Nuclear structure studies of high-spin states with large arrays.

Lecture 1:
at the
Joint ICTP-IAEA Workshop on Nuclear Data : Experiment, Theory and Evaluation

Miramare, Trieste, Italy, August 2016

Paddy Regan
Department of Physics, University of Surrey
Guildford, GU2 7XH
&
National Physical Laboratory, Teddington, UK
p.regan@surrey.ac.uk ; paddy.regan@npl.co.uk

The Chart of the Nuclides

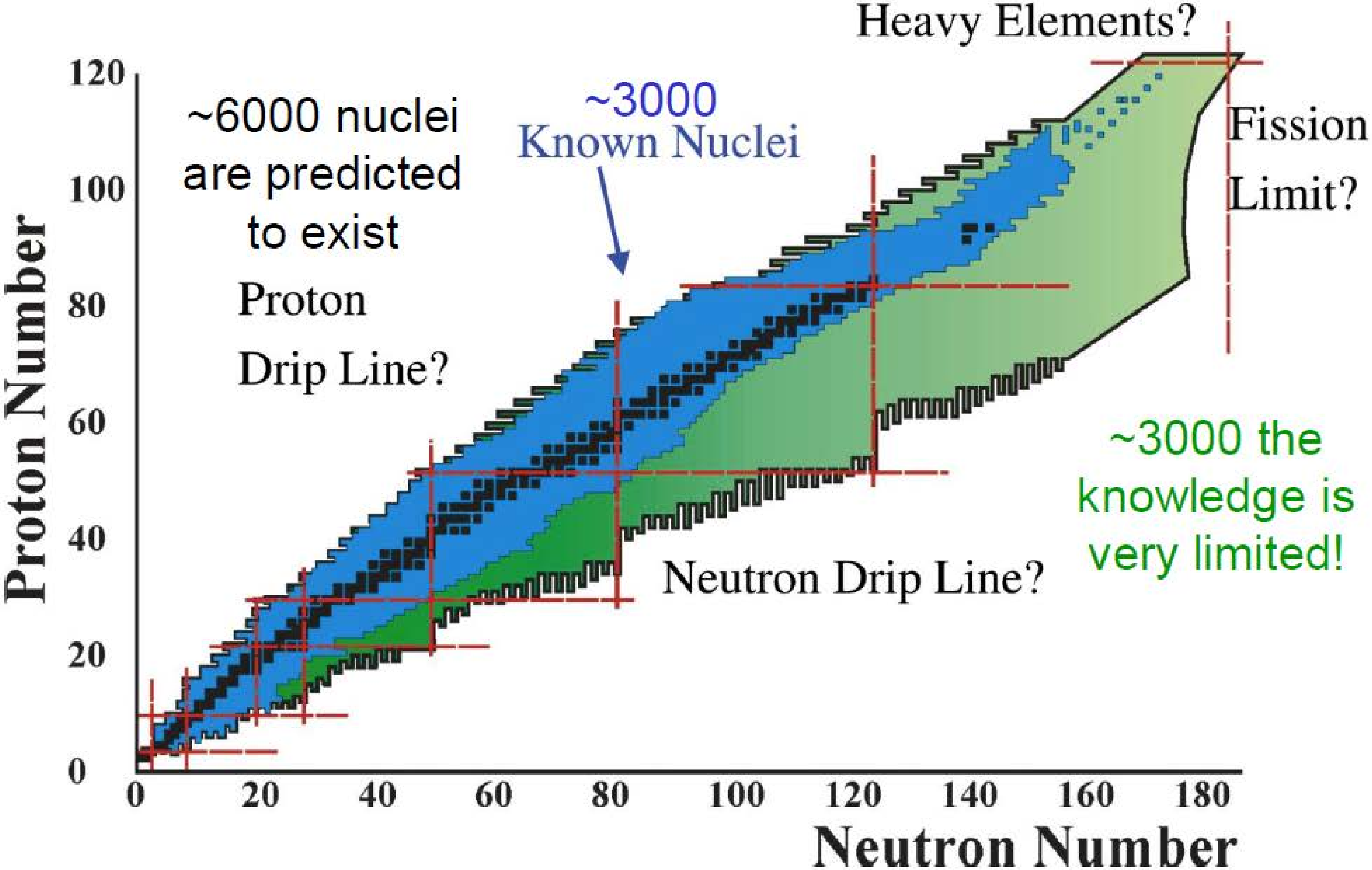

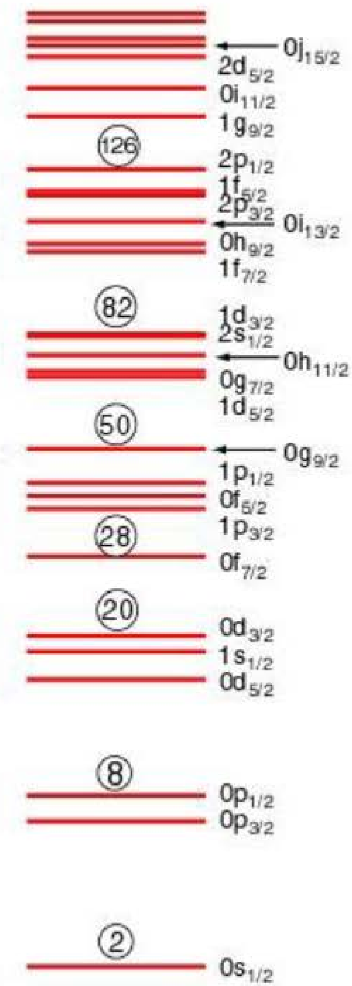

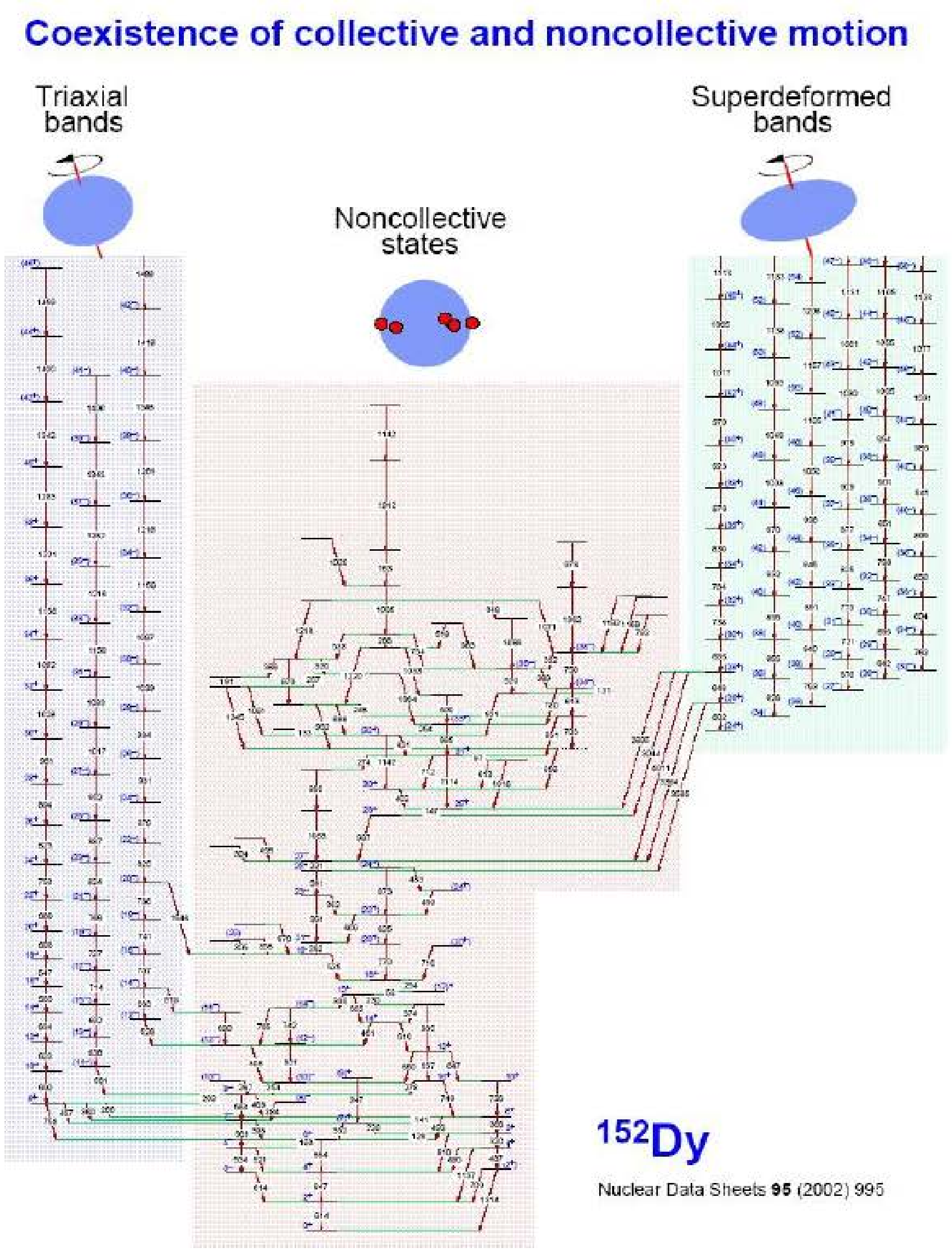

Energy levels are determined by measuring gamma-rays decaying from excited states.

Many, many possible states can be populated…many different gamma-ray energies need to be measured at the same time (in coincidence).

(LN_2 cooled) germanium detectors have the combination of good energy resolution ($\Delta E \sim 2$ keV @ $E_\gamma = 1$ MeV) and acceptable detection efficiency.

Various multi-detector 'arrays' of germanium detectors around the World. e.g., GAMMASPHERE, MINIBALL, GaSp YRASTBALL, JUROGAM, RISING, INGA, EXOGAM, AGATA, GRETINA.

__Fusion-evaporation reactions__ best way to make the highest spins. Nuclear EM decay usually decay via 'near yrast' sequence (since decay prob ~ E_γ^{2L+1})

Compton Suppressed Arrays

For the last ~ 15 - 20 years, large arrays of Compton-suppressed Ge detectors such as EuroBall, JUROBALL , GASP, EXOGAM, TIGRESS, INGA, Gammasphere and others have been the tools of choice for nuclear spectroscopy.

EUROBALL

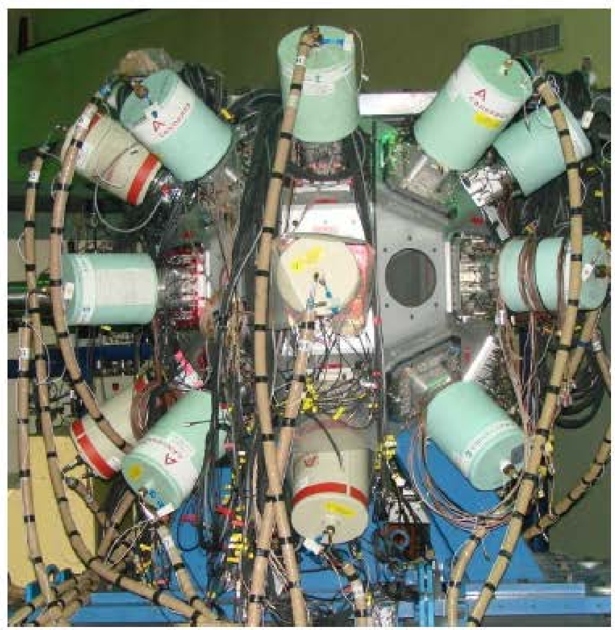

INGA

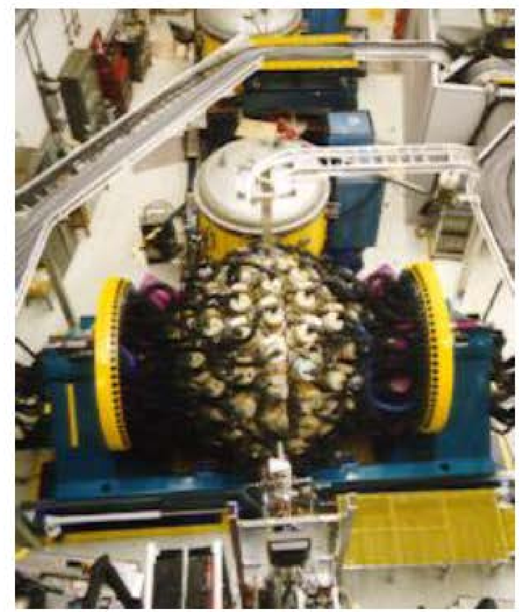

Gammasphere

Angular Momentum World of the Nucleus

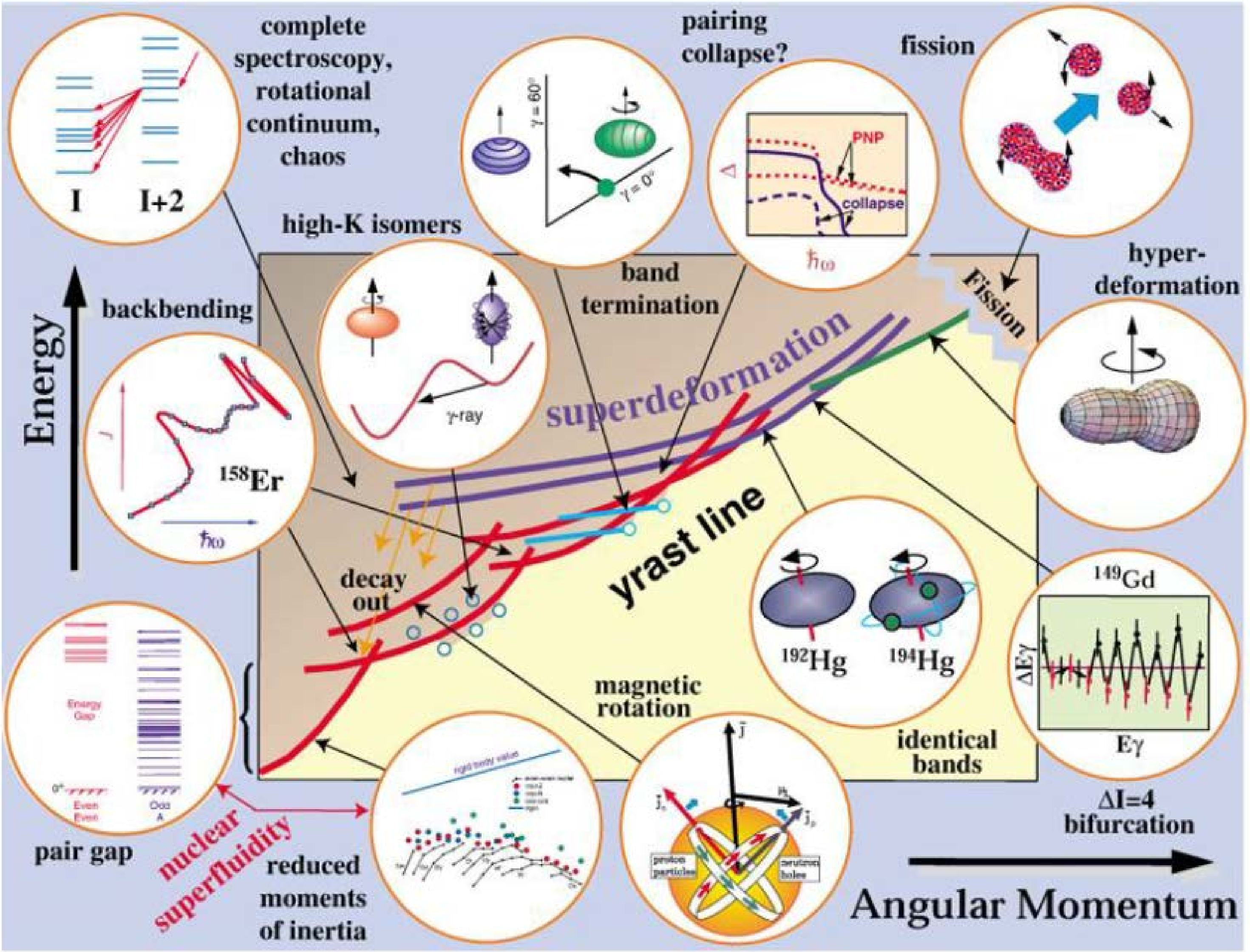

Figure; originated from Prof. M.A.Riley (FSU)

Different nuclear reaction mechanisms?

- Heavy-ion fusion-evaporation reactions (makes mostly neutron-deficient residual nuclei).
- Spontaneous fission sources such as ^{252}Cf (makes mostly neutron-rich residual nuclei).
- Deep-inelastic/multi-nucleon transfer and heavy-ion fusion-fission reactions (makes near-stable/slightly neutron-rich residual nuclei).
- High-energy Projectile fragmentation / projectile fission at e.g., GSI, RIKEN, GANIL, MSU.
- Coulomb excitation, EM excitations via E2 (usually).
- Single particle transfer reactions (p,d)
- Beta decay ; alpha decay ; proton radioactivity
- Other probes (e,e'γ), (γ,γ'), (n,γ), (p,γ), (n,n'γ) etc.

First four generally populate 'near-yrast' states – most useful to see 'higher' spins states and excitations.

Heavy-ion induced nuclear reactions on fixed targets can result in a range of different nuclear reactions taking place.

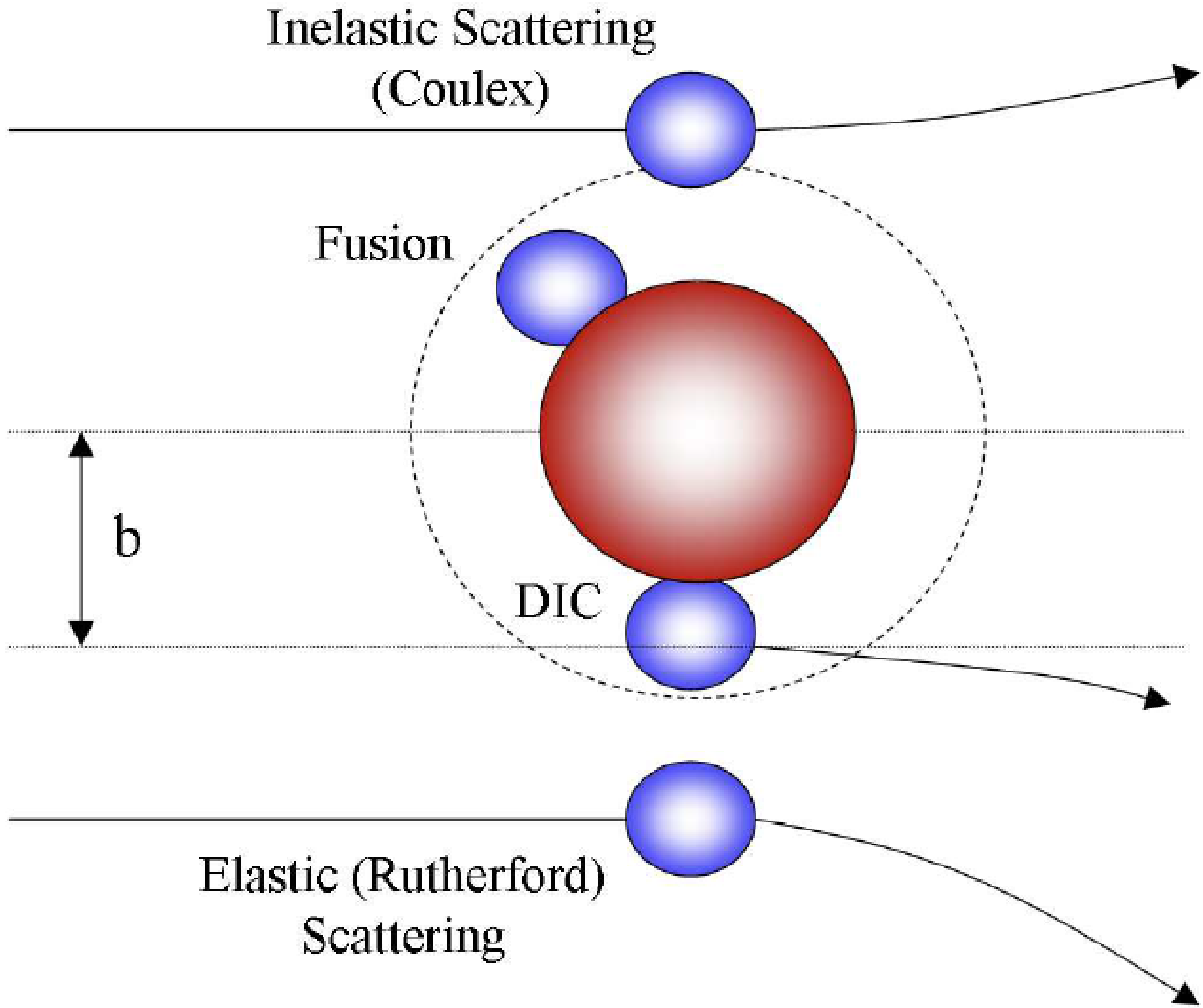

The specifics depends on the (1) beam and target nuclei (A,Z,I);
(2) the beam energy (higher or lower than the Coulomb repulsion between the two nuclei), and (3) the impact parameter, b.

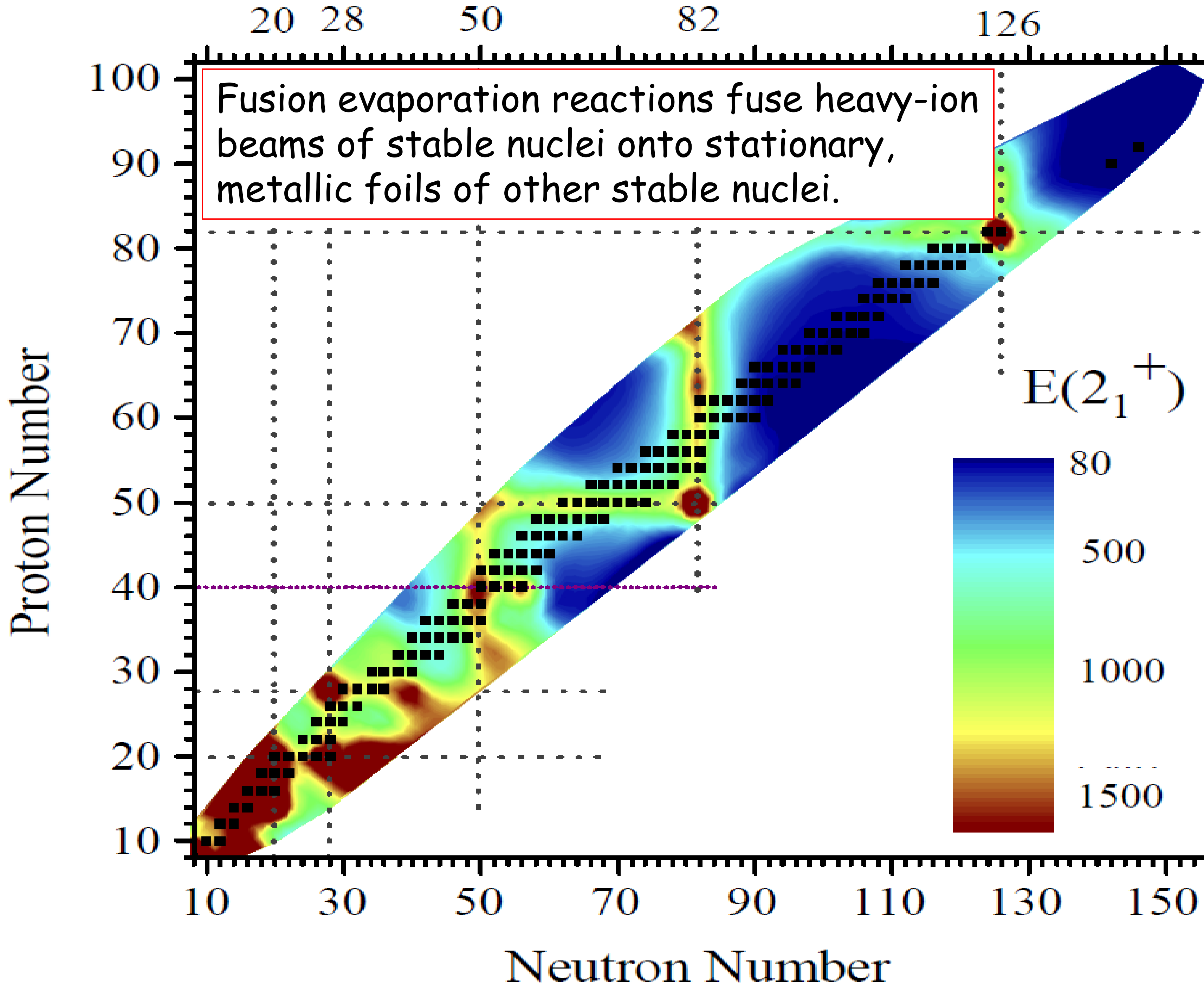

20
28
50
82
126
Fusion evaporation reactions fuse heavy-ion beams of stable nuclei onto stationary, metallic foils of other stable nuclei.
$E(2_1^+)$
80
500
1000
1500
Proton Number
100
90
80
70
60
50
40
30
20
10
10
30
50
70
90
110
130
150
Neutron Number

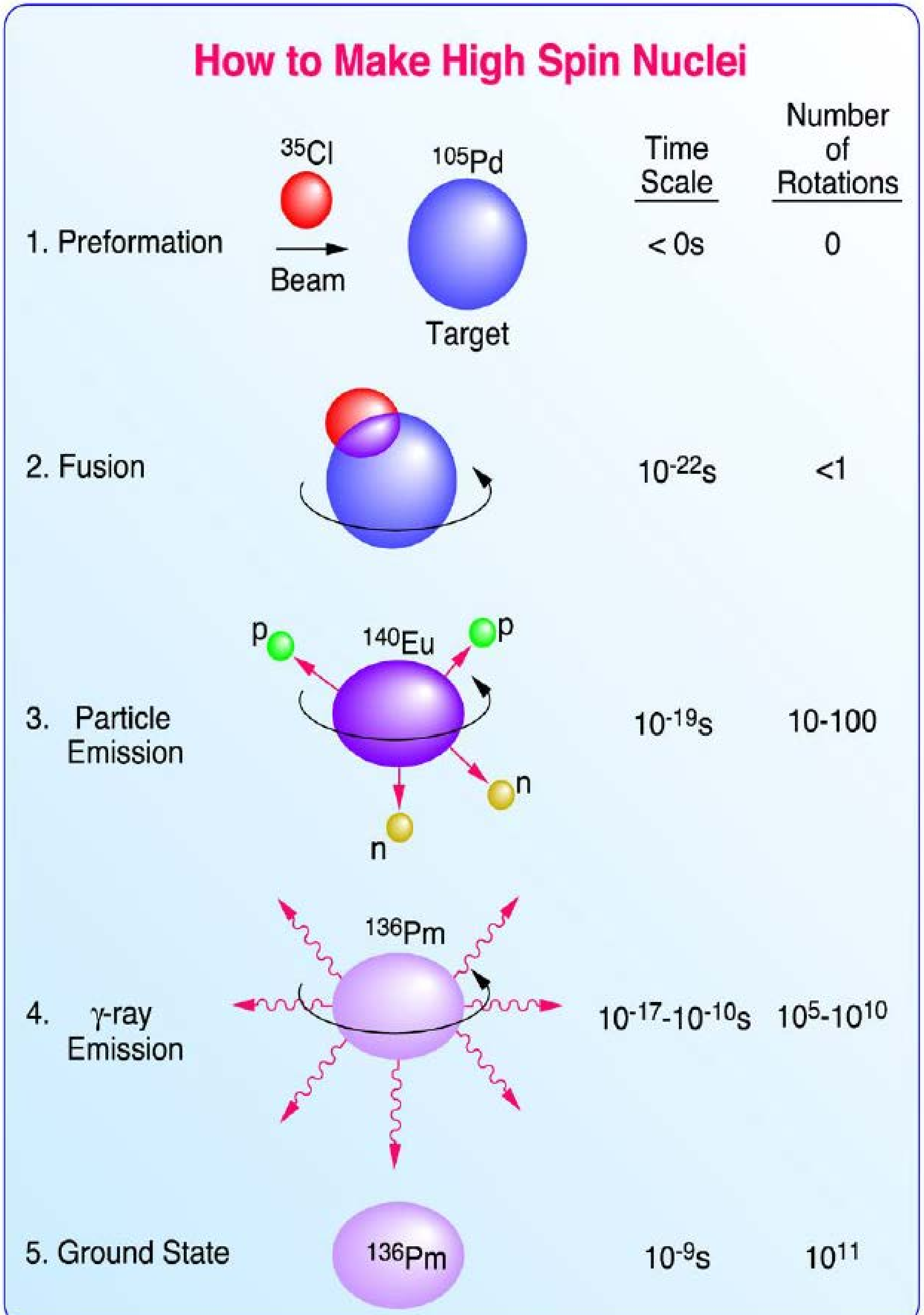

$$E^*_R = E_{Beam} + Q_{reaction} - KE_{recoil}$$

Less particle evaporation corresponds to higher spins states for a particular bombarding energy.

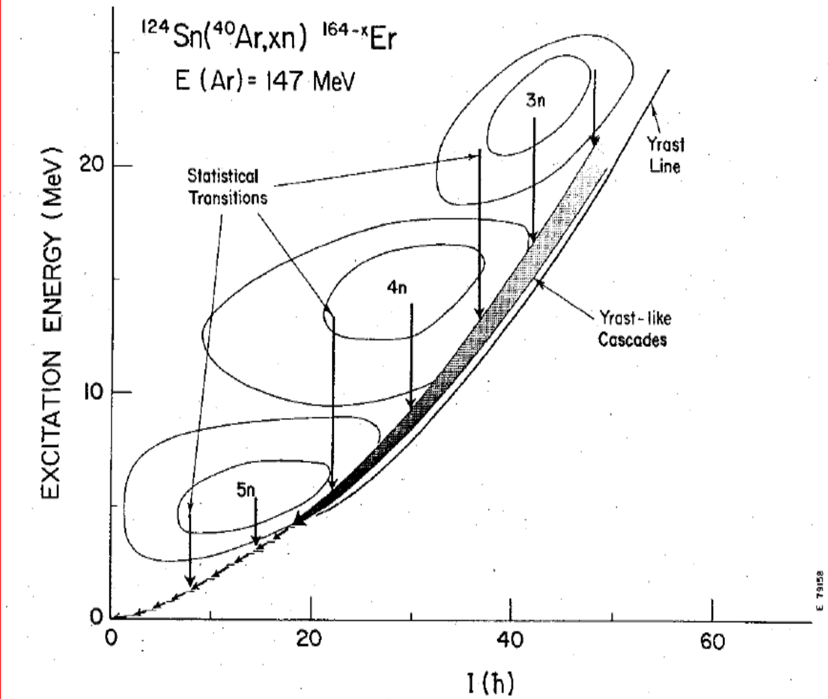

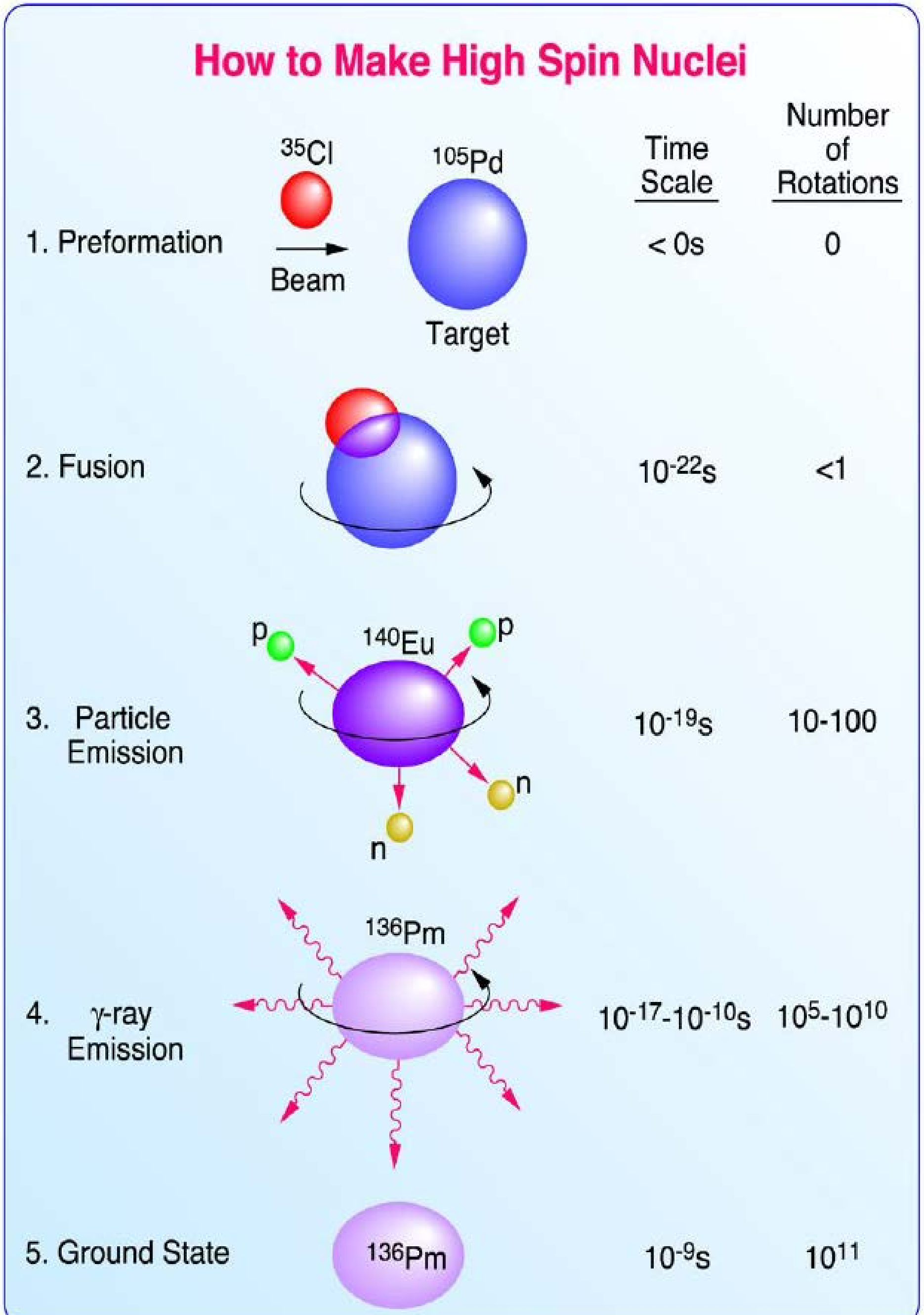

$$E^*_R = E_{Beam} + Q_{reaction} - KE_{recoil}$$

Less particle evaporation corresponds to higher spins states for a particular bombarding energy.

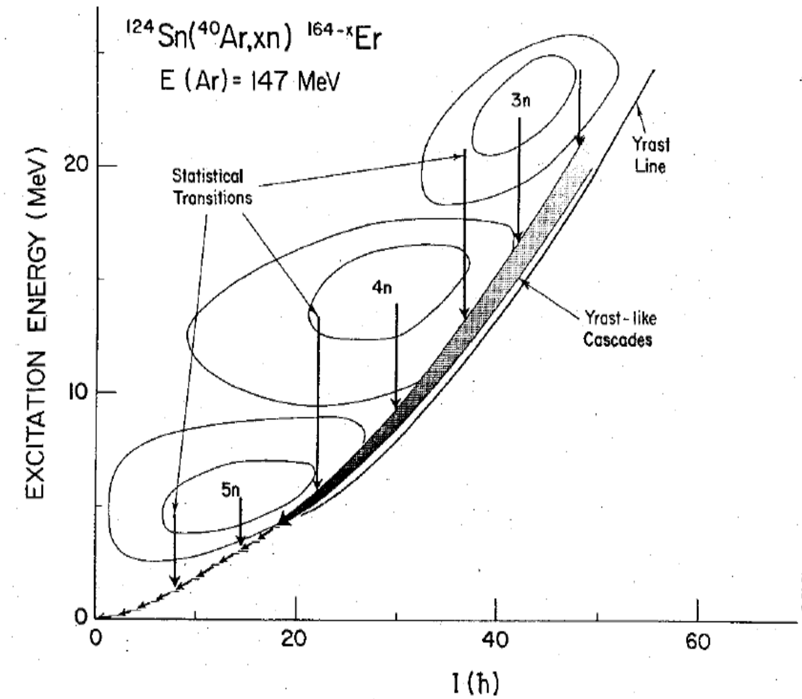

Maximum angular momentum input to compound system (l_{max}) depends on

$\underline{l} = \underline{r} \times \underline{p}$

i.e. beam energy (linked to **p**) and maximum overlap of nuclear radii (**r**)

Example: $^{96}Ru(^{40}Ca,xpyn)^{136}Gd$-xp-yn

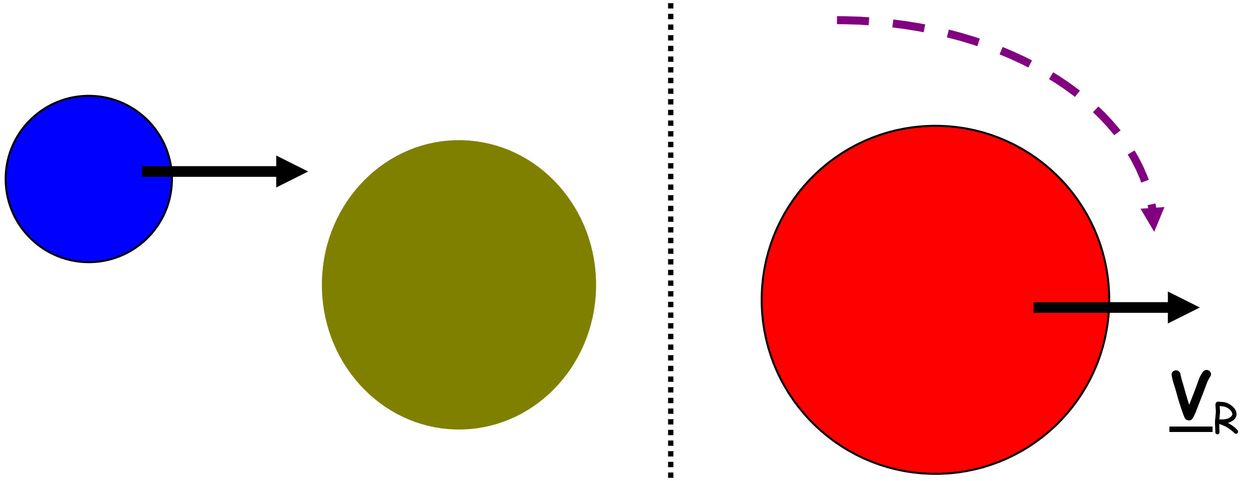

^{40}Ca
Z=20
N=20

^{96}Ru
Z=44
N=52

^{136}Gd (Z=64 N=72).

Hot, compound system recoils backwards at 0° in the lab frame.

Example: ^{96}Ru(^{40}Ca,xpyn)^{136}Gd-xp-yn

$m_B\underline{\mathbf{V}}_B$ $m_T\underline{\mathbf{V}}_T=0$

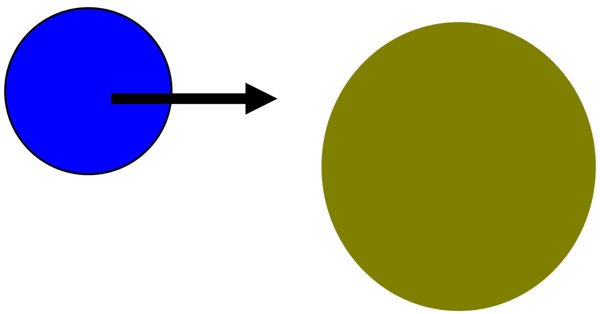

^{40}Ca
Z=20
N=20

^{96}Ru
Z=44
N=52

KE of beam = $\frac{1}{2}\, m_B V_B^{\,2}$

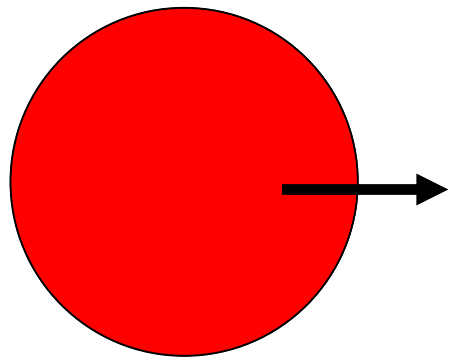

^{136}Gd (Z=64 N=72).
Hot, compound nucleus recoils backwards at 0^o in the lab frame with velocity, $\underline{\mathbf{V}}_R$.

Example: $^{96}Ru(^{40}Ca,xpyn)^{136}Gd$-xp-yn

$m_B\underline{\mathbf{V}}_B$

$m_T\underline{\mathbf{V}}_T=0$

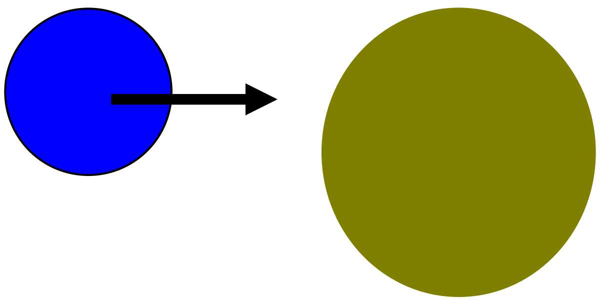

^{40}Ca
Z=20
N=20

^{96}Ru
Z=44
N=52

KE of beam = $\frac{1}{2}\, m_B V_B^{\,2}$

$m_R\underline{\mathbf{V}}_R = (m_B+m_T)\underline{\mathbf{V}}_R = m_B\underline{\mathbf{V}}_B$. Therefore,

$\underline{\mathbf{V}}_R=(m_B)\underline{\mathbf{V}}_B/(m_B+m_T)$

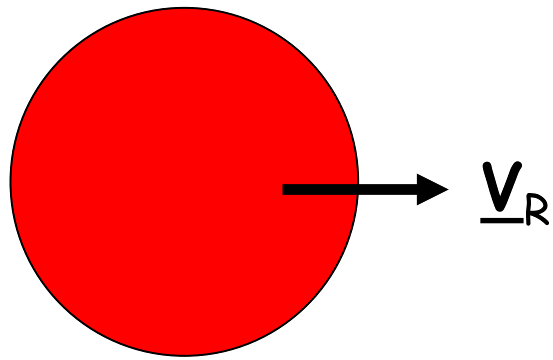

^{136}Gd (Z=64 N=72).
Hot, compound nucleus recoils backwards at 0° in the lab frame with velocity, $\underline{\mathbf{V}}_R$.

Example: $^{96}Ru(^{40}Ca,xpyn)^{136}Gd$-xp-yn

$m_B\underline{\mathbf{V}}_B$

$m_T\underline{\mathbf{V}}_T=0$

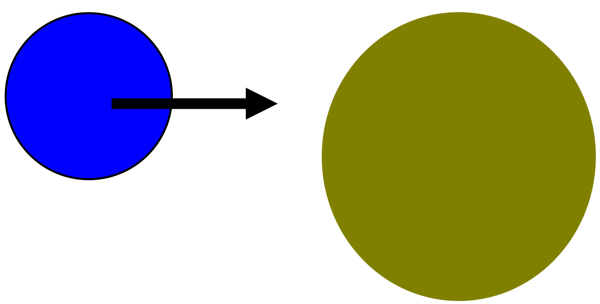

^{40}Ca
Z=20
N=20

^{96}Ru
Z=44
N=52

KE of beam = $\frac{1}{2} m_B V_B^2$

$m_R\underline{\mathbf{V}}_R = (m_B+m_T)\underline{\mathbf{V}}_R = m_B\underline{\mathbf{V}}_B$. Therefore,

$\underline{\mathbf{V}}_R=(m_B)\underline{\mathbf{V}}_B/(m_B+m_T)$

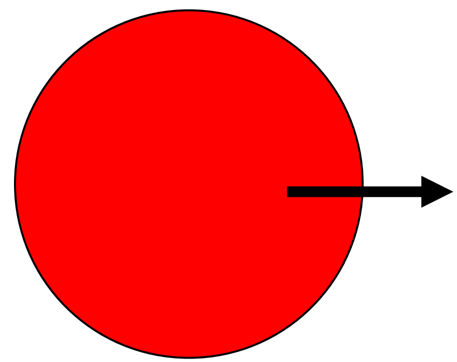

^{136}Gd (Z=64 N=72).
Hot, compound nucleus recoils backwards at 0° in the lab frame with velocity, v_R.

KE of recoiling nucleus = $\frac{1}{2}(M_B+M_T)V^2_R$

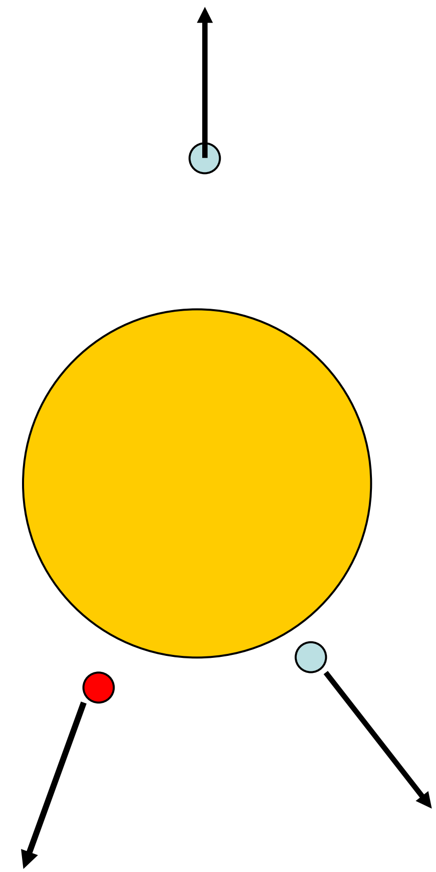

Light particles p,n,α evaporated.
Sn,Sp ~ 1-15 MeV.

Example: ^{96}Ru(^{40}Ca,xpyn)^{136}Gd-xp-yn

$m_B\underline{\mathbf{V}}_B$

$m_T\underline{\mathbf{V}}_T=0$

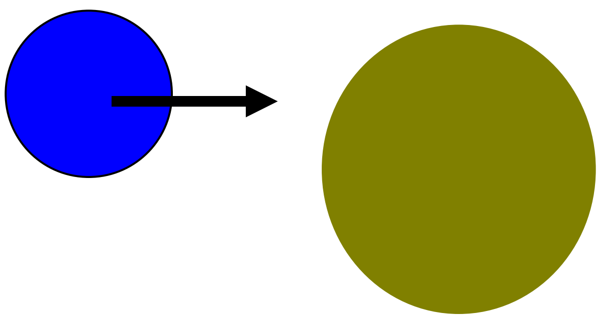

^{40}Ca
Z=20
N=20

^{96}Ru
Z=44
N=52

KE of beam = $\frac{1}{2}\, m_B v_B^{\,2}$

$m_R\underline{\mathbf{V}}_R = (m_B+m_T)\underline{\mathbf{V}}_R = m_B\underline{\mathbf{V}}_B$. Therefore,
$\underline{\mathbf{V}}_R=(m_B)\underline{\mathbf{V}}_B/(m_B+m_T)$

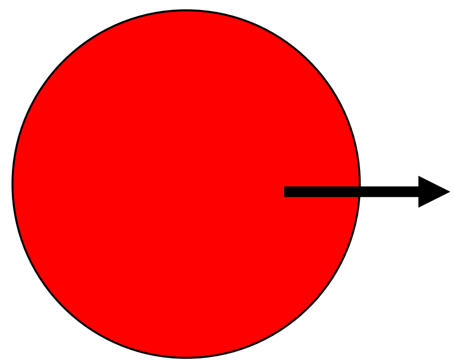

^{136}Gd (Z=64 N=72).
Hot, compound nucleus recoils backwards at 0° in the lab frame with velocity, v_R.
KE of recoiling nucleis $= \frac{1}{2}\,(M_B+M_T)V^2_R$

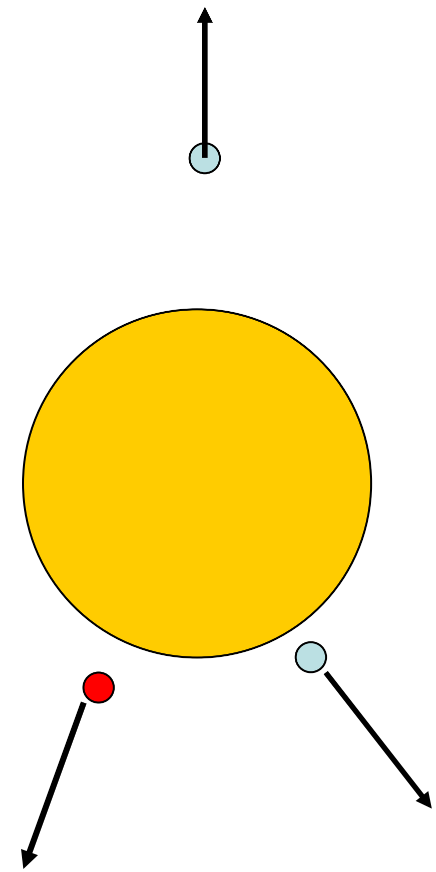

^{136}Gd+3p = ^{133}Pm
^{136}Gd+2pn=^{133}Sm
^{136}Gd+3pn=^{134}Pm
^{136}Gd+2p2n=^{132}Sm

Production of High-Spin States

$$E_{ex} = E_{cm} + Q_{fus} \tag{2.1.1}$$

E_{cm} is the kinetic energy of the collision which is transfered to the compound system. It can be calculated by taking the kinetic energy of the beam, E_B and subtracting the kinetic energy of the recoiling compound system, E_R. Thus

$$E_{cm} = E_B - E_R \tag{2.1.2}$$

By conservation of momentum, for beam and target masses of M_B and M_T respectively, the velocity of the recoiling compound, V_R can be calculated using

$$M_B V_B = (M_T + M_B) V_R \tag{2.1.3}$$

and by conservation of energy,

$$E_{cm} = E_B - \frac{1}{2}(M_T + M_B) V_R^2 \tag{2.1.4}$$

substituting in for V_R, and recalling that $E_B = \frac{1}{2} M_B V_B^2$, we obtain

$$E_{cm} = E_B \left(1 - \frac{M_B}{M_T + M_B}\right) \tag{2.1.5}$$

Example: $^{96}Ru(^{40}Ca,xpyn)^{136}Gd$-xp-yn

$m_B\underline{\mathbf{V}}_B$

$m_T\underline{\mathbf{V}}_T=0$

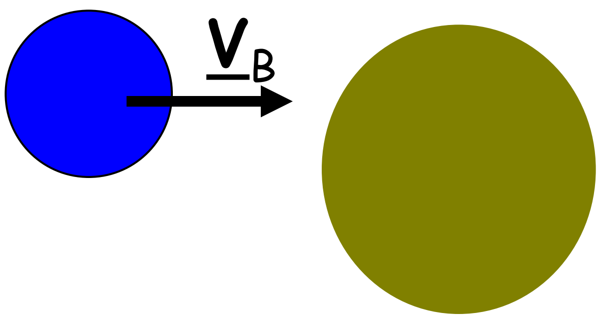

^{40}Ca
Z=20
N=20

^{96}Ru
Z=44
N=52

KE of beam = $\frac{1}{2}\, m_B v_B^2$

$m_R\underline{\mathbf{V}}_R = (m_B+m_T)\underline{\mathbf{V}}_R = m_B\underline{\mathbf{V}}_B$. Therefore,
$\underline{\mathbf{V}}_R=(m_B)\underline{\mathbf{V}}_B/(m_B+m_T)$

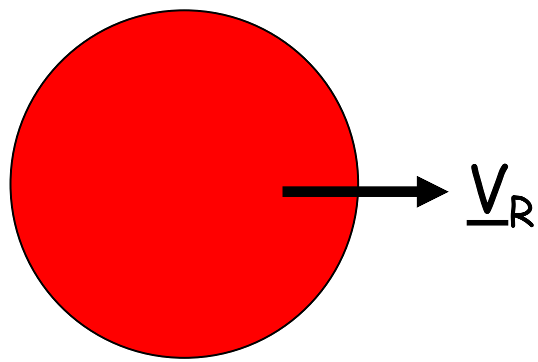

^{136}Gd (Z=64 N=72).
Hot, compound nucleus recoils backwards at 0° in the lab frame with velocity, $\underline{\mathbf{V}}_R$.
KE of recoiling nucleis = $\frac{1}{2}\,(M_B+M_T)V^2_R$

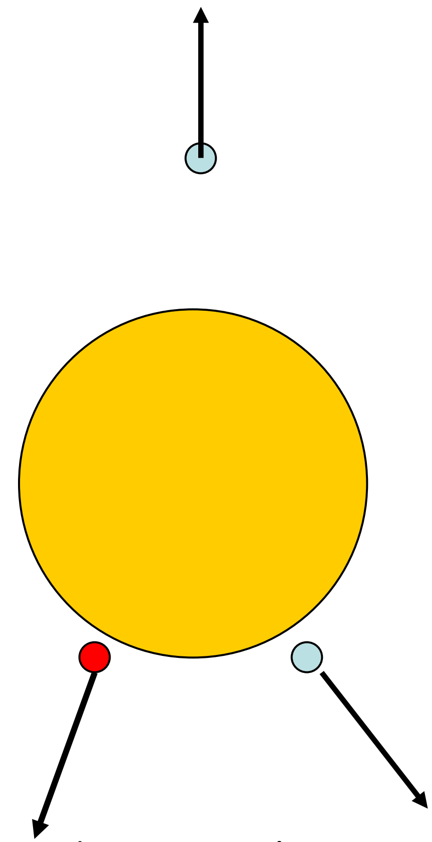

Light particle emission causes small recoil cone in lab frame due to cons. of linear momentum.

Doppler Shifts

Moving source – nucleus which emits gamma-ray ;
Stationary observer - Ge detector.

$$E_S = E_0 \frac{\sqrt{1-\beta^2}}{1-\beta\cos\theta} \approx E_0(1+\beta\cos\theta)$$

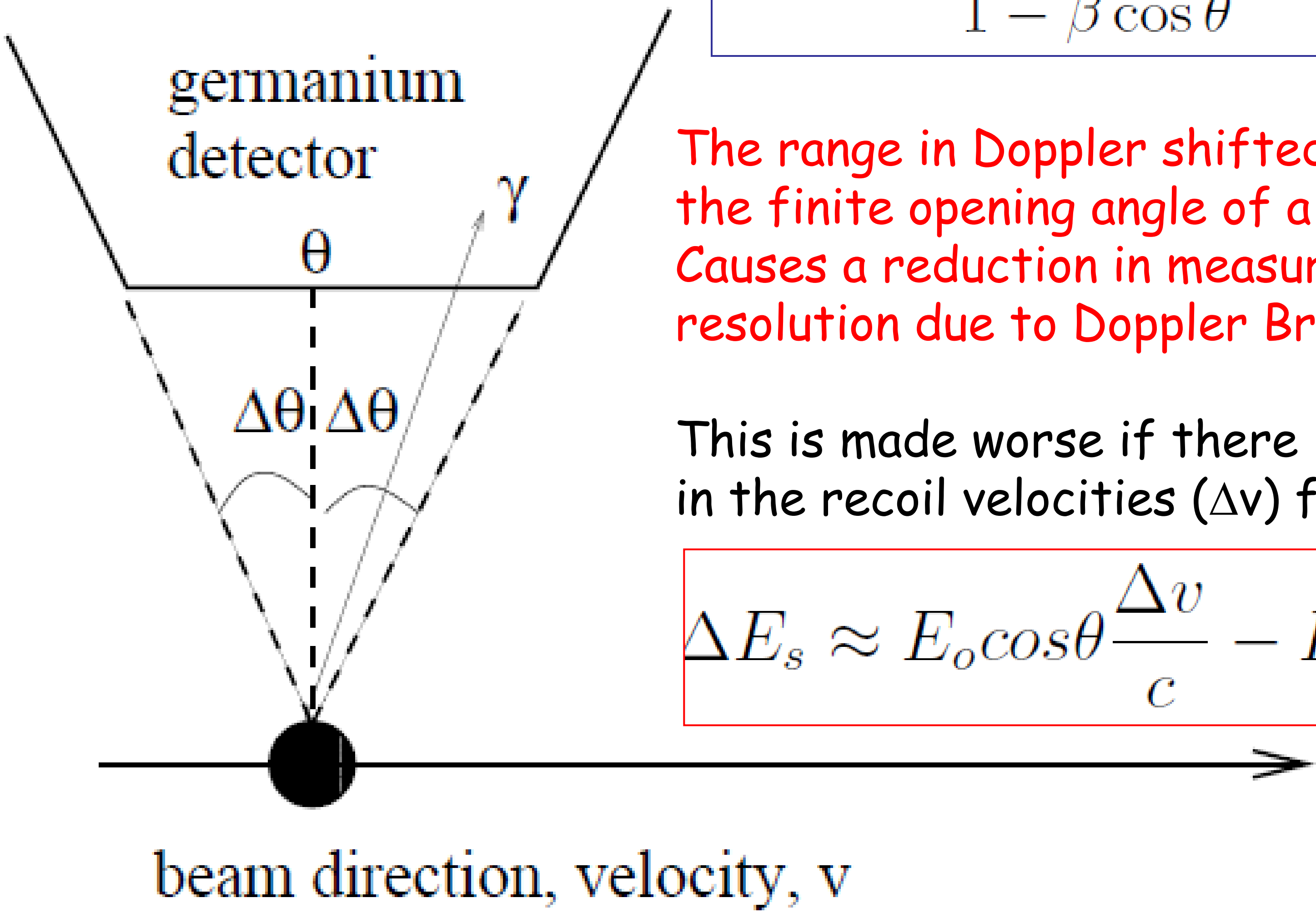

The range in Doppler shifted energy across the finite opening angle of a detector (Δθ) Causes a reduction in measured energy resolution due to Doppler Broadening.

This is made worse if there is also a spread in the recoil velocities (Δv) for the recoils.

$$\Delta E_s \approx E_o cos\theta \frac{\Delta v}{c} - E_o \frac{v}{c} sin\theta \Delta\theta$$

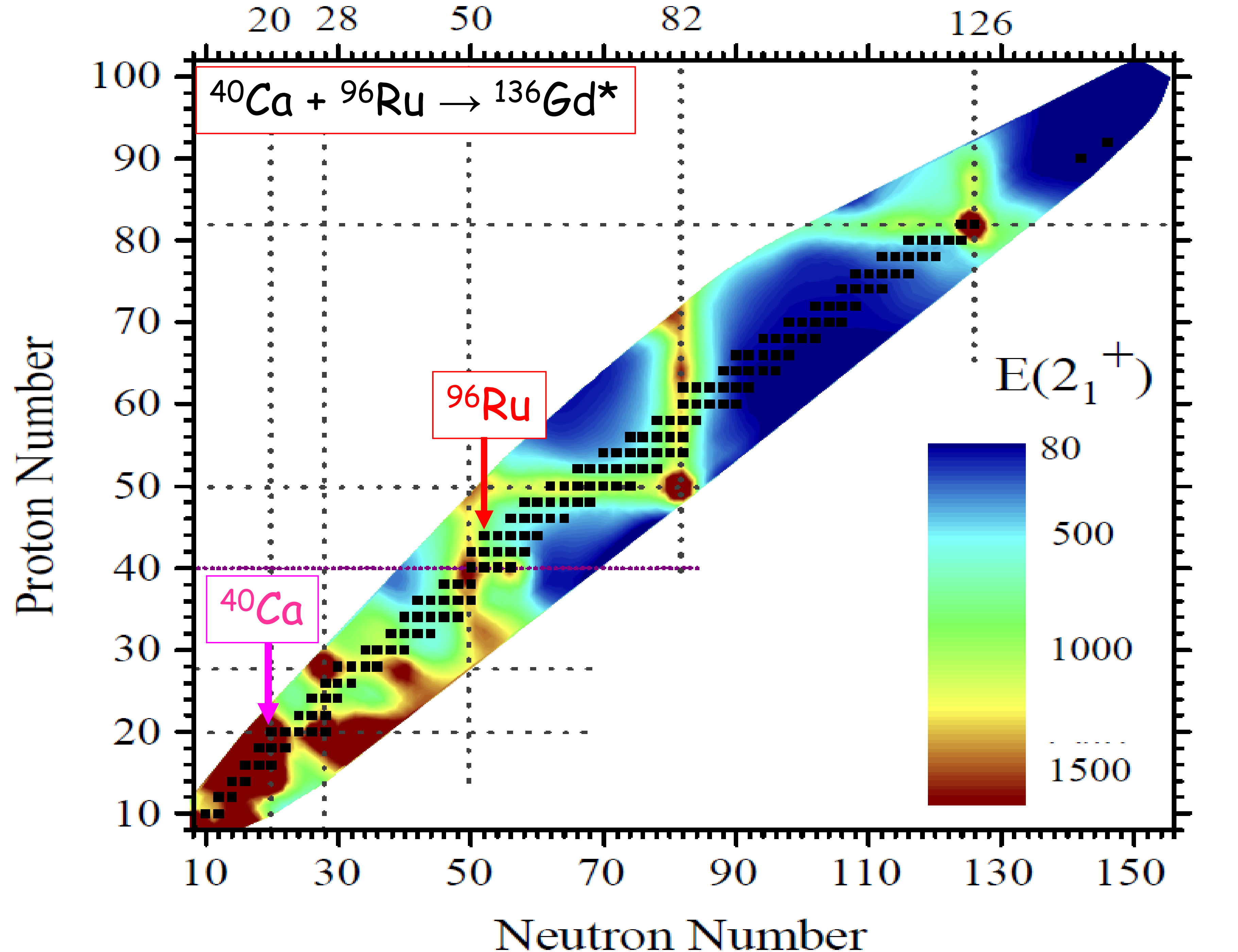

$^{40}Ca + ^{96}Ru \rightarrow ^{136}Gd^*$
^{96}Ru
^{40}Ca
$E(2_1^+)$
80
500
1000
1500
20
28
50
82
126
Proton Number
Neutron Number
10
30
50
70
90
110
130
150
10
20
30
40
50
60
70
80
90
100

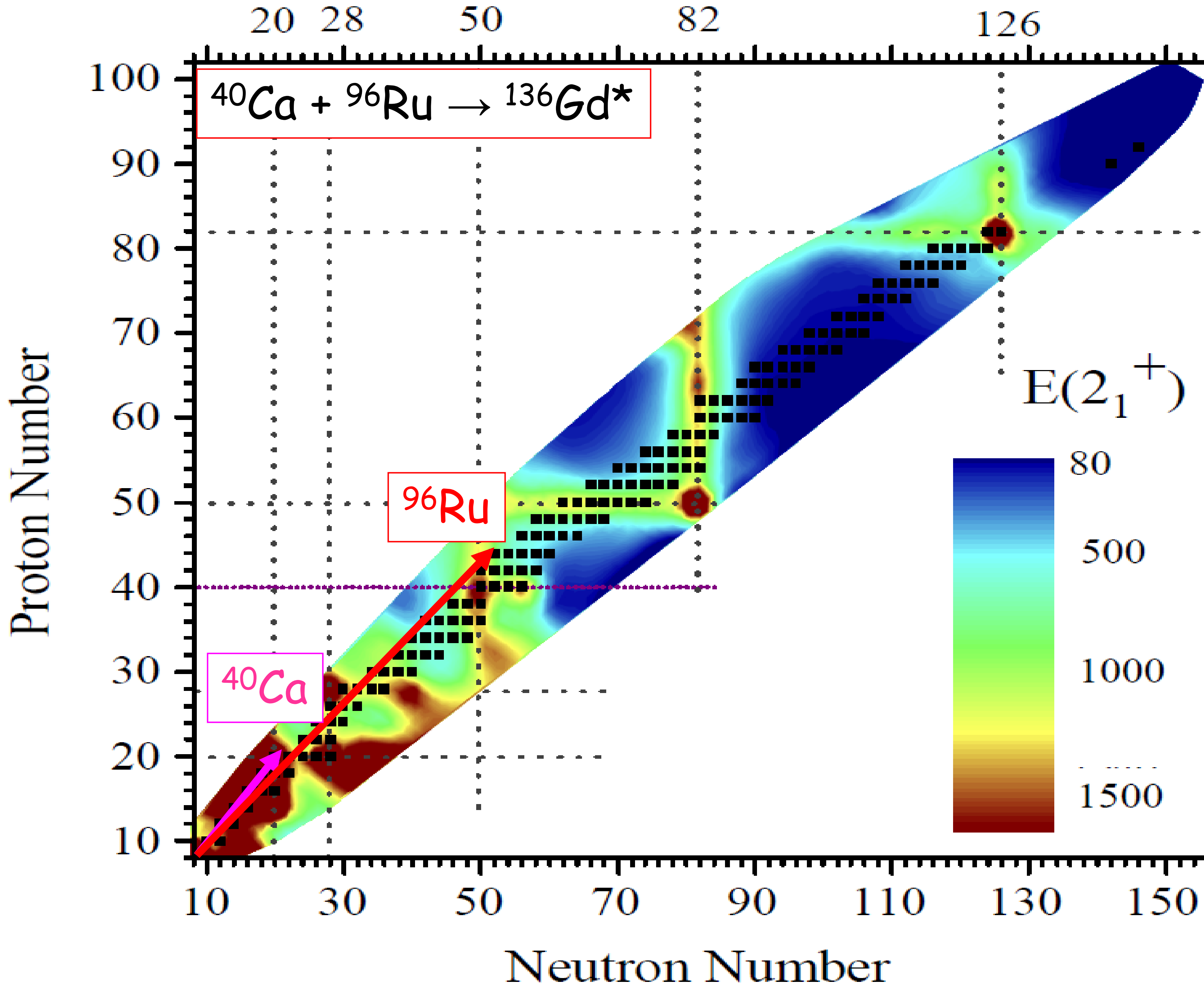

$^{40}Ca + ^{96}Ru \rightarrow ^{136}Gd^*$
^{96}Ru
^{40}Ca
$E(2_1^+)$
80
500
1000
1500
20
28
50
82
126
Proton Number
Neutron Number
10
30
50
70
90
110
130
150
100
90
80
70
60
40
20

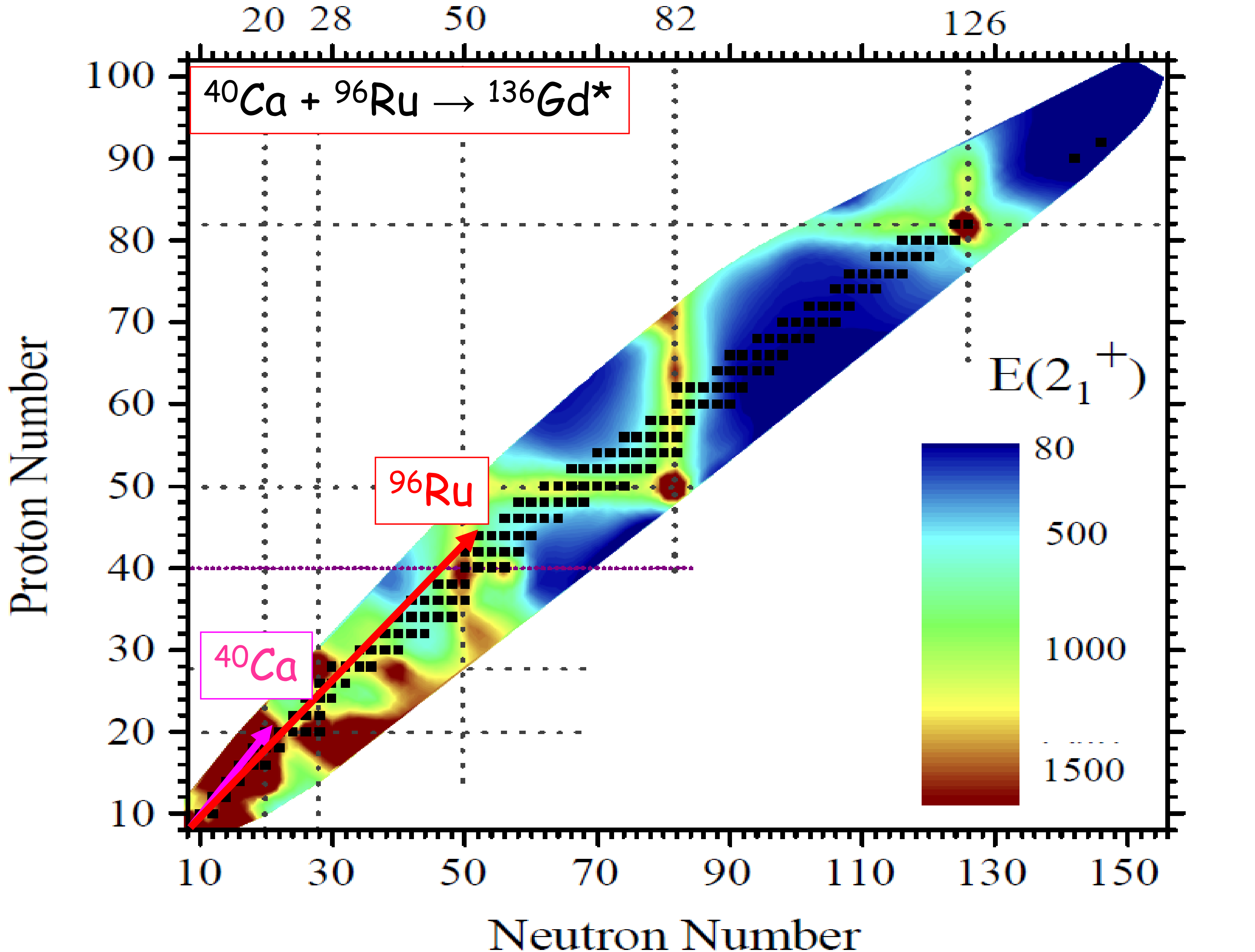

$^{40}Ca + ^{96}Ru \rightarrow ^{136}Gd^*$
^{96}Ru
^{40}Ca
$E(2_1^+)$
80
500
1000
1500
20 28 50 82 126
Proton Number
Neutron Number
10 30 50 70 90 110 130 150
10 20 30 40 50 60 70 80 90 100

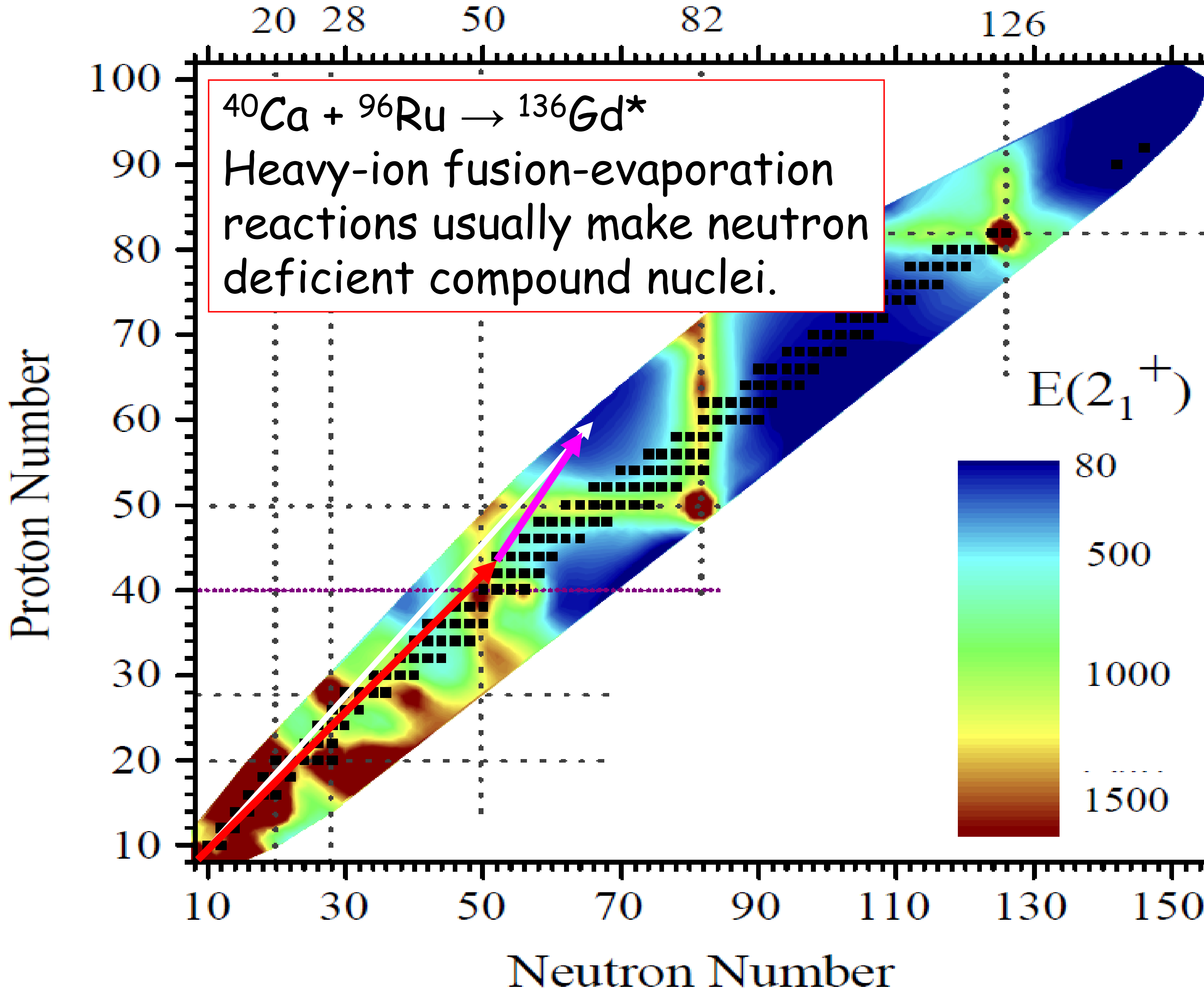

$^{40}Ca + ^{96}Ru \rightarrow ^{136}Gd^*$
Heavy-ion fusion-evaporation reactions usually make neutron deficient compound nuclei.
20
28
50
82
126
100
90
80
70
60
50
40
30
20
10
Proton Number
$E(2_1^+)$
80
500
1000
1500
10
30
50
70
90
110
130
150
Neutron Number

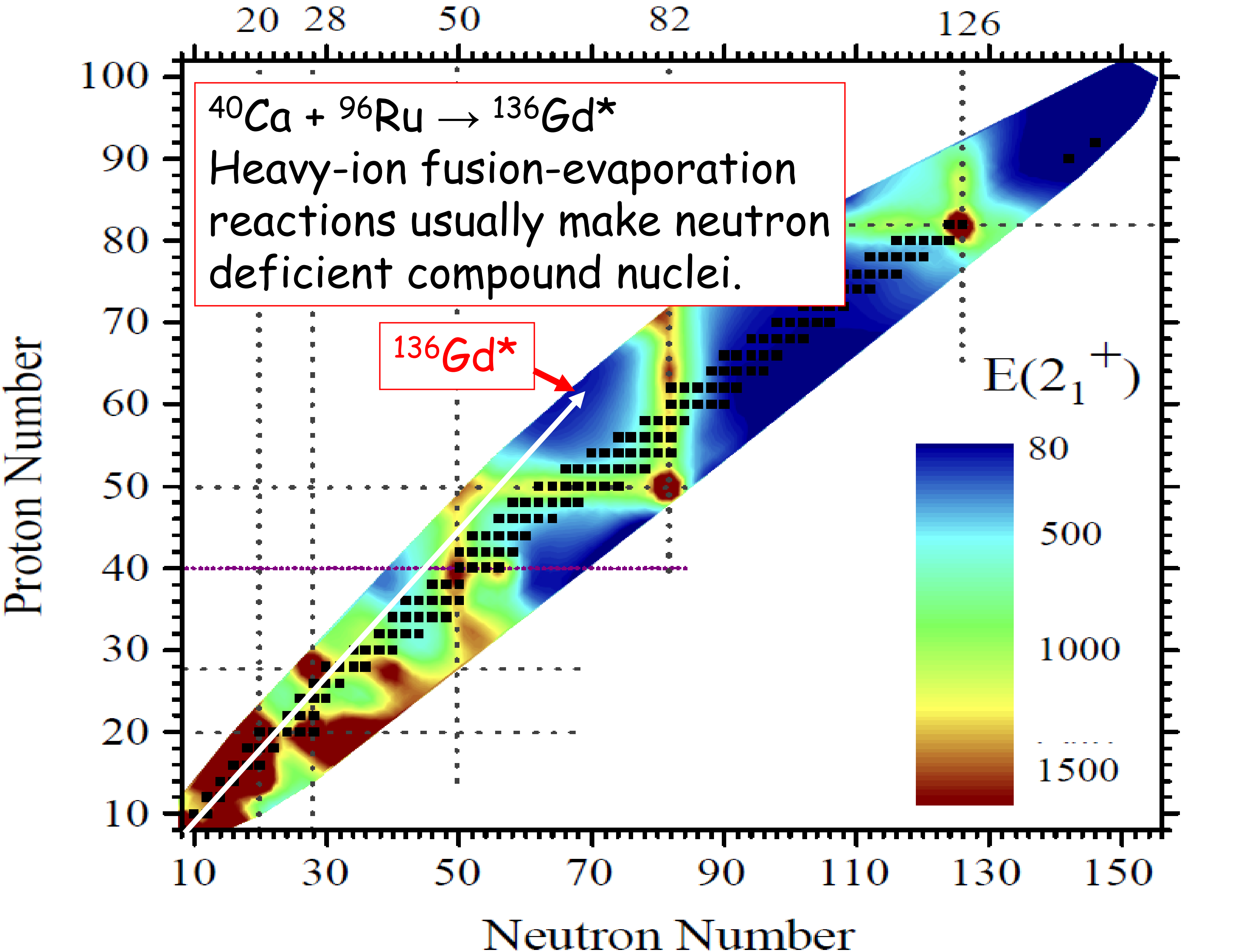

$^{40}Ca + ^{96}Ru \rightarrow ^{136}Gd^*$
Heavy-ion fusion-evaporation reactions usually make neutron deficient compound nuclei.
$^{136}Gd^*$
$E(2_1^+)$
80
500
1000
1500
Proton Number
Neutron Number
20 28 50 82 126
100 90 80 70 60 50 40 30 20 10
10 30 50 70 90 110 130 150

Do you evaporate protons or neutrons?

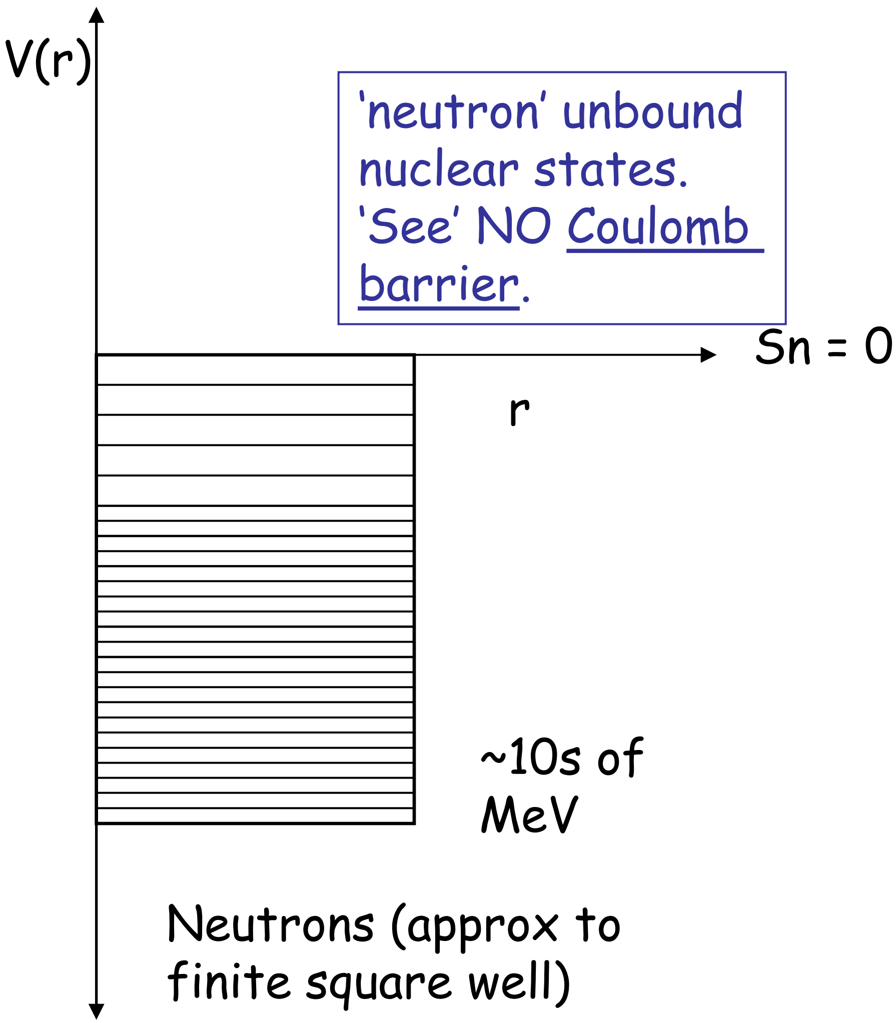

Do you evaporate protons or neutrons?

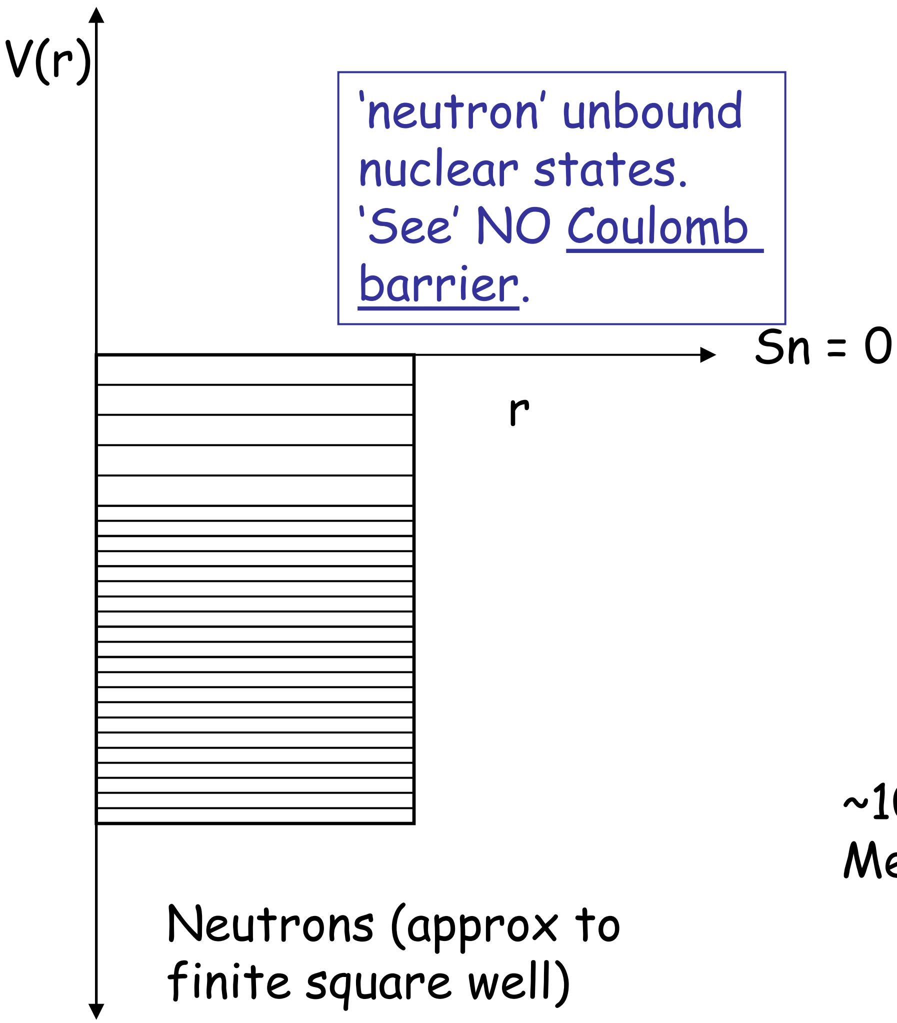

Neutrons (approx to finite square well)

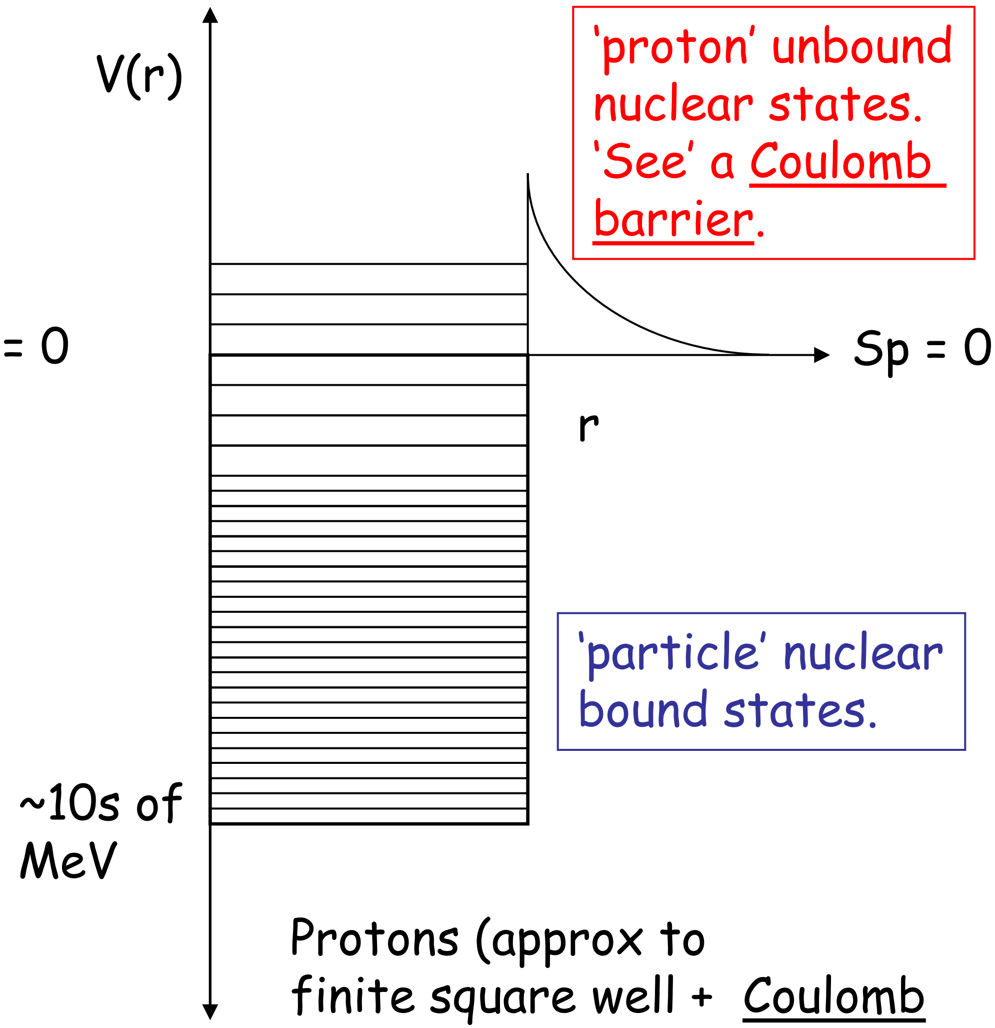

Protons (approx to finite square well + Coulomb Barrier above Sp=0)

Near stable (compound) nuclei, Sp ~ Sn ~ 5-8 MeV.

Coulomb barrier means (HI,xn) favoured over (HI,xp)

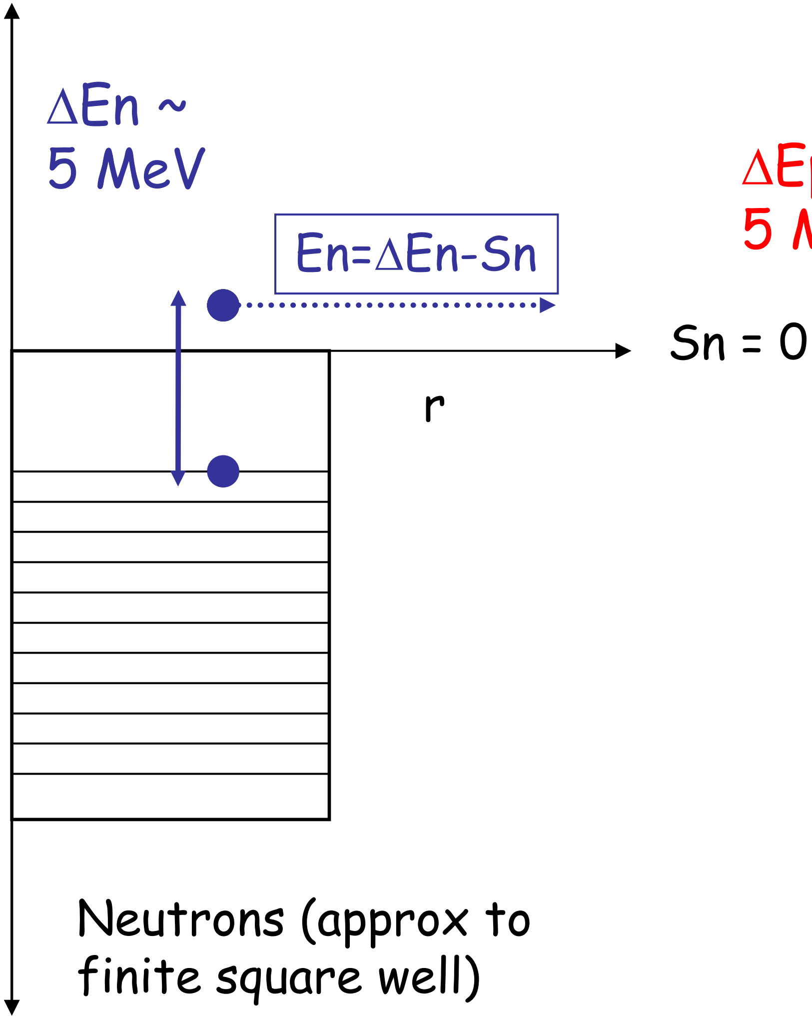

Neutrons (approx to finite square well)

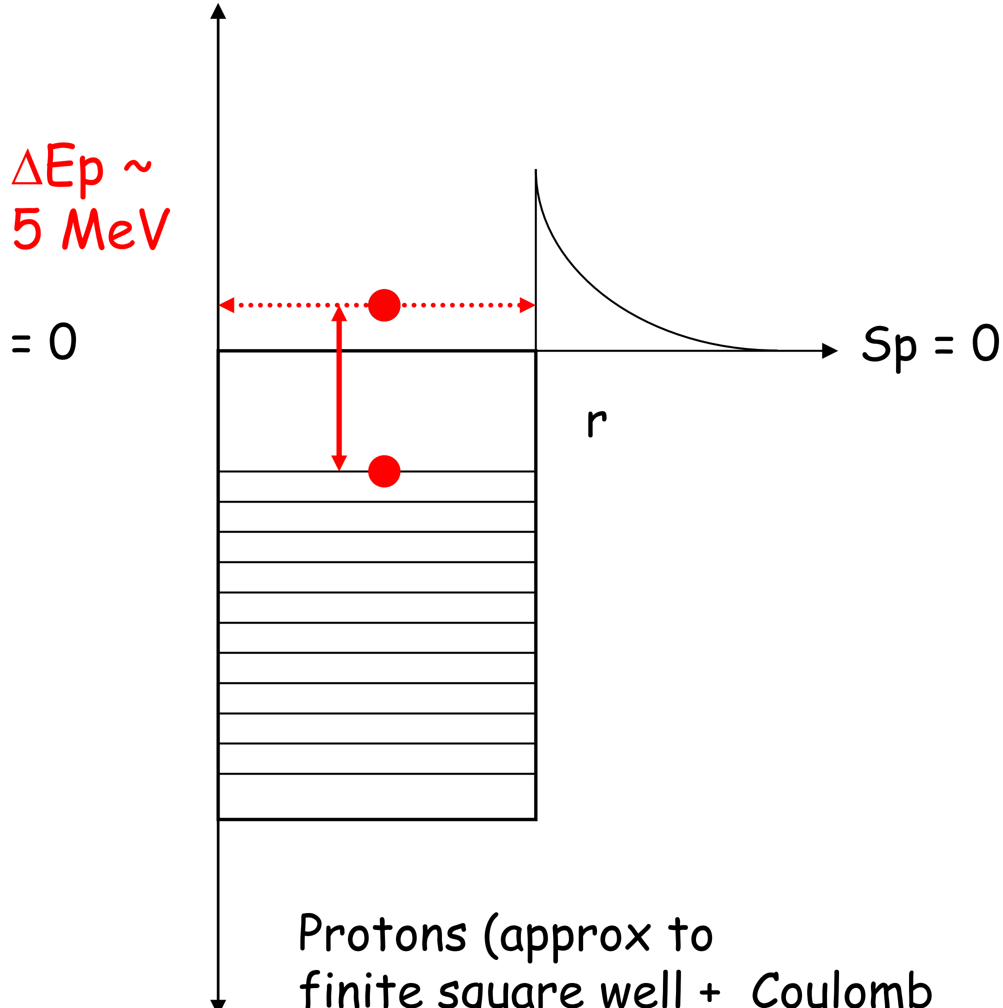

Protons (approx to finite square well + Coulomb Barrier above Sp=0)

Angular Momentum Input in HIFE Reactions?

$$\hbar l_{max} = \mu v R$$

$$\frac{1}{2}\mu v^2 = E_{cm} - V_c$$

Reduced mass of system,
$\mu = m_b.m_T / (m_B+m_T)$

$$l_{max}^2 = \frac{2\mu R^2}{\hbar^2}\left(E_{cm} - V_c\right)$$

^{98}Mo + ^{12}C → ^{110}Cd fusion evaporation calculations using PACE4 S.F. Ashley, PhD thesis, University of Surrey (2007)

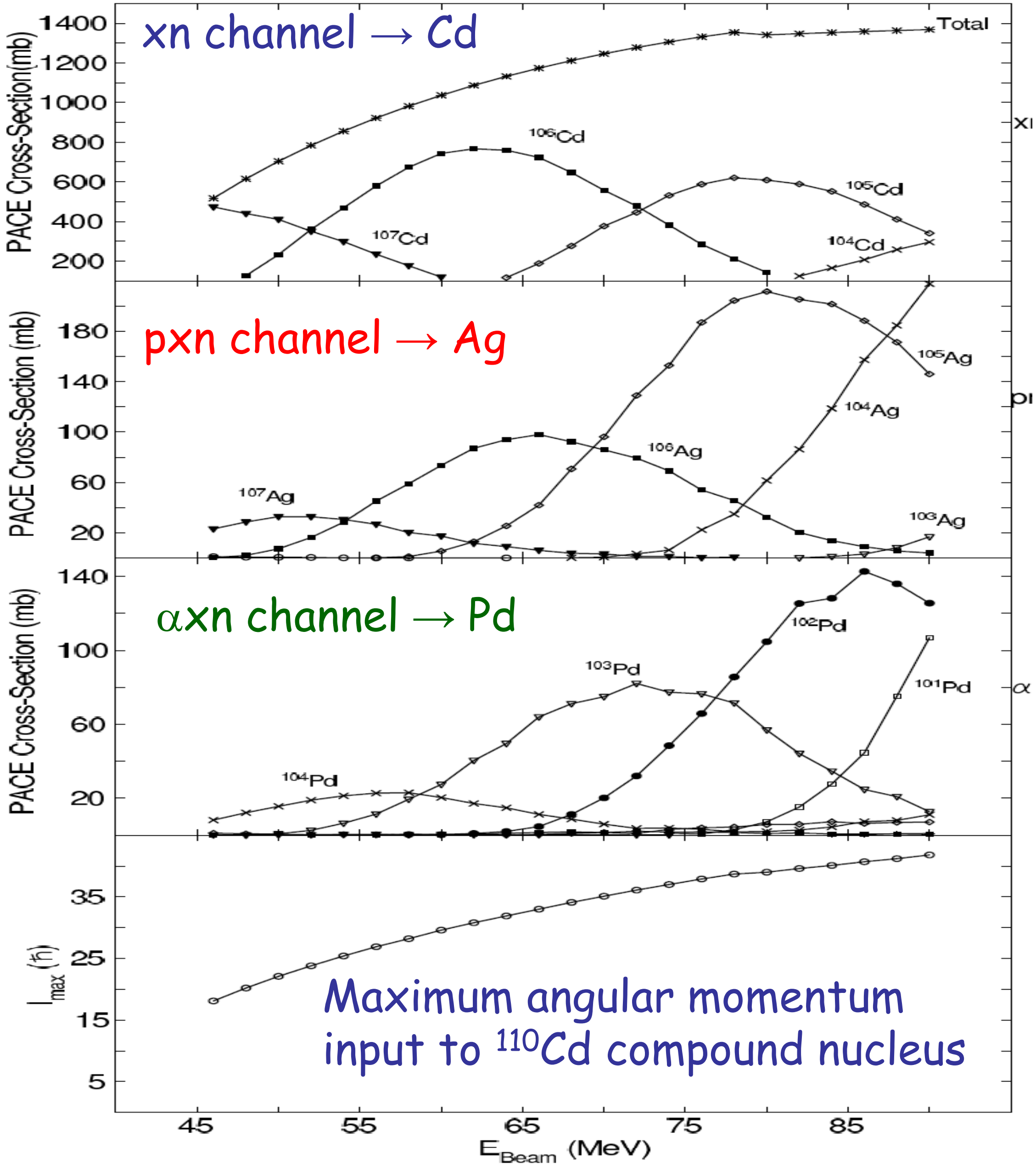

Increasing the beam energy increases the maximum input angular momentum,

but

Causes more nucleons to be evaporated (on average).

Also, increasing the beam energy increases the recoil velocity.

For the ^{110}Cd compound nucleus:
S_n = 9.9 MeV
S_p = 8.9 MeV

Coulomb barrier means neutron evaporation is much favoured.

Very neutron-deficient (compound) nuclei, e.g. ^{136}Gd, S_p= 2.15 MeV, S_n=12.94 MeV

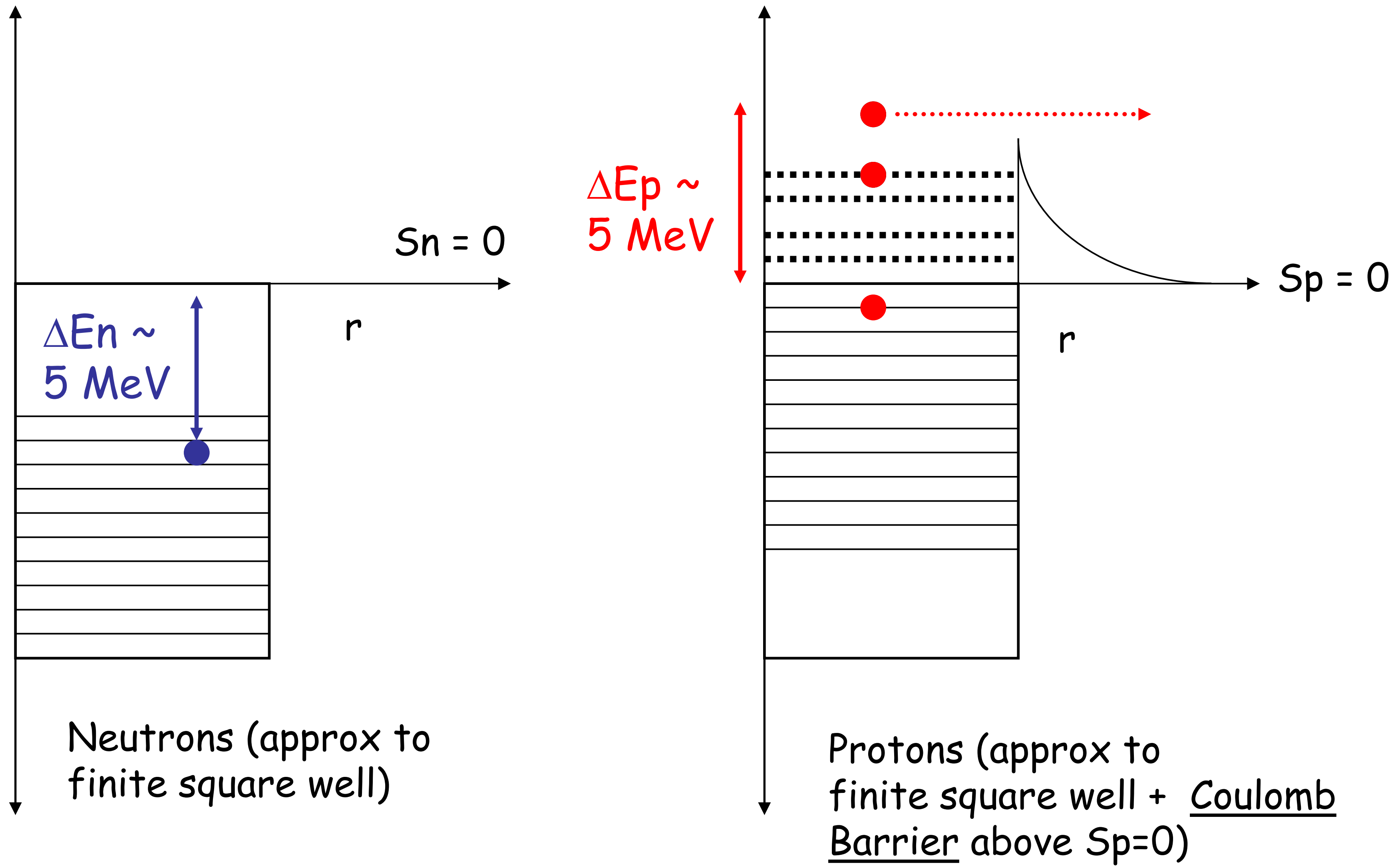

Excitation Functions?

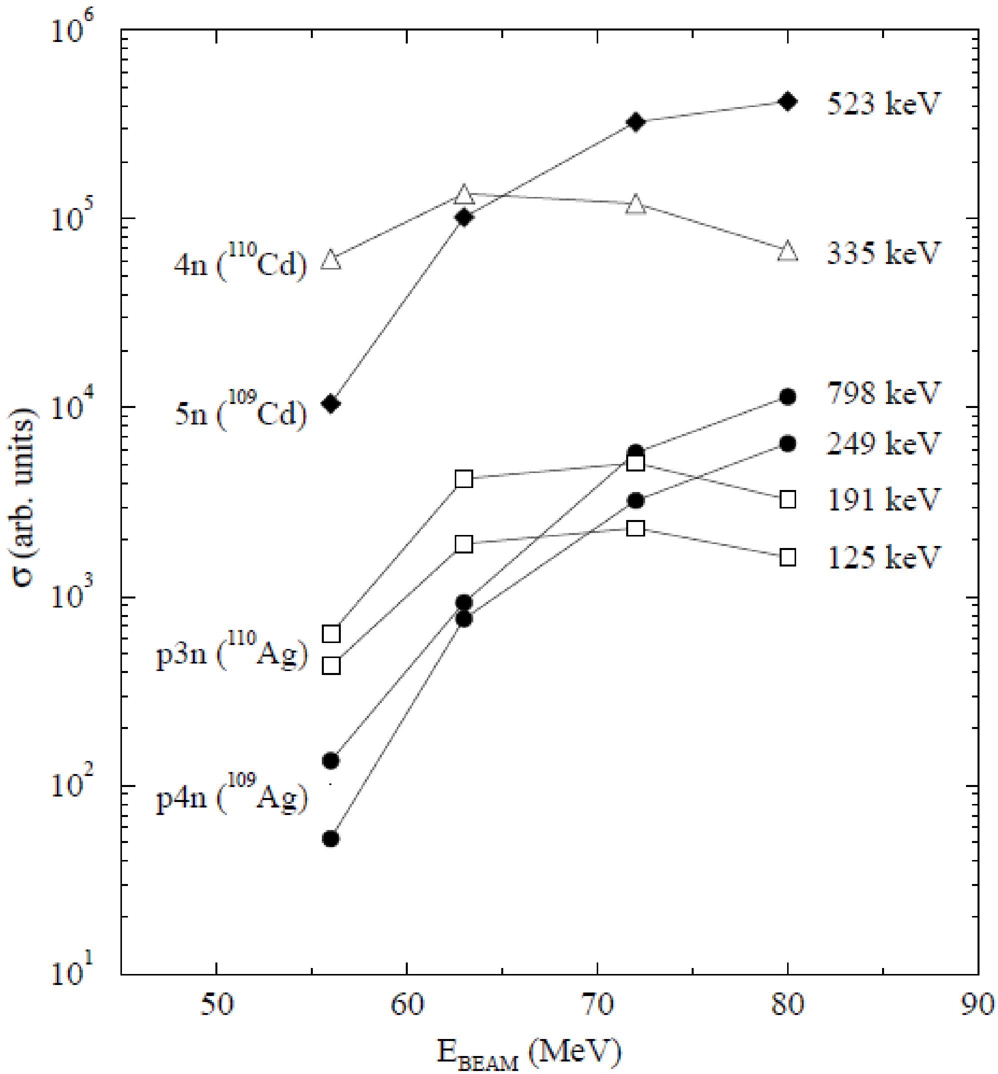

Excitation function for various products of the reaction $^{18}O+^{96}Zr$

P.H. Regan et al., Phys. Rev. **C49** (1994) 1885

Basic EM Selection Rules?

$$|I_i + I_f| \geq L \geq |I_i - I_f|$$

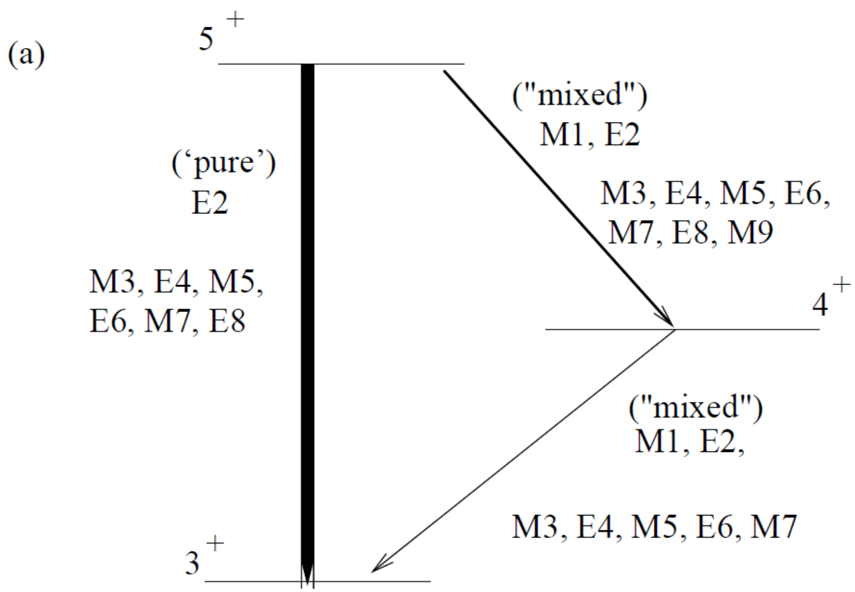

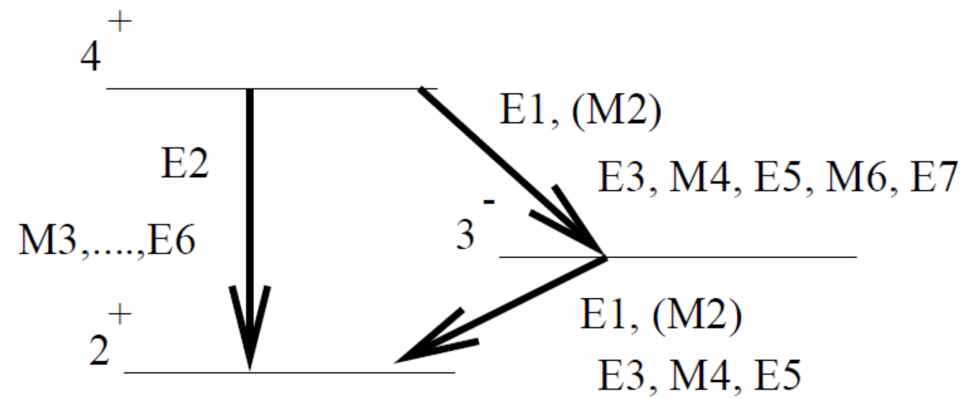

The transition probability for a state decaying from state J_i to state J_f, separated by energy E_γ, by a transition of multipole order L is given by [1, 7]

$$T_{fi}(\lambda L) = \frac{8\pi(L+1)}{\hbar L\left((2L+1)!!\right)^2}\left(\frac{E_\gamma}{\hbar c}\right)^{2L+1} B(\lambda L : J_i \rightarrow J_f) \qquad (1.1.2)$$

where $B(\lambda L : J_i \rightarrow J_f)$ is called the *reduced matrix element.*

DCO and DCO Ratios

JULY 15, 1940 PHYSICAL REVIEW VOLUME 58

On Directional Correlation of Successive Quanta

DONALD R. HAMILTON*
Harvard University, Cambridge, Massachusetts

(Received May 6, 1940)

A theoretical investigation shows that there should be a correlation between the directions of propagation of the quanta emitted in two successive transitions of a single radiating system. This correlation is described by a function $W(\theta)$ which gives the relative probability that the second quantum will be emitted at an angle θ with the first; W is determined by the angular momenta of the three levels involved in the two transitions and by the multipole order of the radiation emitted in these transitions. The explicit forms of W for all angular momenta and for dipole and quadrupole radiation are given; experimental determination of W in any given case should limit these factors to a small number of possibilities. This has particular interest as a means of investigating the nuclear energy levels involved in γ-radiation; here W should be observable by measuring the variation with θ of gamma-gamma coincidence counting rates.

$$w(\theta) = a_0 + a_2 \cos^2\theta + a_4 \cos^4\theta$$

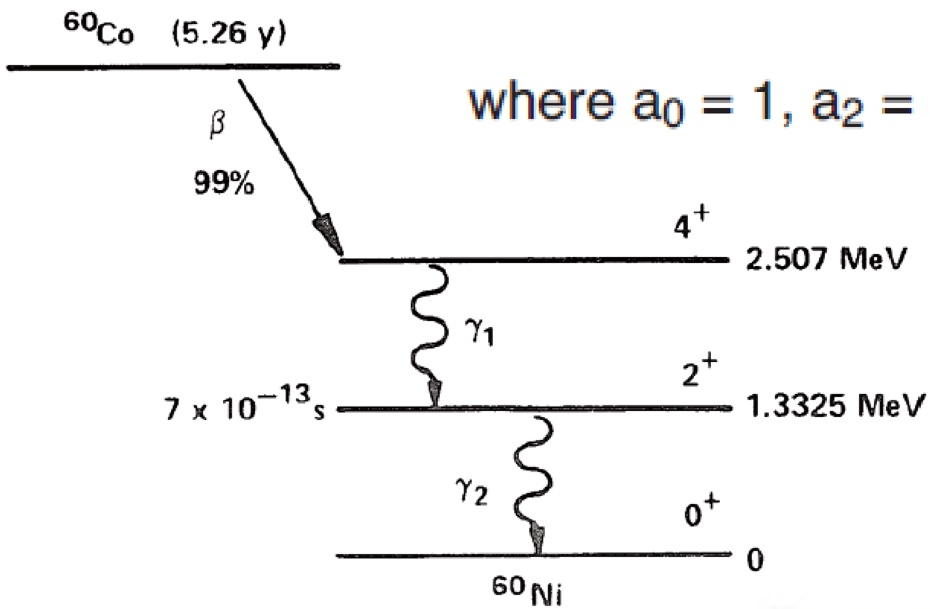

where $a_0 = 1$, $a_2 = 1/8$, and $a_4 = 1/24$.

$$G(\theta) = \frac{w(\theta)}{w(90°)}$$

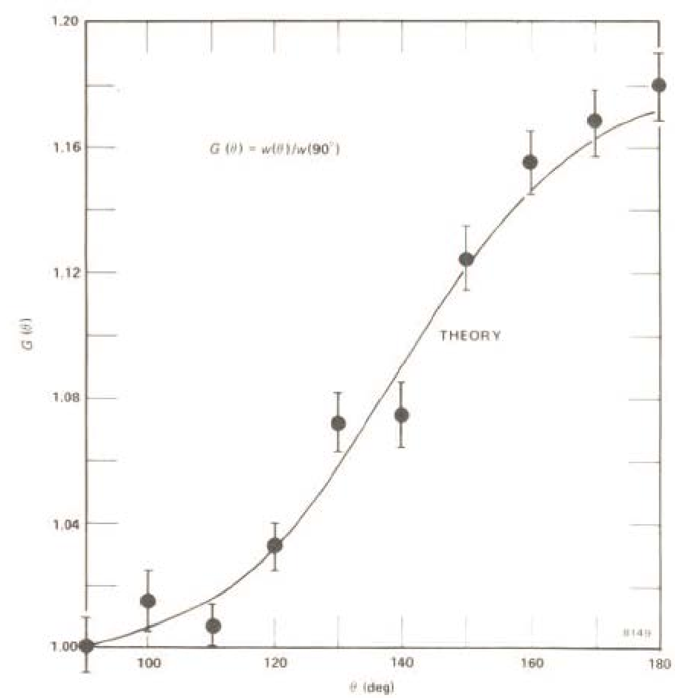

Dropping a constant factor, our correlation function for calculation is

$$\mathbf{W}(\theta)=1+(\mathbf{R}/\mathbf{Q})\cos^2\theta+(\mathbf{S}/\mathbf{Q})\cos^4\theta.$$

TABLE I. *R/Q, for both transitions dipole.*

	$\Delta J=-1$	$\Delta J=0$	$\Delta J=1$
$\Delta j=-1$	$\frac{1}{13}$	$\frac{-(2J-1)}{(14J+13)}$	$\frac{J(2J-1)}{(26J^2+67J+40)}$
$\Delta j=0$	$\frac{-(2J+3)}{(14J+1)}$	$\frac{(2J-1)(2J+3)}{(12J^2+12J+1)}$	
$\Delta j=1$	$\frac{(J+1)(2J+3)}{(26J^2-15J-1)}$		

TABLE II. *R/Q, for first transition quadrupole, second dipole.*

	$\Delta J=1$	$\Delta J=0$	$\Delta J=-1$
$\Delta j=2$	$\frac{-3}{29}$	$\frac{3(2J+3)}{(26J-3)}$	$\frac{-3(J+1)(2J+3)}{(58J^2-23J+3)}$
$\Delta j=1$	$\frac{3(J-5)}{(55J+61)}$	$\frac{-3(2J+3)(J-5)}{(58J^2+49J-15)}$	$\frac{3(2J+3)(J-5)}{(110J^2-49J+15)}$
$\Delta j=0$	$\frac{(2J-3)(2J+5)}{(36J^2+92J+61)}$	$\frac{-(2J-3)(2J+5)}{5(4J^2+4J-1)}$	$\frac{(2J-3)(2J+5)}{(36J^2-20J+5)}$
$\Delta j=-1$	$\frac{3(2J-1)(J+6)}{(110J^2+269J+174)}$	$\frac{-3(2J-1)(J+6)}{(58J^2+67J-6)}$	$\frac{3(J+6)}{(55J-6)}$
$\Delta j=-2$	$\frac{-3J(2J-1)}{(58J^2+139J+84)}$	$\frac{3(2J-1)}{(26J+29)}$	$\frac{-3}{29}$

Dropping a constant factor, our correlation function for calculation is

$$W(\theta)=1+(R/O)\cos^2\theta+(S/O)\cos^4\theta.$$

TABLE III. R/Q, *for both transitions quadrupole.*

	$\Delta J=0$	$\Delta J=-1$	$\Delta J=-2$
$\Delta j=-2$	$\frac{-(2J-3)(2J+1)}{(2J+3)(6J+5)}$	$\frac{(J+3)}{(17J+15)}$	$\frac{1}{8}$
$\Delta j=-1$	$\frac{(5J-2)(2J-3)(2J+5)}{(20J^3+52J^2+41J+6)}$	$\frac{-(17J^2+17J-30)}{(35J^2+35J+6)}$	$\frac{(J-2)}{(17J+2)}$
$\Delta j=0$	$\frac{-(2J-3)(4J^2+4J-7)(2J+5)}{(2J-1)(2J+3)(4J^2+4J-1)}$	$\frac{(5J+7)(2J-3)(2J+5)}{(20J^3+8J^2-3J+3)}$	$\frac{-(2J+1)(2J+5)}{(2J-1)(6J+1)}$
$\Delta j=1$		$\frac{-(2J+3)(17J^3+69J^2-77J-105)}{(70J^4-9J^3-73J^2-27J-9)}$	$\frac{(2J+3)(J^2+18J+5)}{(34J^3-57J^2+8J+3)}$
$\Delta j=2$			$\frac{(J+1)(2J+3)(2J^2-9J+1)}{(2J-1)(16J^3-42J^2+29J+3)}$

	$\Delta J=2$	$\Delta J=1$
$\Delta j=-2$	$\frac{J(2J-1)(2J^2+13J+12)}{(2J+3)(16J^3+90J^2+161J+84)}$	$\frac{(2J-1)(J^2-16J-12)}{(34J^3+159J^2+224J+96)}$
$\Delta j=-1$		$\frac{-(2J-1)(17J^3-18J^2-164J-24)}{(70J^4+289J^3+374J^2+188J+24)}$

TABLE IV. S/Q, *for both transitions quadrupole.*

	$\Delta J=0$	$\Delta J=-1$	$\Delta J=-2$
$\Delta j=-2$	$\frac{4(J-1)(2J-3)}{3(2J+3)(6J+5)}$	$\frac{-4(2J-3)}{3(17J+15)}$	$\frac{1}{24}$
$\Delta j=-1$	$\frac{-16(J-1)(2J-3)(2J+5)}{3(20J^3+52J^2+41J+6)}$	$\frac{16(2J-3)(2J+5)}{3(35J^2+35J+6)}$	$\frac{-4(2J+5)}{3(17J+2)}$
$\Delta j=0$	$\frac{16(J-1)(J+2)(2J-3)(2J+5)}{3(2J-1)(2J+3)(4J^2+4J-1)}$	$\frac{-16(J+2)(2J-3)(2J+5)}{3(20J^3+8J^2-3J+3)}$	$\frac{4(J+2)(2J+5)}{3(2J-1)(6J+1)}$
$\Delta j=1$		$\frac{16(2J-3)(2J+3)(J+2)(2J+5)}{3(70J^4-9J^3-73J^2-27J-9)}$	$\frac{-4(2J+3)(J+2)(2J+5)}{3(34J^3-57J^2+8J+3)}$
$\Delta j=2$			$\frac{(J+1)(2J+3)(J+2)(2J+5)}{3(2J-1)(16J^3-42J^2+29J+3)}$

	$\Delta J=2$	$\Delta J=1$
$\Delta j=-2$	$\frac{J(2J-1)(J-1)(2J-3)}{3(2J+3)(16J^3+90J^2+161J+84)}$	$\frac{-4(2J-1)(J-1)(2J-3)}{3(34J^3+159J^2+224J+96)}$
$\Delta j=-1$		$\frac{16(2J-1)(J-1)(2J-3)(2J+5)}{3(70J^4+289J^3+374J^2+188J+24)}$

JULY 15, 1940 PHYSICAL REVIEW VOLUME 58

On Directional Correlation of Successive Quanta

DONALD R. HAMILTON*
Harvard University, Cambridge, Massachusetts
(Received May 6, 1940)

First real ‘evidence’ of angular correlations between successive gamma rays;

Radioactive decays of

^{60}Co ($I^{\pi}=5^{+}$, $T_{1/2}=5.27$ yrs to ^{60}Ni)
^{46}Sc ($I^{\pi}=4^{+}$, $T_{1/2}=84$ days to 46Ti)
^{88}Y ($I^{\pi}=4-$, $T^{1/2}=107$ days to ^{88}Sr)
^{134}Cs ($I^{\pi}=4^{+}$, $T_{1/2}=2.1$ yrs to ^{134}Ba).

(note, says ^{86}Y in paper, means ^{88}Y)

Angular Correlation of Successive Gamma-Ray Quanta

EDWARD L. BRADY AND MARTIN DEUTSCH
Massachusetts Institute of Technology, Cambridge, Massachusetts
September 10, 1947

THEORETICAL considerations[1,2] predict a directional correlation of successive quanta of the form

$$W(\theta)=1+\sum_{i=1}^{l} A_i \cos^{2i}\theta$$

if $2l$ is the highest multipole order occurring. Attempts to demonstrate this effect experimentally have heretofore been inconclusive.[3] We have studied coincidences between successive gamma-rays of Co^{60}, Sc^{46}, Y^{86} (106 day), and Cs^{134} at angles 180° and 90° between the counters, and found a pronounced anisotropy in the first two named and no correlation within the experimental error in the last two. Our results, together with the gamma-ray energies concerned, are shown in Table I. The quantity $(W(\pi)$

TABLE I. Anisotropy of gamma-ray coincidences.

Source	Co^{60}	Sc^{46}	Y^{86}	Cs^{134}
ϵ	0.21 ± 0.025	0.20 ± 0.035	-0.05 ± 0.03	0.01 ± 0.04
Gamma-rays Mev	1.1, 1.3	0.89, 1.12	0.91, 1.89	0.58, 0.78
Reference	4	5	6	7

$-W(\pi/2))/W(\pi/2)$ should be equal to ΣA_i. Our results

The probability, per unit solid angle, that two successive gamma-rays are emitted at an angle θ is proportional to

$$W(\theta) = 1 + \sum_{1}^{l} a_i \cos^{2i}\theta$$

where $2l$ is the order of the lowest multipole in the cascade. Thus, if both gamma-rays are quadrupoles $W(\theta) = 1 + a_1 \cos^2\theta + a_2 \cos^4\theta$. If one is a dipole $W(\theta) = 1 + a_1 \cos^2\theta$, etc. A further restriction on the number of terms in $W(\theta)$ is $a_i = 0$ for $i > J_2$. J_2 is the spin of the intermediate state in the cascade. Thus if J_2 is zero or $\frac{1}{2}$, the angular correlation will always be isotropic; if J_2 is 1 or $\frac{3}{2}$, the correlation will at most contain terms in $\cos^2\theta$. The coefficients a_1 and a_2 have been given by Hamilton[2] for all possible combinations of angular momenta. In Table I we have listed the values of these coefficients from Hamilton's paper for the values of J which are of interest in connection with our experiments. Coefficients for octupole radiation should be very useful, but have not yet been published. If the transition involves mixed multipoles, e.g., electric quadrupole and magnetic dipole components, the situation becomes very complicated and the coefficients depend not only on the relative intensities of the two components but also on their relative phases.[5]

PHYSICAL REVIEW VOLUME 78, NUMBER 5 JUNE 1, 1950

Angular Correlation of Successive Gamma-Rays*

E. L. Brady† and M. Deutsch
Laboratory for Nuclear Science and Engineering, Department of Physics and Chemistry Department, Massachusetts Institute of Technology, Cambridge, Massachusetts

(Received February 6, 1950)

The angular correlation of successive gamma-rays emitted by six even-even nuclei has been investigated and found to be anisotropic in every case, and of the magnitude expected theoretically. Effects of external magnetic fields and of chemical binding on the correlations are found to be smaller than the experimental uncertainty for some exploratory experiments. Interpretation of the results in terms of the nuclear states involved is in general possible by use of additional evidence such as relative transition probabilities.

Table I. Coefficients for the angular correlation with the spin of the ground state $J_1 = 0$.

J_2	J_3	Multipoles	a_1	a_2
1	0	Dipole–Dipole	1	0
1	1	Dipole–Dipole	−1/3	0
1	2	Dipole–Dipole	−1/3	0
1	1	Quadrupole–Dipole	−1/3	0
1	2	Quadrupole–Dipole	3/7	0
1	3	Quadrupole–Dipole	−3/29	0
2	3	Dipole–Quadrupole	−3/29	0
2	2	Dipole–Quadrupole	3/7	0
2	1	Dipole–Quadrupole	−1/3	0
2	0	Quadrupole–Quadrupole	−3	4
2	1	Quadrupole–Quadrupole	5	−16/3
2	2	Quadrupole–Quadrupole	−15/13	16/13
2	3	Quadrupole–Quadrupole	0	−1/3
2	4	Quadrupole–Quadrupole	1/8	1/24

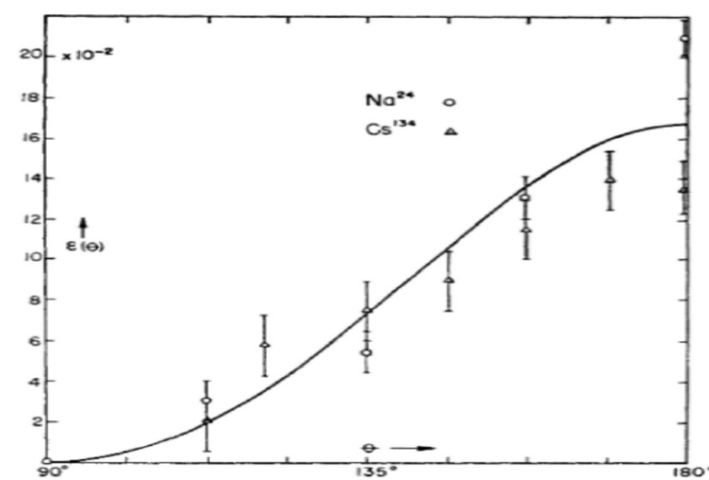

Fig. 4. Correlation of gamma-rays from Cs^{134} and Na^{24}.

PHYSICAL REVIEW C **93**, 024301 (2016)

High-precision γ-ray spectroscopy of the cardiac PET imaging isotope ^{82}Rb and its impact on dosimetry

M. N. Nino,[1] E. A. McCutchan,[2] S. V. Smith,[3] C. J. Lister,[4] J. P. Greene,[5] M. P. Carpenter,[5] L. Muench,[3] A. A. Sonzogni,[2] and S. Zhu[5]
[1]*Department of Physics and Astronomy, Hofstra University, Hempstead, New York 11549, USA*
[2]*National Nuclear Data Center, Brookhaven National Laboratory, Upton, New York 11973, USA*
[3]*Collider Accelerator Department, Brookhaven National Laboratory, Upton, New York 11973, USA*
[4]*Department of Physics and Applied Physics, University of Massachusetts Lowell, Lowell, Massachusetts 01854, USA*
[5]*Physics Division, Argonne National Laboratory, Argonne, Illinois 60439, USA*
(Received 2 October 2015; revised manuscript received 21 December 2015; published 1 February 2016)

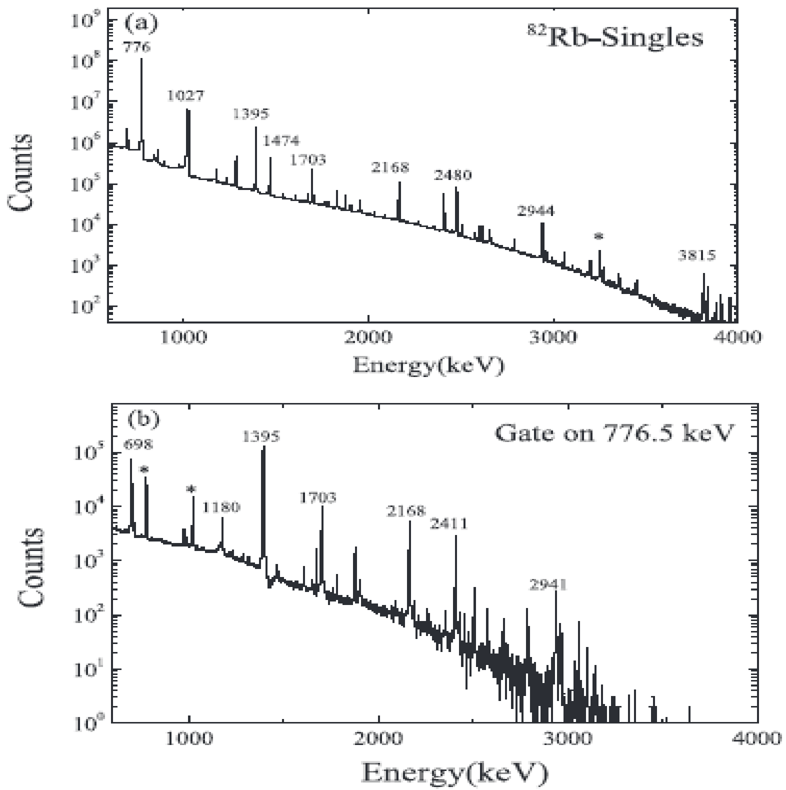

FIG. 1. (a) Singles spectrum from the decay of ^{82}Rb. (b) Spectrum obtained by gating on the 776-keV transition in ^{82}Kr. In both panels, strong transitions belonging to the decay of ^{82}Rb are labeled by their energy in keV, while background lines are indicated with a *.

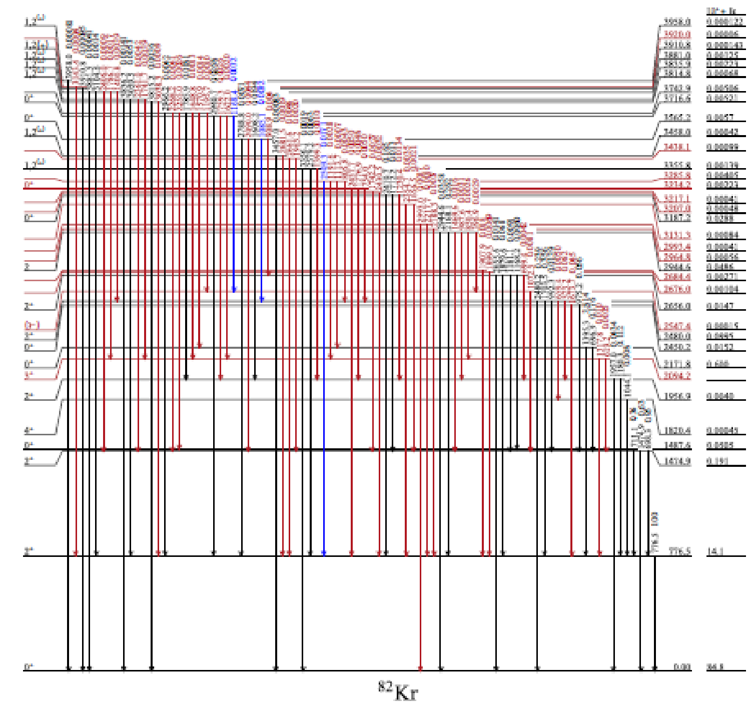

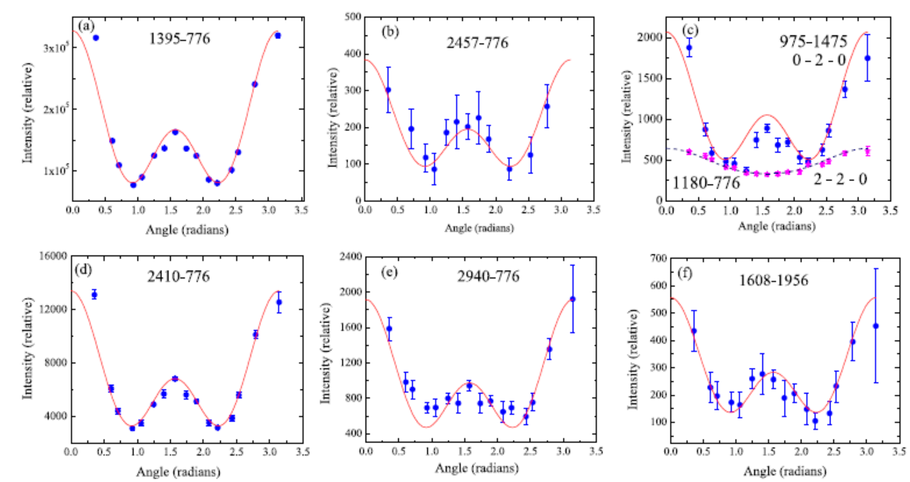

FIG. 6. Angular correlation analysis of confirmed and newly identified $0^+ \rightarrow 2^+ \rightarrow 0^+$ cascade transitions in ^{82}Kr. Solid circles give the measured intensity as a function of angle between detectors while solid lines are the theoretical predictions for a 0-2-0 sequence. Numbers in each panel give the cascade energies, in keV. In panel (c), the angular correlation of the 1180-776.5 cascade (stars) is given along with the theoretical predictions for a 2-2-0 sequence with $\delta = -0.52$ (dotted line).

Reaction mechanism itself can provide alignment of angular Momentum sub-states.

Should see angular DISTRIBUTIONS following Fusion-evaporation reactions.

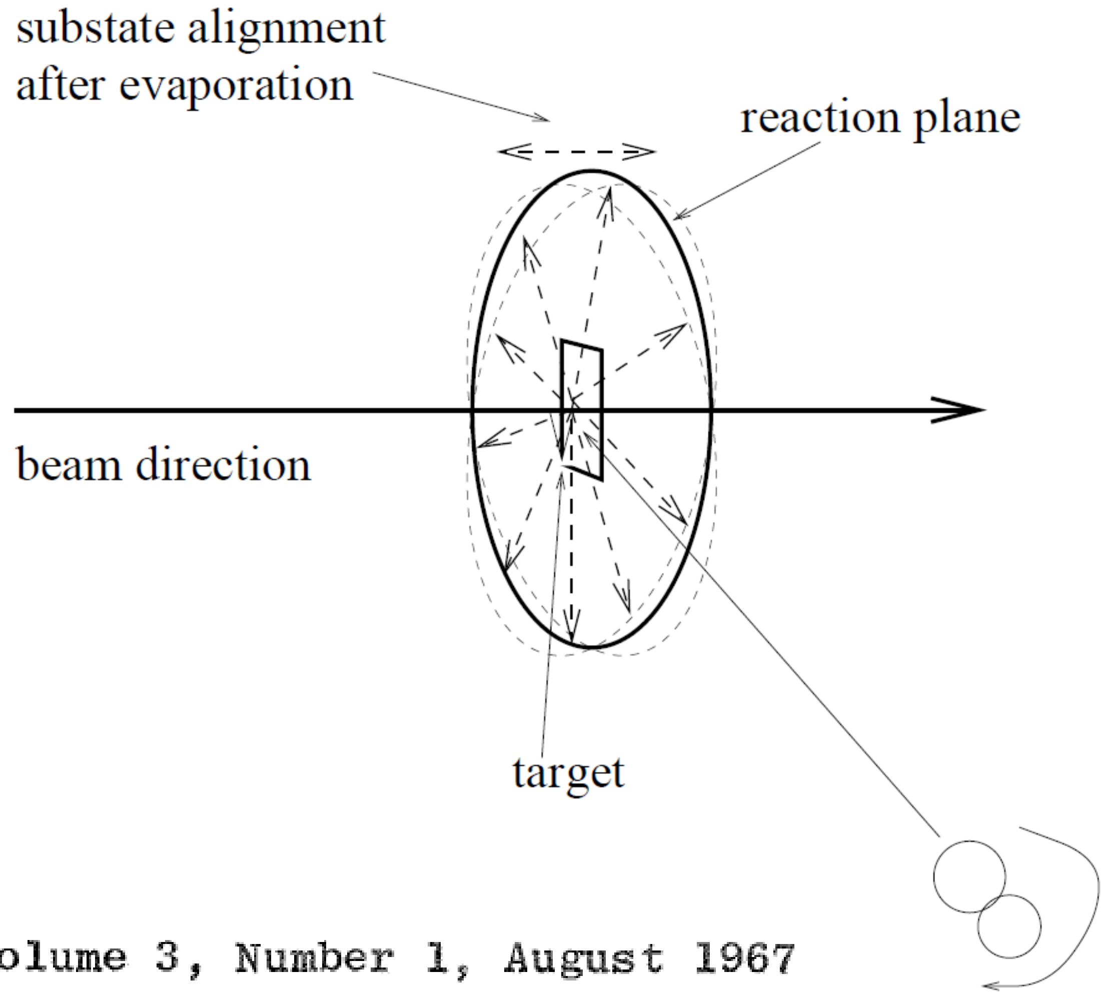

NUCLEAR DATA, Section A, Volume 3, Number 1, August 1967

TABLES OF COEFFICIENTS FOR ANGULAR DISTRIBUTION OF GAMMA RAYS FROM ALIGNED NUCLEI *

T. YAMAZAKI

Lawrence Radiation Laboratory,
University of California, Berkeley, California

$$W(\theta) = \sum_k A_k P_k(\cos\theta)$$

For $\Delta I=2$ EM transitions, the singles angular distribution is of the form:

$$W(\theta) = A_0 \{1 + A_2 P_2(\cos\theta) + A_4 P_4(\cos\theta)\}$$

$$P_2(\cos\theta) = \tfrac{1}{2}(3\cos^2\theta - 1)$$

$$P_4(\cos\theta) = \tfrac{1}{8}(35\cos^4\theta - 30\cos^2\theta + 3)$$

E Der Mateosian and A.W. Sunyar, *Atomic Data and Nuclear Data Tables* **13** (1974) p407

K.S. Krane, R.M. Steffen and R.M. Wheeler, *Nuclear Data Tables* **11** (1973) p351

$$A = 2\left(\frac{W(37^\circ) - W(79^\circ)}{W(37^\circ) + W(79^\circ)}\right)$$

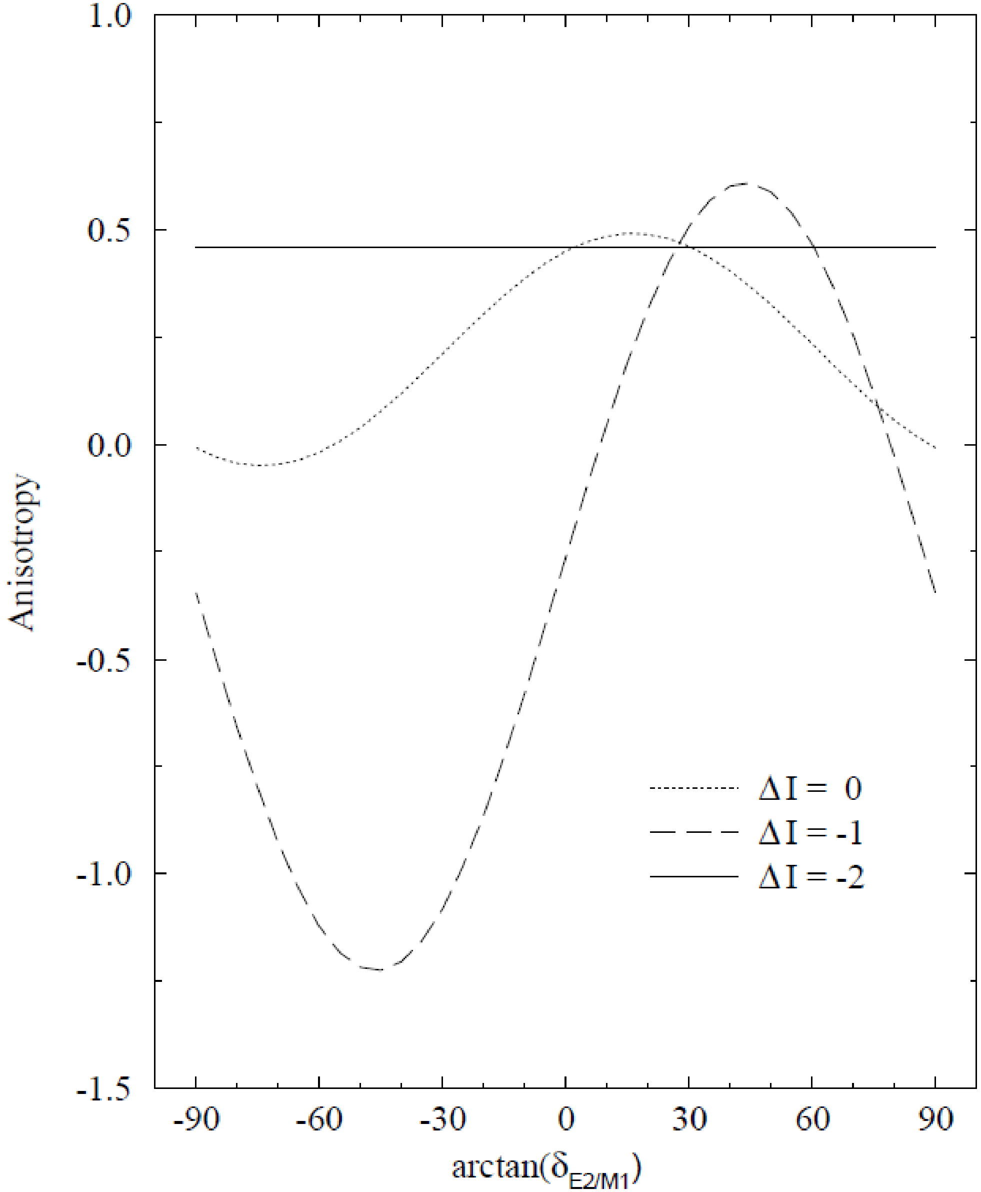

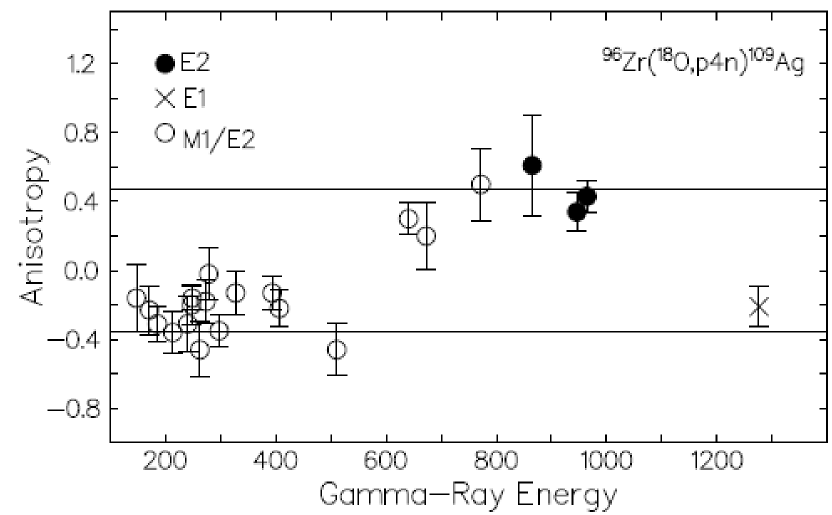

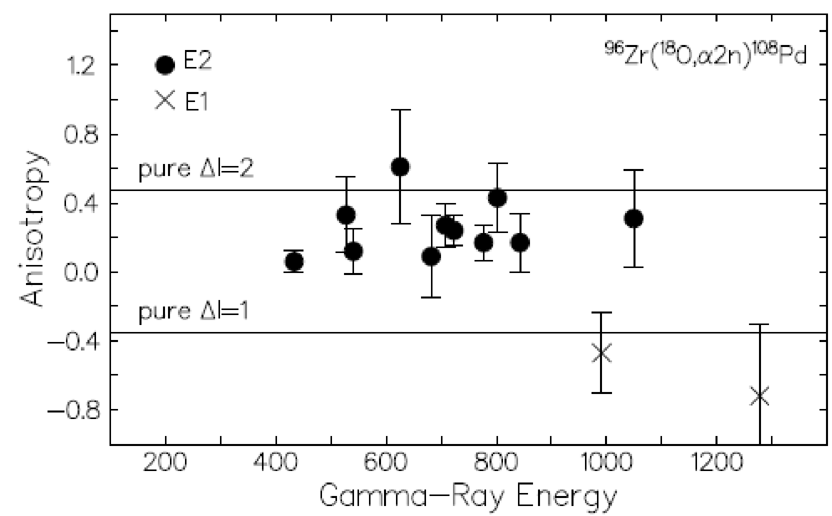

K.R. Pohl *et al. Phys. Rev.* **C53** (1996) p2682

Selection and identification of high-spins states.

- Need a top quality gamma-ray spectrometer to measure full-energies of emitted gamma rays from (high-spin) excited nuclear states.

- Helpful to have some sort of channel selection device (e.g., recoil separator; fragment detector).

- Timing between reaction and detection of gamma ray(s) and also the time differences between individual gamma rays in a decay sequences can also be helpful in channel selection and decay scheme building.

- Use EM selection rules, transition rates and DCO/W(θ) etc. to assign spin and parities to excited states.

Compton Suppression

Gammasphere

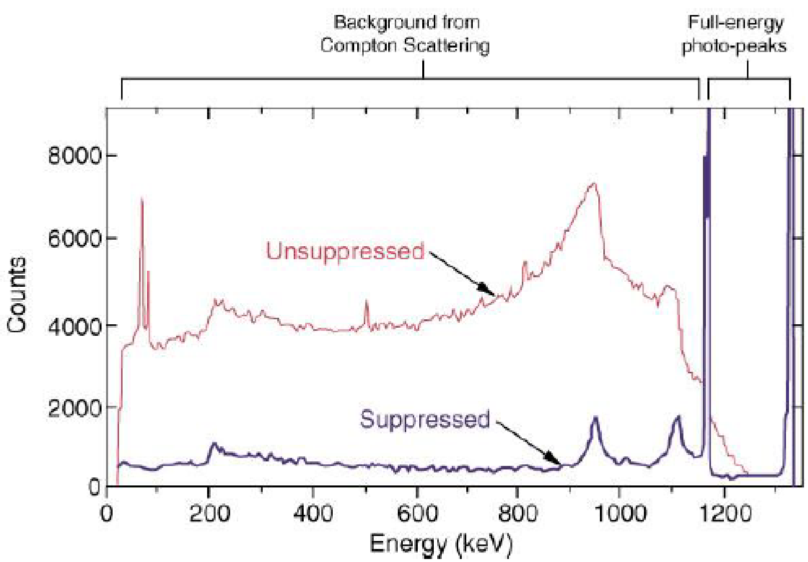

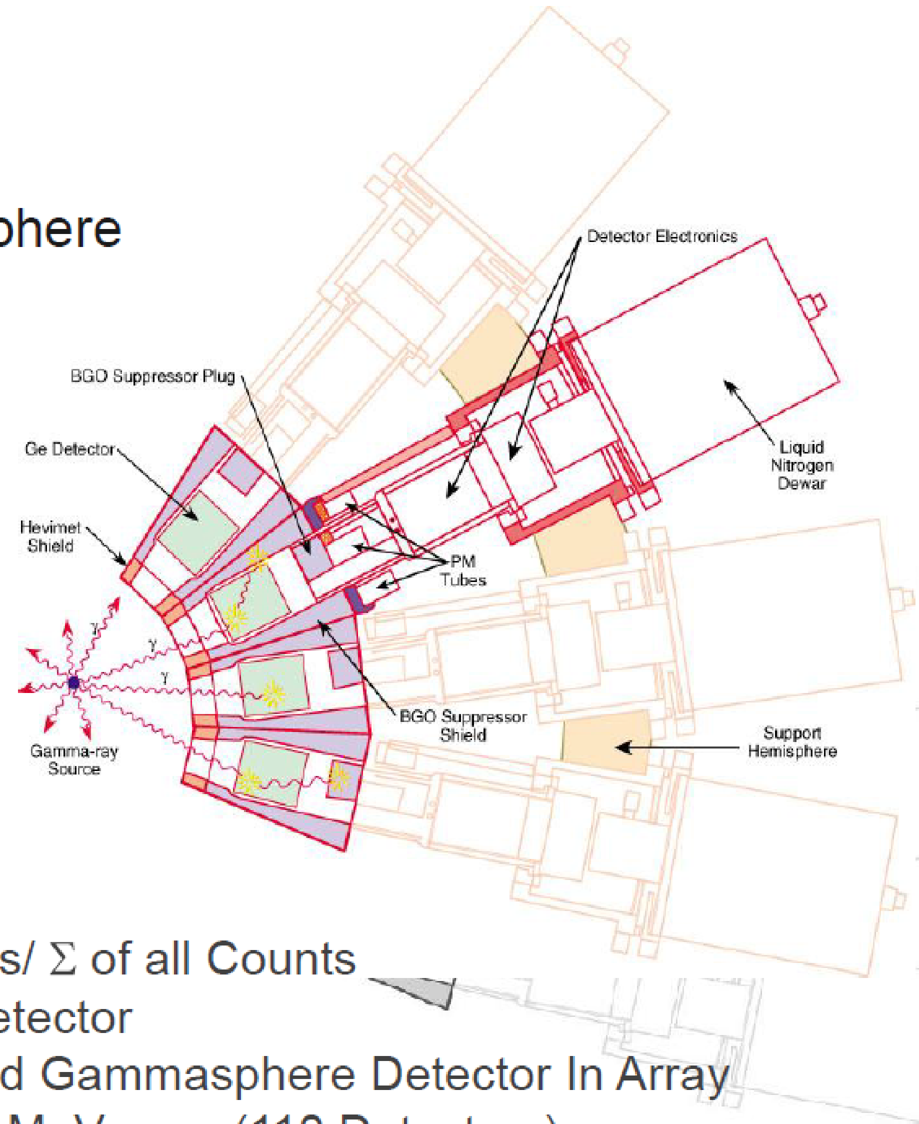

- Peak to Total (P/T) = Σ Photo Peaks/ Σ of all Counts
- P/T ~ 0.20 for 70% Co-axial Ge Detector
- P/T ~ 0.55 for Compton Suppressed Gammasphere Detector In Array
- Photopeak efficiency is ~10% for 1 MeV γ ray (110 Detectors)
- δE = 2.5 keV at 1MeV

Recoil (Mass) Separators

Gas Filled

- Pros: High Efficiency
- Cons: No Mass Resolution
- Examples: RITU (Jyvaskyla), BGS (Berkeley)

Vacuum

- Pros: Mass Resolution
- Conn: Low Efficiency
- Examples: FMA (Argonne), RMS (Oak Ridge)

Using Fragment Mass Analyzer (FMA) for High Spin Studies

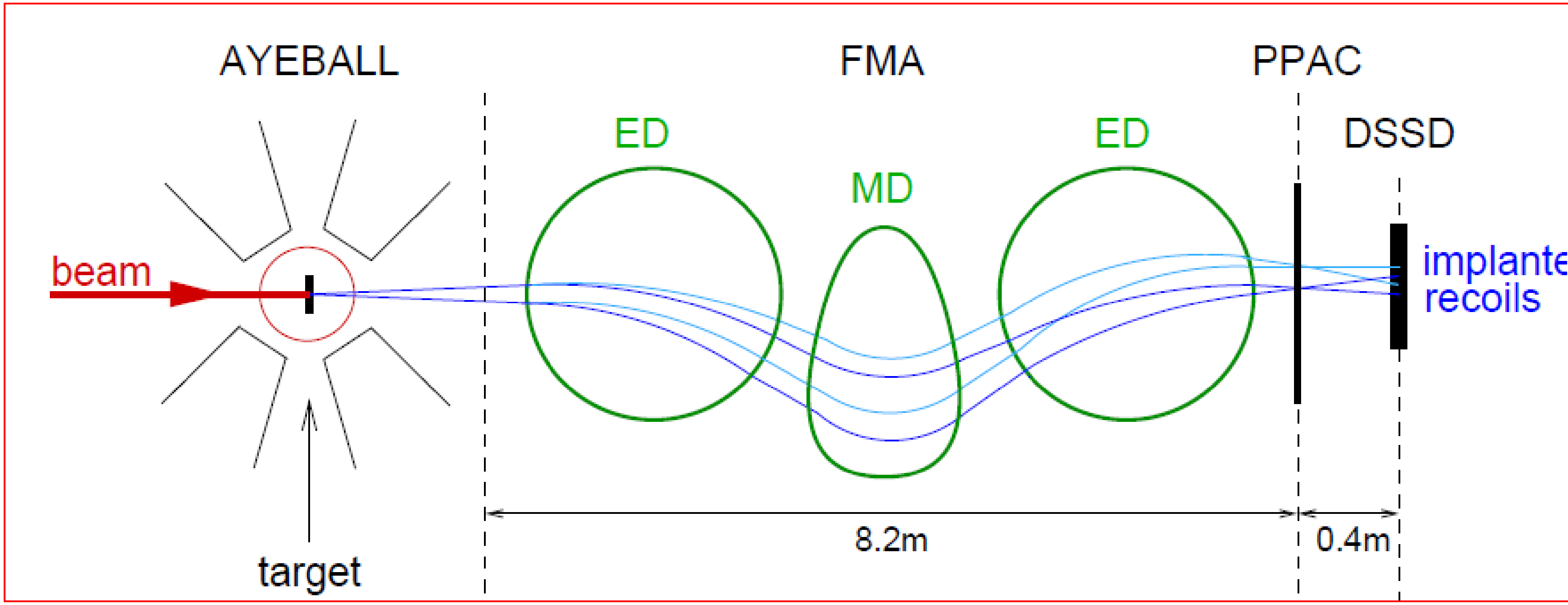

- Separates ions produced at the target position as a function of M/q at the focal plane.
- 8.9 meters long with a +/- 20% energy acceptance.
- Mass resolution is ~ 350:1.
- Multiple detector configurations at focal plane.

PHYSICAL REVIEW C, VOLUME 60, 064308

Near yrast study of the *fpg* shell nuclei ^{58}Ni, ^{61}Cu, and ^{61}Zn

S. M. Vincent,[1,*] P. H. Regan,[1] S. Mohammadi,[1,†] D. Blumenthal,[2] M. Carpenter,[2] C. N. Davids,[2] W. Gelletly,[1] S. S. Ghugre,[3] D. J. Henderson,[2] R. V. F. Janssens,[2] M. Hjorth-Jensen,[4] B. Kharraja,[5] C. J. Lister,[2] C. J. Pearson,[1] D. Seweryniak,[2] J. Schwartz,[2,6] J. Simpson,[7] and D. D. Warner[7]

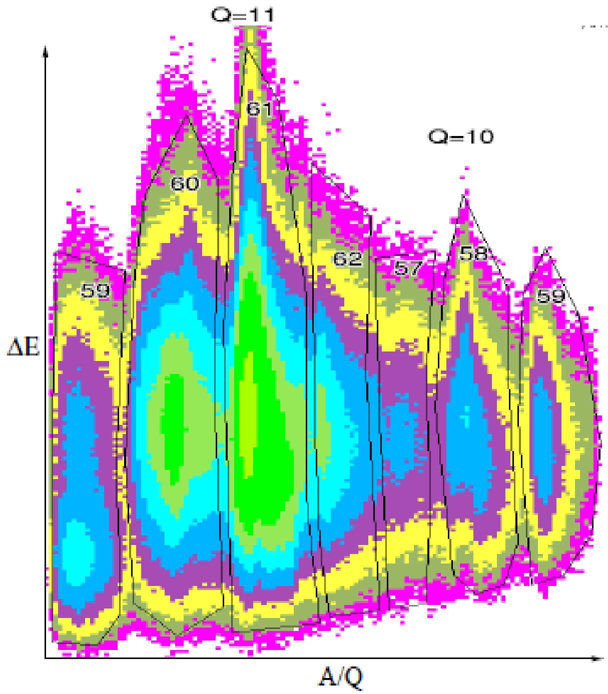

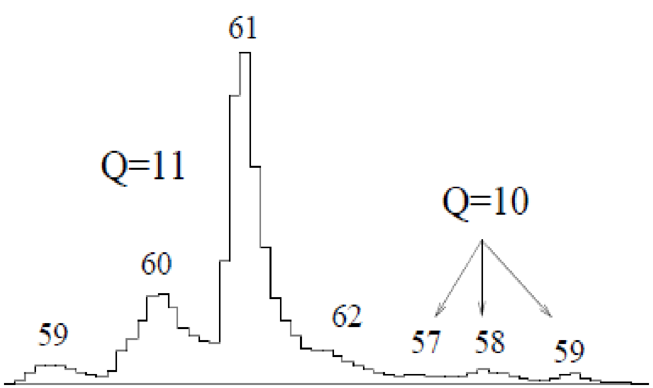

^{24}Mg beam on ^{40}Ca target @65 MeV.

Compound =^{64}Ge
Recoils focussed through Argonne FMA, separated by A/Q.

Observed recoils
2p+^{62}Zn
2pn+^{61}Zn
3p+^{61}Cu
4p+^{60}Ni
3pn+^{60}Cu
α2p+^{58}Ni

and ^{64}Zn ?? (from ^{44}Ca in target).

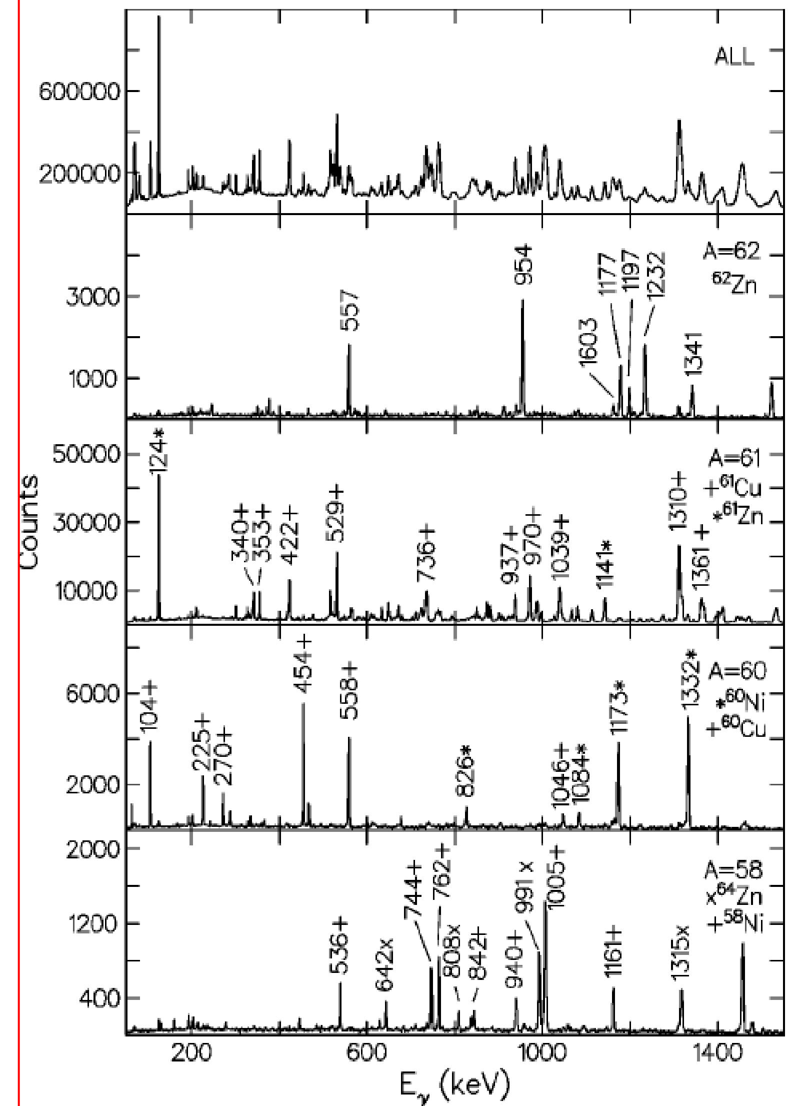

Can be used to select very weak channels (1 part in 10^6 or less);
Good example is SHE studies where most compound nuclei fission.

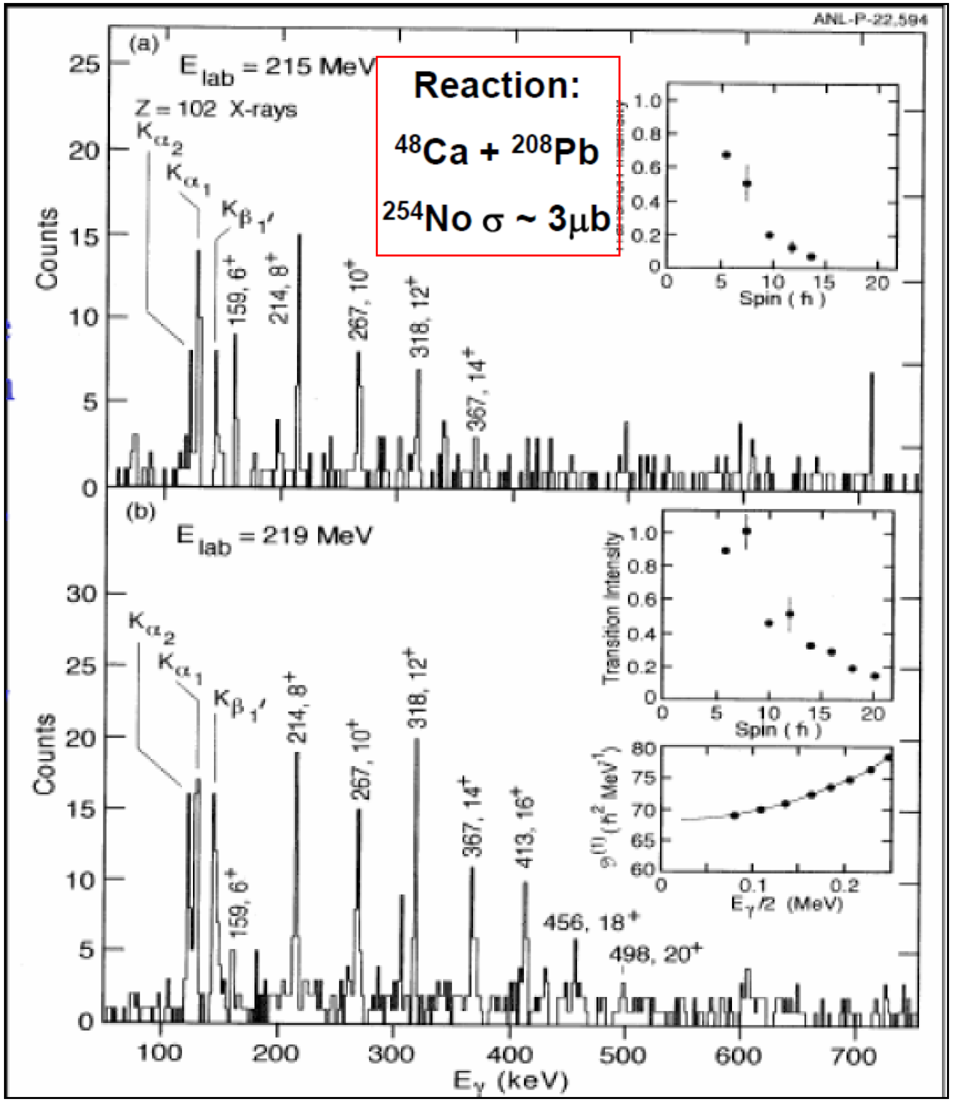

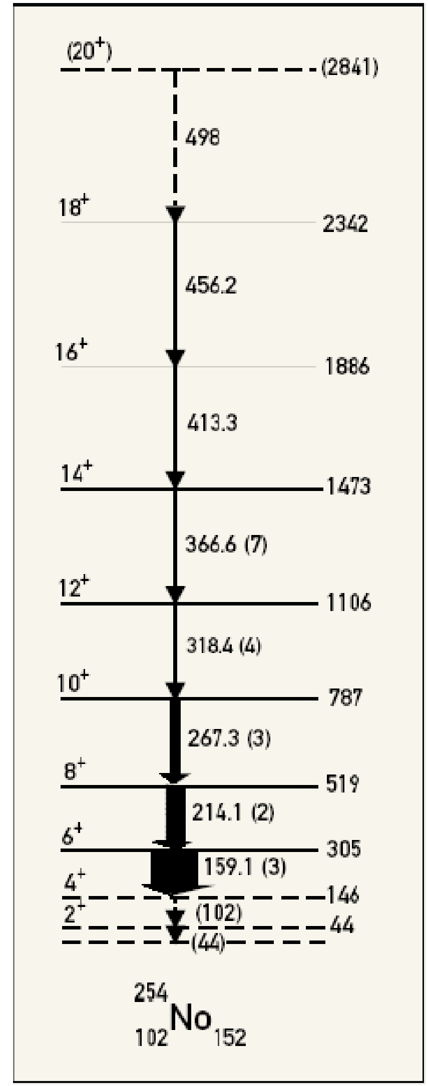

. Reiter *et al*., Phys. Rev. Lett. 82 (1999) 509

Recoil Decay Tagging (Isotopic Identification)

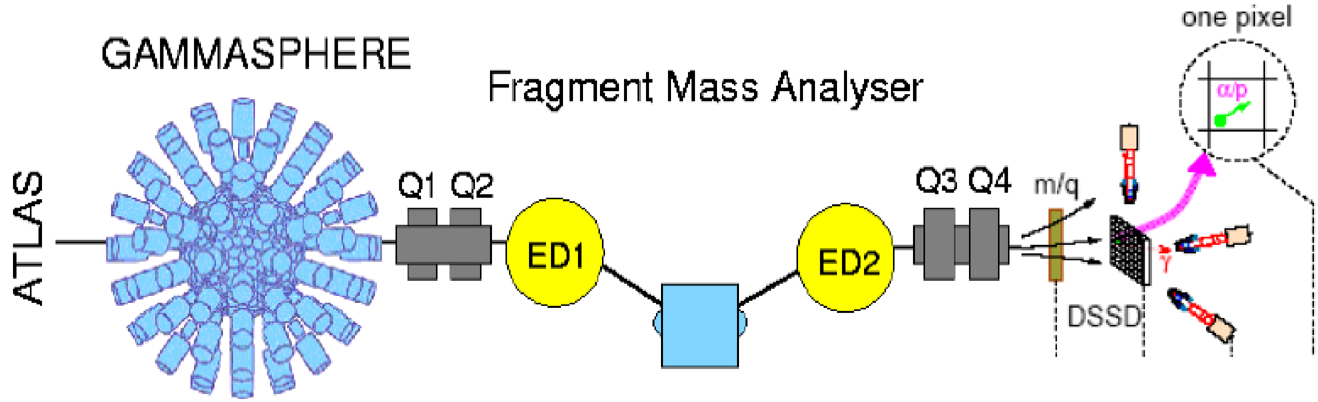

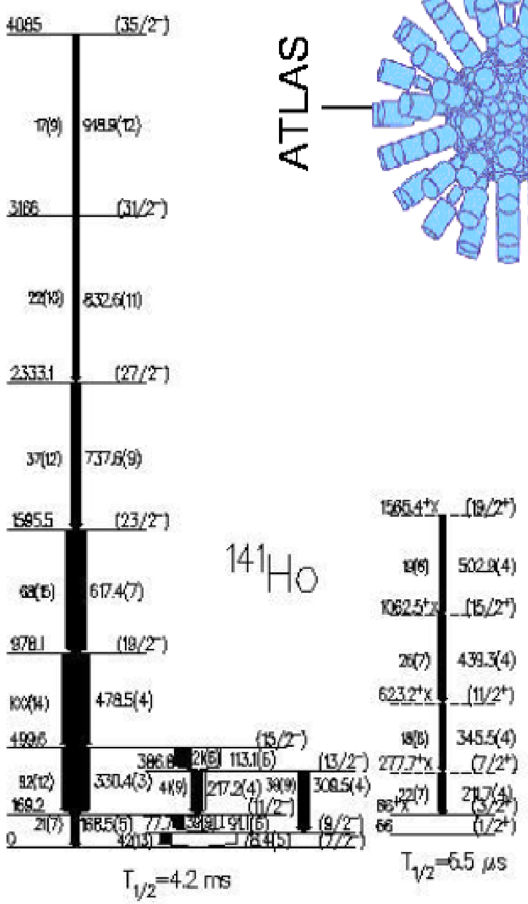

σ=300nb σ=50nb

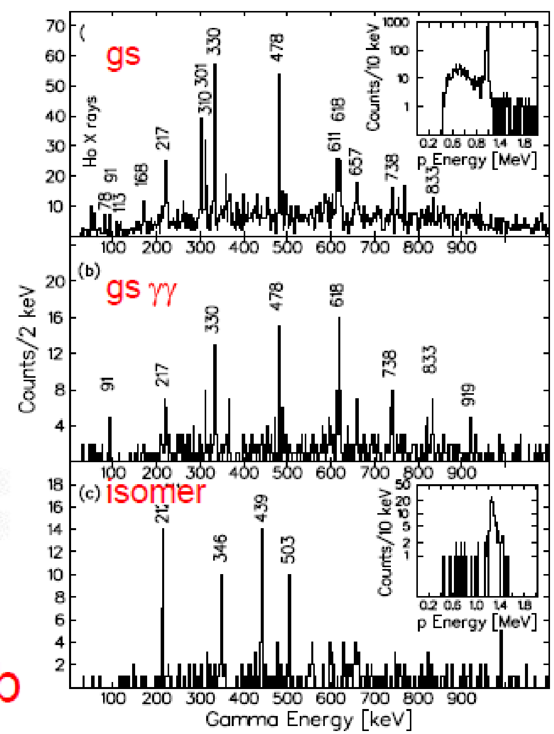

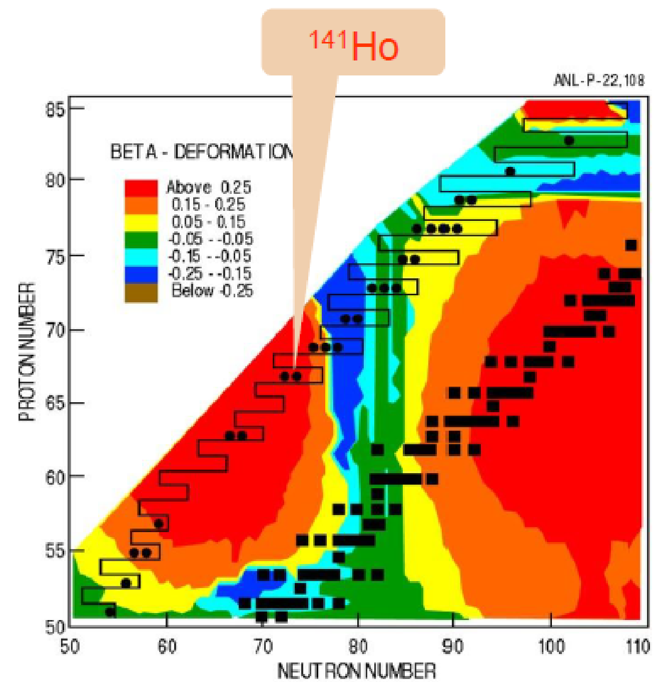

D. Seweryniak *et al.*, PRL 86 (2001) 1458.

Can use 'fine structure' in radioactivity to select decays to specific states (i.e., different single particle configurations).

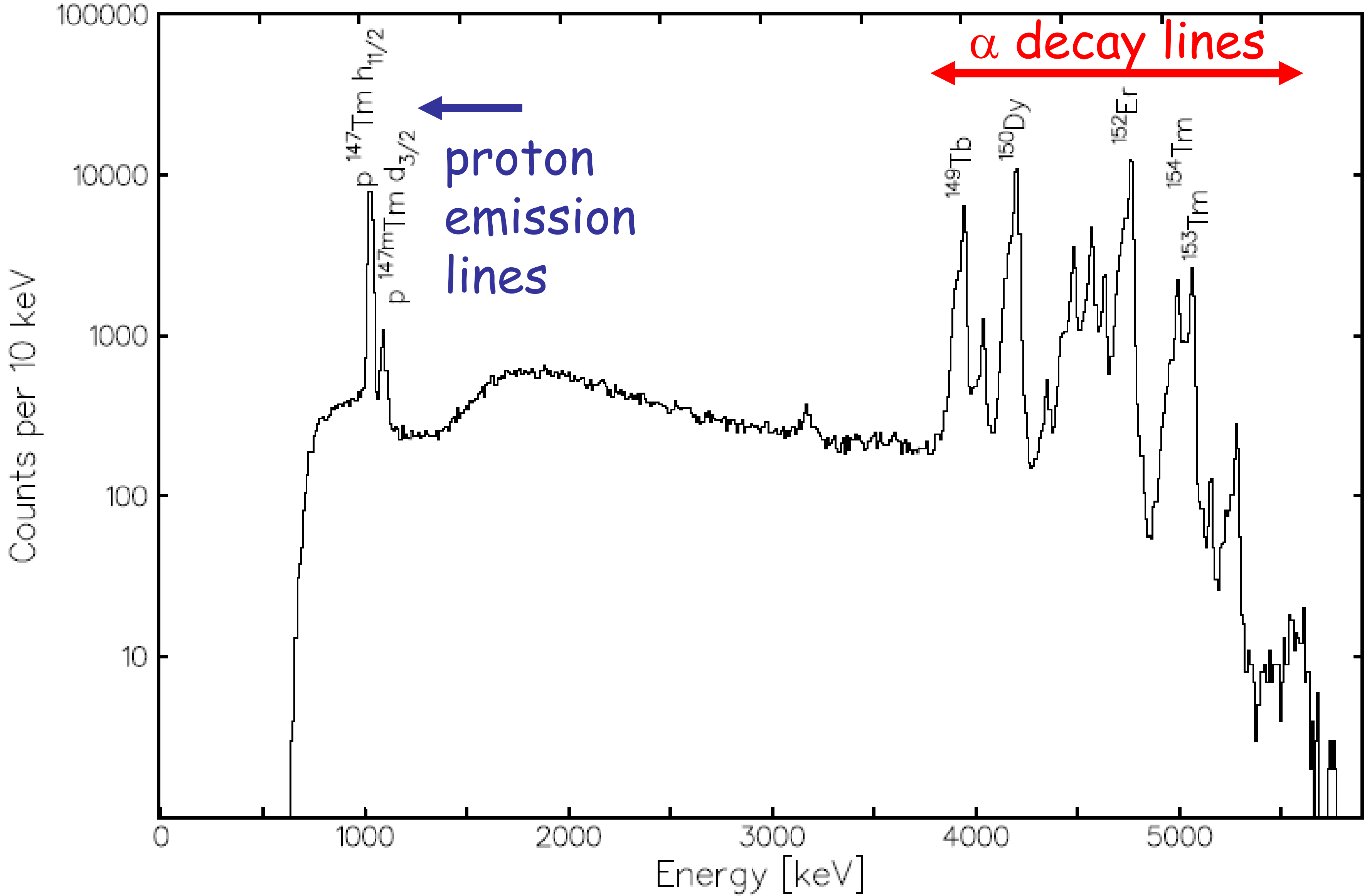

D. Seweyniak *et al.* *Phys. Rev.* **C55** (1997) R2137

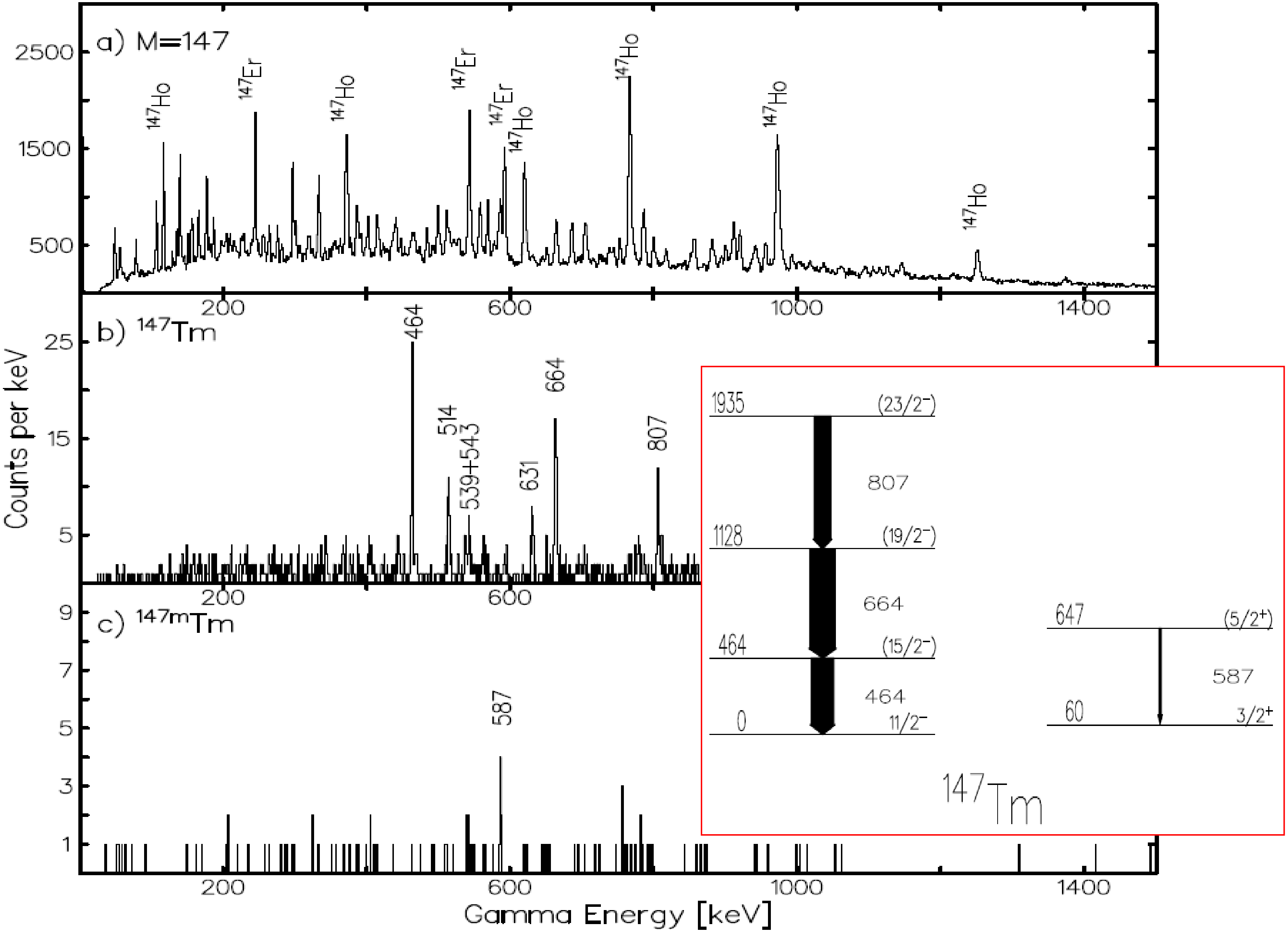

D. Seweyniak *et al.* *Phys. Rev.* **C55** (1997) R2137

Some high-spin nuclear physics phenomena.

- What happens to the nucleus under rotational stress?
  - Observe sequences of 'rotational bands' in many nuclei.
  - Single particle effects/excitations can 'compete'
    - 'alignments' and 'backbending'.
    - Coriolis effects; moment of inertia differences; band crossings.
  - Other (stable) deformed nuclear shapes exist.
    - Static octupole (β_3) deformations; parity doublets.
  - Very stable, very elongated nuclear charge and mass distributions ('superdeformation').

Quasi-particle aligned angular momentum

Total **aligned** angular momentum (I_x) can be calculated using Pythagoras theorem:

$$I_x(I) = \sqrt{I(I+1) - K^2} \approx \sqrt{\left(I+\frac{1}{2}\right)^2 - K^2}$$

The rotational frequency can be derived (from the canonical relation) to give

$$\omega \approx \frac{E_\gamma}{\sqrt{(I+\frac{3}{2})^2 - K^2} - \sqrt{(I-\frac{1}{2})^2 - K^2}}$$

Many plots of I (= Ix) for even-even nuclei ground state sequences vs. ω show 'discontinuities' at the 'critical' frequency.

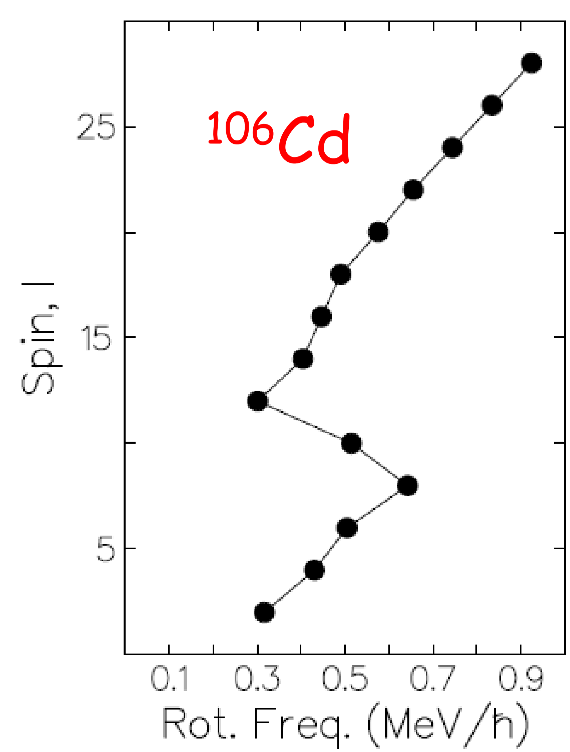

Rotation of nuclear core can cause 'breaking' of nuclear pairs close to the nuclear (Fermi) surface.
Biggest energy effect from Coriolis interaction is for orbitals with largest j_x values (i.e. high-J, low-Ω Nilsson orbitals).

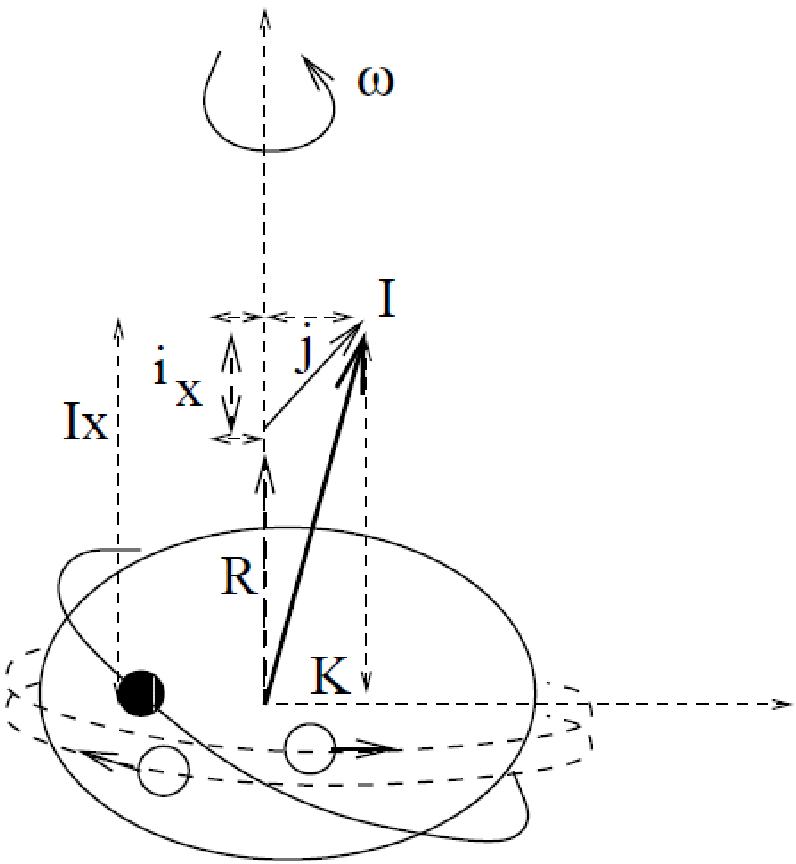

Rotation of nuclear core can cause 'breaking' of nuclear pairs close to the nuclear (Fermi) surface.
Biggest energy effect from Coriolis interaction is for orbitals with largest j_x values (i.e. high-J, low-Ω Nilsson orbitals).

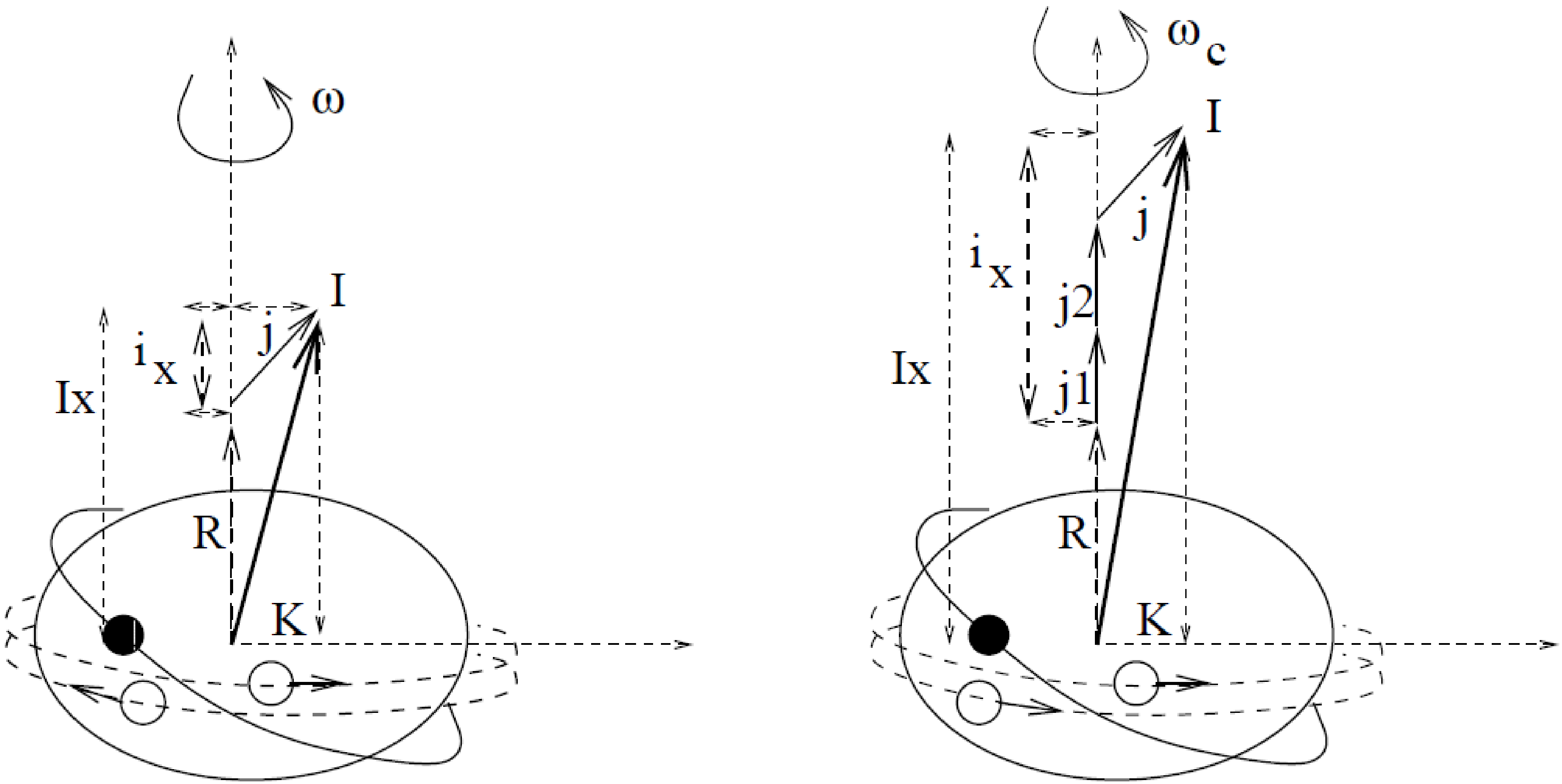

The experimental data can give a value for the total angular momentum of state, aligned parallel to the axis of rotation, Ix (from Pythagoras)

$$I_x(I) = \sqrt{I(I+1) - K^2} \approx \sqrt{\left(I + \frac{1}{2}\right)^2 - K^2}$$

Single particle contribution to 'aligned' angular momentum can be separated from the collective, rotational contribution to Ix.

$$i_x(\omega) = I_x(\omega) - I_{\text{ref}}(\omega)$$

The core, collective angular momentum component of the total Ix can be parameterised as a function of rotational frequency (ω) using the 'Harris parameters' to fit the nuclear moment of inertia.

$$I_{\text{ref}} = \left(\mathcal{I}_{(0)} + \mathcal{I}_{(2)}\omega^2\right)\omega$$

$$E_{rot}(I) = \frac{\hbar^2}{2\mathcal{I}^{(0)}(I)} I(I+1)$$

The kinematic moment of inertia is given by

$$\mathcal{I}^{(1)}(I) = \frac{I}{\omega}$$

while the dynamic moment is given by

$$\mathcal{I}^{(2)} = \frac{dI}{d\omega} \approx \frac{4\hbar}{\Delta E_\gamma}$$

$$\omega = \frac{dE(I)}{dI_x(I)} \approx \frac{E(I+1) - E(I-1)}{I_x(I+1) - I_x(I-1)}$$

$$I_x(I) = \sqrt{I(I+1) - K^2} \approx \sqrt{\left(I + \frac{1}{2}\right)^2 - K^2}$$

$$\omega \approx \frac{E_\gamma}{\sqrt{(I+\frac{3}{2})^2 - K^2} - \sqrt{(I-\frac{1}{2})^2 - K^2}}$$

^{106}Cd Yrast Band

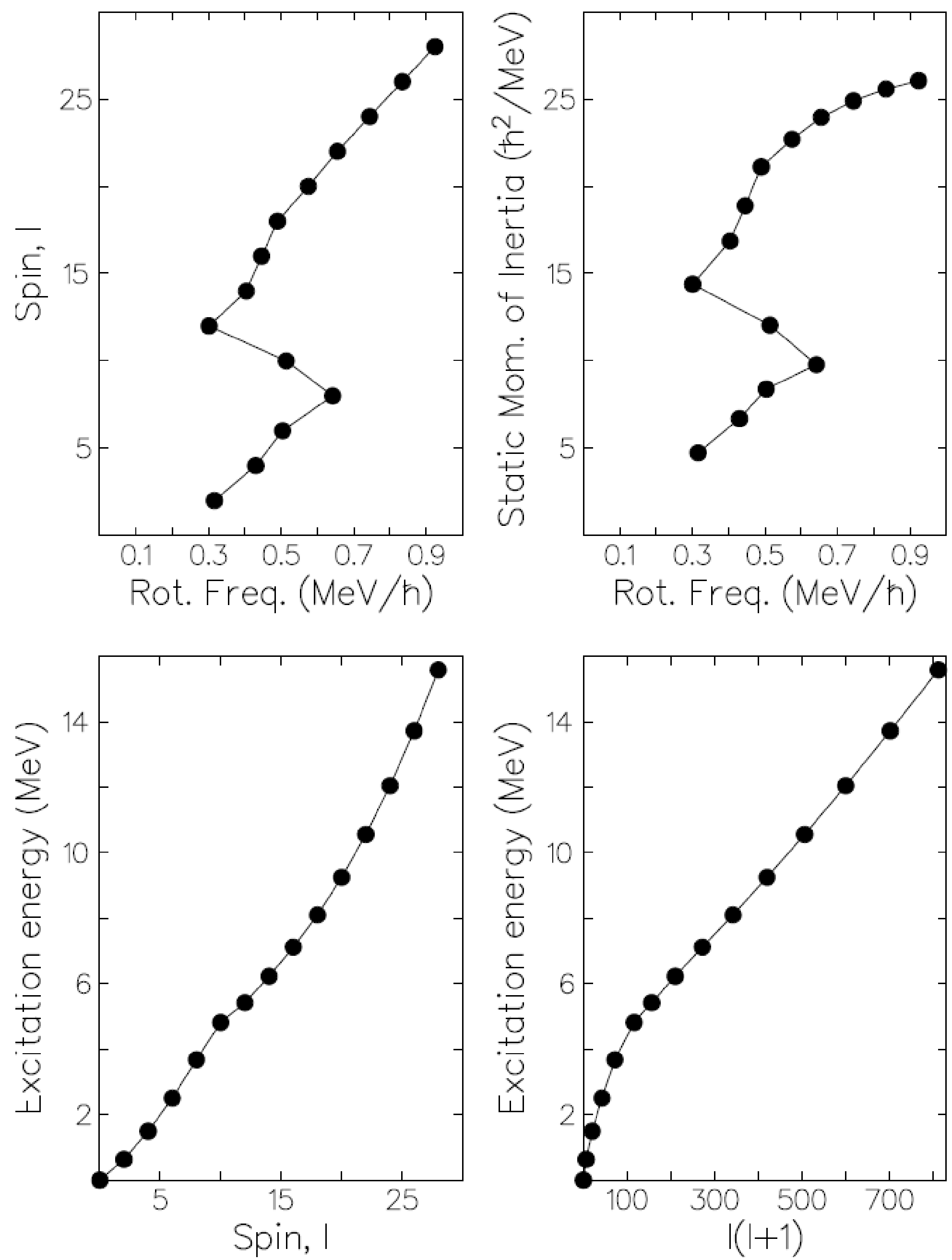

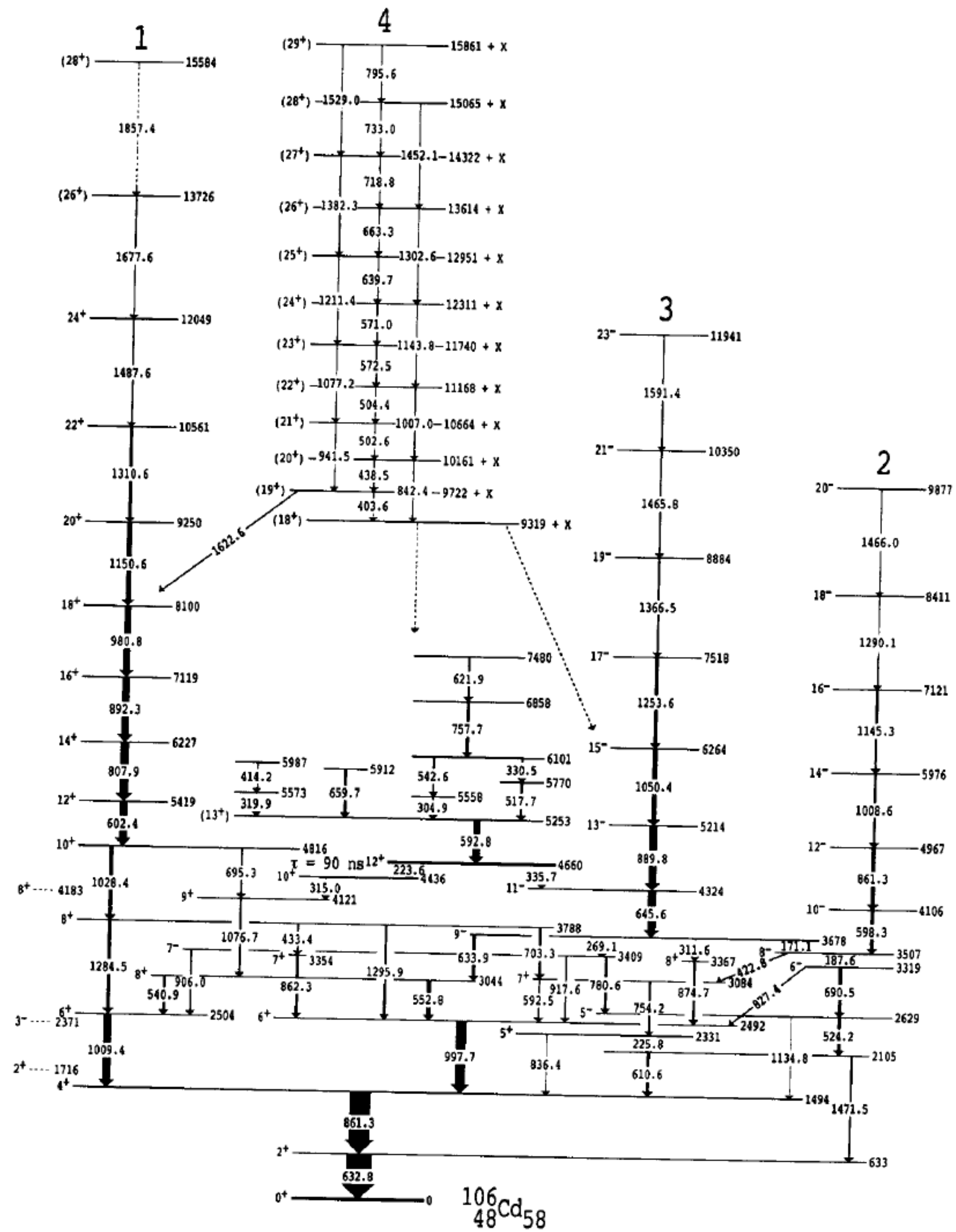
1
4
3
2
(28+) 15584
1857.4
(26+) 13726
1677.6
24+ 12049
1487.6
22+ 10561
1310.6
20+ 9250
1150.6
18+ 8100
980.8
16+ 7119
892.3
14+ 6227
807.9
12+ 5419
602.4
10+ 4816
1028.4
8+ 4183
8+
1284.5
6+
3- 2371
1009.4
2+ 1716
4+
(29+) 15861 + X
795.6
(28+) 1529.0 15065 + X
733.0
(27+) 1452.1 14322 + X
718.8
(26+) 1382.3 13614 + X
663.3
(25+) 1302.6 12951 + X
639.7
(24+) 1211.4 12311 + X
571.0
(23+) 1143.8 11740 + X
572.5
(22+) 1077.2 11168 + X
504.4
(21+) 1007.0 10664 + X
502.6
(20+) 941.5 10161 + X
438.5
(19+) 842.4 9722 + X
403.6
(18+) 9319 + X
1622.6
23- 11941
1591.4
21- 10350
1465.8
19- 8884
1366.5
17- 7518
1253.6
15- 6264
1050.4
13- 5214
889.8
11- 4324
645.6
20- 9877
1466.0
18- 8411
1290.1
16- 7121
1145.3
14- 5976
1008.6
12- 4967
861.3
10- 4106
598.3
7480
621.9
6858
757.7
6101
542.6
330.5
5770
5558
517.7
304.9
5253
5987
414.2
5573
319.9
(13+)
5912
659.7
592.8
12+ 4660
τ = 90 ns
10+ 223.6 4436
335.7
695.3
9+ 315.0 4121
3788
9-
1076.7
433.4
7- 7+ 3354
8+ 906.0
540.9
2504
862.3
1295.9
633.9 3044
552.8
703.3
269.1 3409
311.6
8+ 3367
8- 171.1 3678
3507
6- 187.6 3319
422.8
3084
7+ 917.6
780.6
874.7
827.4
592.5
5- 754.2
2492
2629
690.5
524.2
6+
5+ 2331
225.8
2105
997.7
836.4
610.6
1134.8
1494
1471.5
861.3
2+ 633
632.8
0+ 0
$^{106}_{48}Cd_{58}$

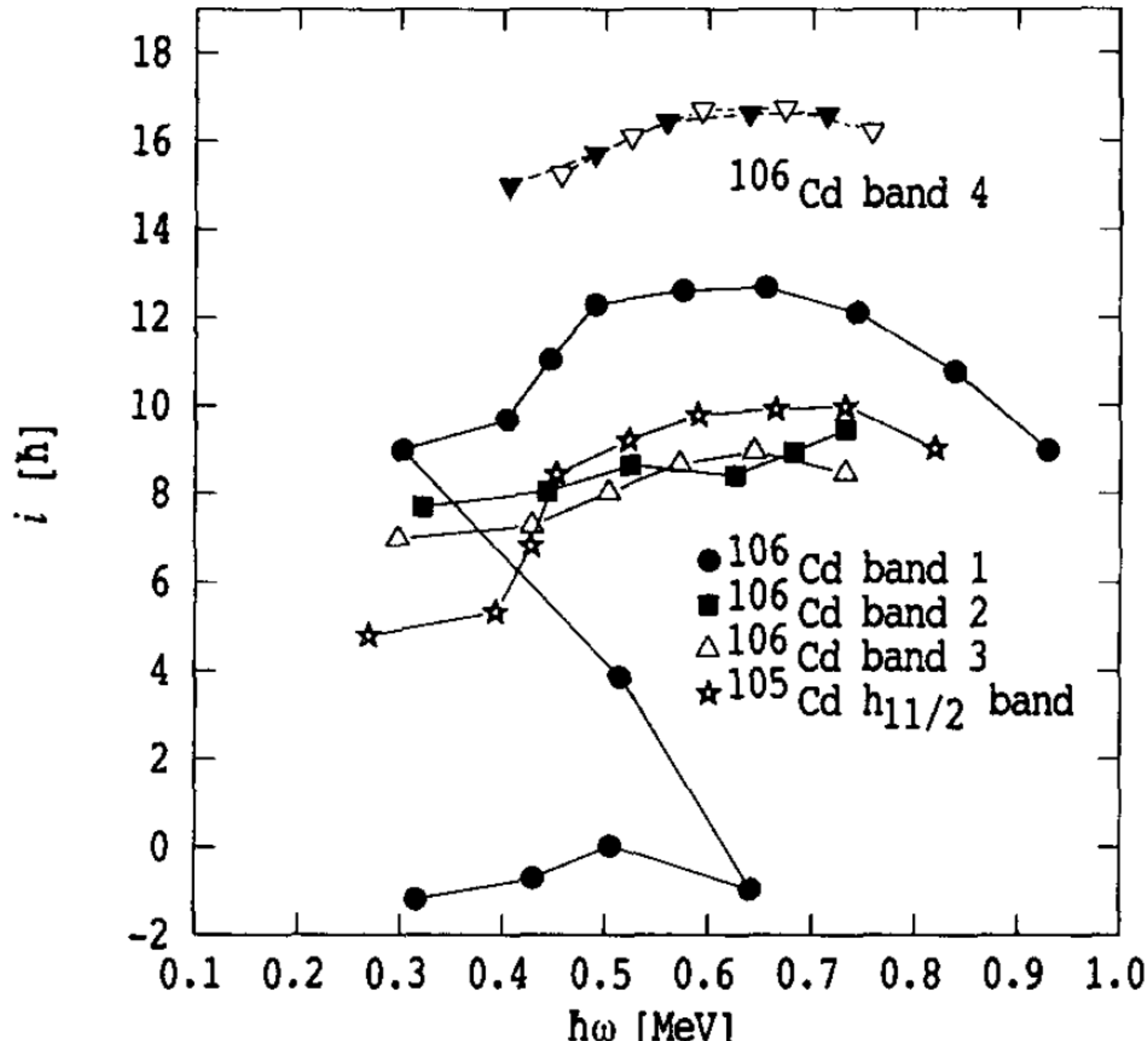

18
16
14
12
10
8
6
4
2
0
-2
0.1 0.2 0.3 0.4 0.5 0.6 0.7 0.8 0.9 1.0
i [ħ]
ħω [MeV]
106Cd band 4
106Cd band 1
106Cd band 2
106Cd band 3
105Cd h11/2 band

PHYSICAL REVIEW C **68**, 044313 (2003)

Binary-reaction spectroscopy of ^{99,100}Mo: Intruder alignment systematics in $N=57$ and $N=58$ isotones

P. H. Regan,[1,2,*] A. D. Yamamoto,[1,2] F. R. Xu,[3] C. Y. Wu,[4] A. O. Macchiavelli,[5] D. Cline,[4] J. F. Smith,[7] S. J. Freeman,[7] J. J. Valiente-Dobón,[1] K. Andgren,[1,6] R. S. Chakrawarthy,[7] M. Cromaz,[5] P. Fallon,[5] W. Gelletly,[1] A. Gorgen,[5] A. Hayes,[4] H. Hua,[4] S. D. Langdown,[1,2] I-Y. Lee,[5] C. J. Pearson,[1] Zs. Podolyák,[1] R. Teng,[4] and C. Wheldon[1,8]

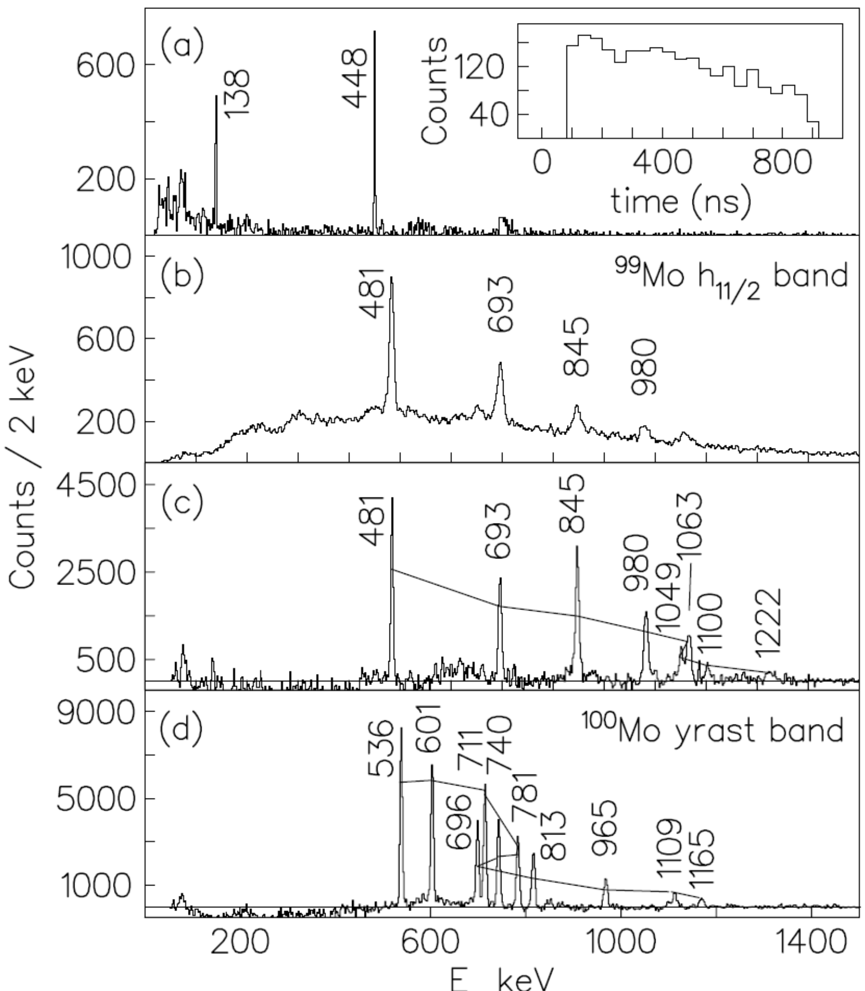

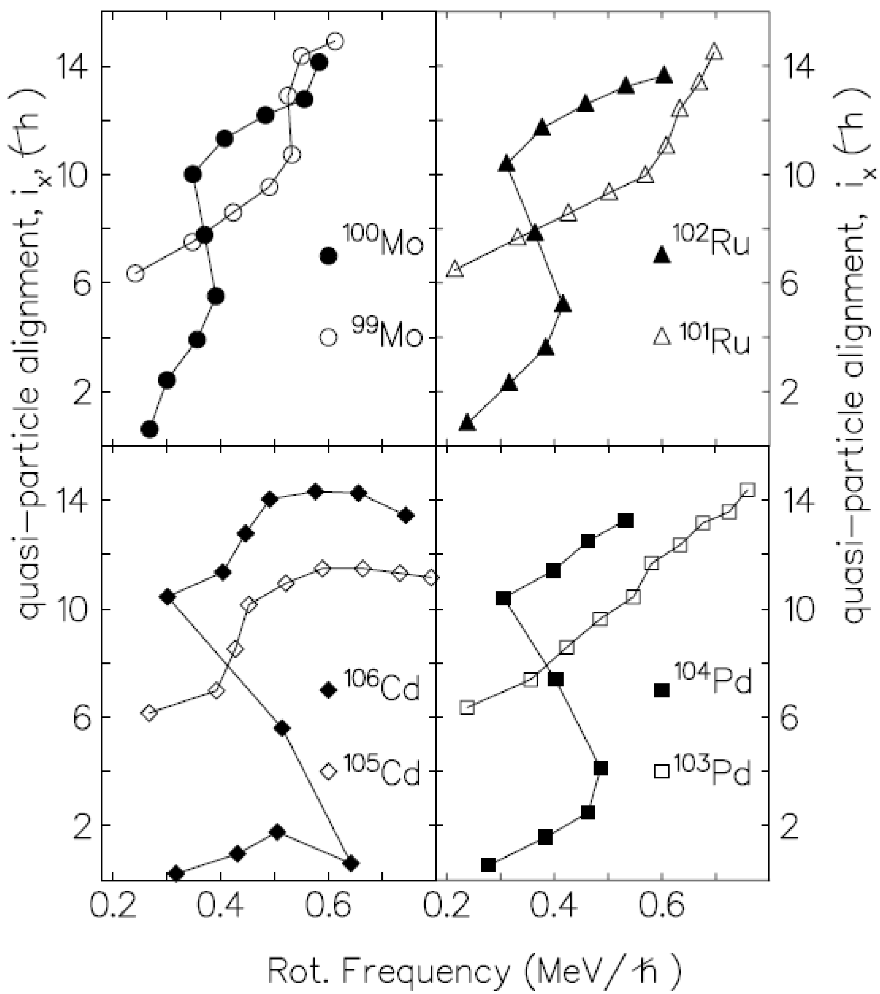

Collective Model B(E2), B(M1) values ?

The reduced in-band transition probabilities[1] are given by,

$$B(E2; I_i K \rightarrow I_f K) = \frac{5}{16\pi} e^2 Q_o^2 | < I_i 2 K 0 | I_f K > |^2$$

$$B(M1; I_i K \rightarrow I_f K) = \frac{3}{4\pi} e^2 | < I_i 1 K 0 | I_f K > |^2 (g_K - g_R)^2 K^2$$

where Q_o is the intrinsic quadrupole moment and g_K and g_R are the intrinsic and rotational gyromagnetic ratios respectively. The relevant Clebsch-Gordon coefficients[2] are given below.

$$\begin{aligned} E2(\Delta I = 2) &= \left[\frac{3(I-K)(I-K-1)(I+K)(I+K-1)}{(2I-2)(2I-1)I(2I+1)} \right]^{1/2} \\ E2(\Delta I = 1) &= -K \left[\frac{3(I-K)(I+K)}{(I-1)I(2I+1)(I+1)} \right]^{1/2} \qquad (2.4.57) \\ M1(\Delta I = 1) &= - \left[\frac{(I-K)(I+K)}{I(2I+1)} \right]^{1/2} \end{aligned}$$

[1] K.E.G. Löbner in, The Electromagnetic Interaction in Nuclear Spectroscopy, W.D. Hamilton (Ed), North-Holland (1975) Chapter 5

[2] The Theory of Atomic Spectra, Condon and Shortley (1935) reprinted (1963) p76-77

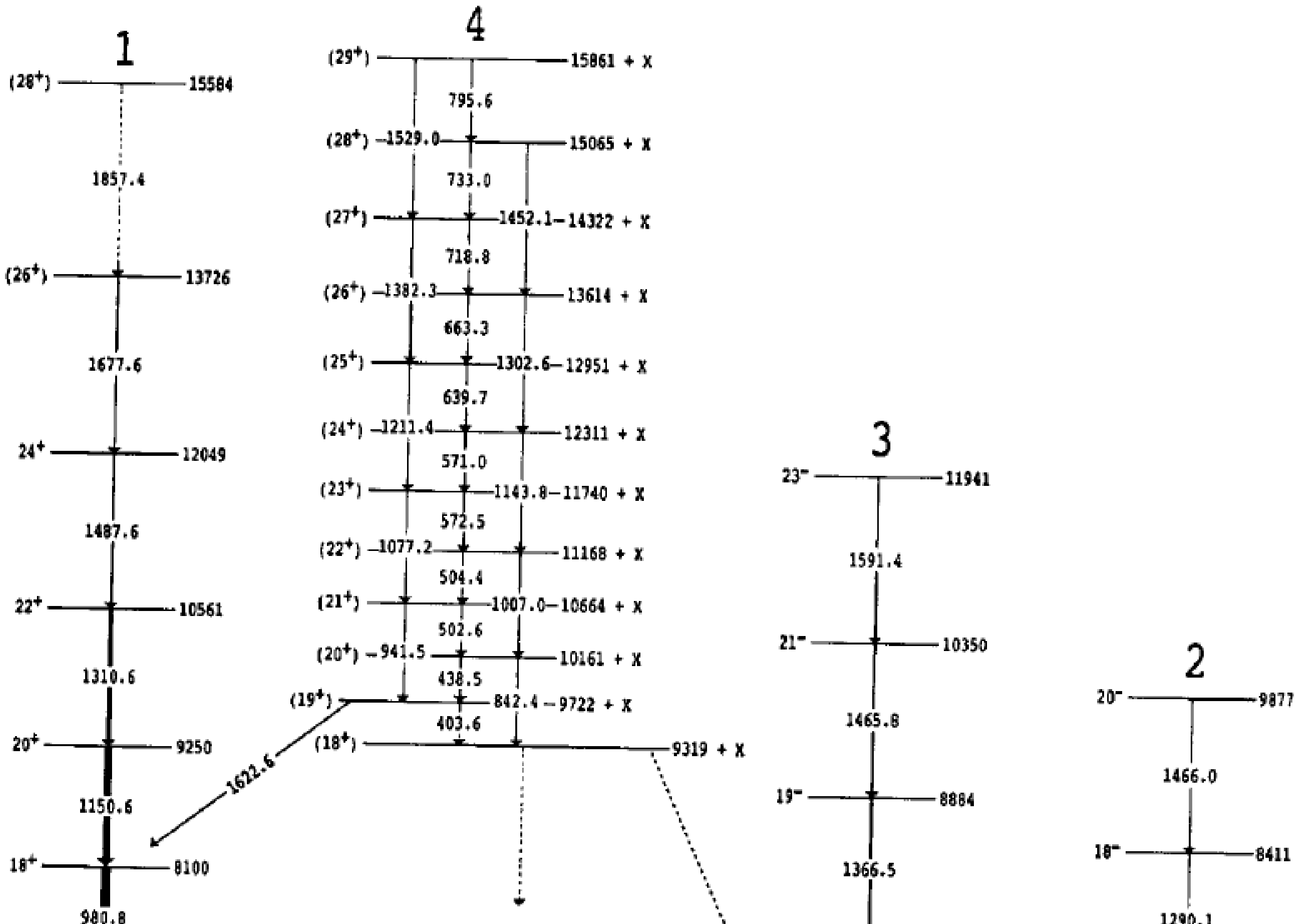
1
(28+) 15584
1857.4
(26+) 13726
1677.6
24+ 12049
1487.6
22+ 10561
1310.6
20+ 9250
1150.6
18+ 8100
980.8
1622.6
4
(29+) 15861 + X
795.6
(28+) 1529.0 15065 + X
733.0
(27+) 1452.1 14322 + X
718.8
(26+) 1382.3 13614 + X
663.3
(25+) 1302.6 12951 + X
639.7
(24+) 1211.4 12311 + X
571.0
(23+) 1143.8 11740 + X
572.5
(22+) 1077.2 11168 + X
504.4
(21+) 1007.0 10664 + X
502.6
(20+) 941.5 10161 + X
438.5
(19+) 842.4 9722 + X
403.6
(18+) 9319 + X
3
23- 11941
1591.4
21- 10350
1465.8
19- 8884
1366.5
2
20- 9877
1466.0
18- 8411
1290.1

$$B(\mathrm{M1}) = \frac{3}{8\pi}\frac{K^2}{I^2}\left[\left(g^{(1)} - g_R\right)\left(\sqrt{I^2 - K^2} - i_x^{(1)}\right) - \left(g^{(2)} - g_R\right)i_x^{(2)}\right]^2$$

$$B(\mathrm{E2}\colon I \to I-2) = \frac{5}{16\pi}Q_0^2\frac{3(I-K)(I-K-1)(I+K)(I+K+1)}{(2I-2)(2I-1)I(2I+1)}$$

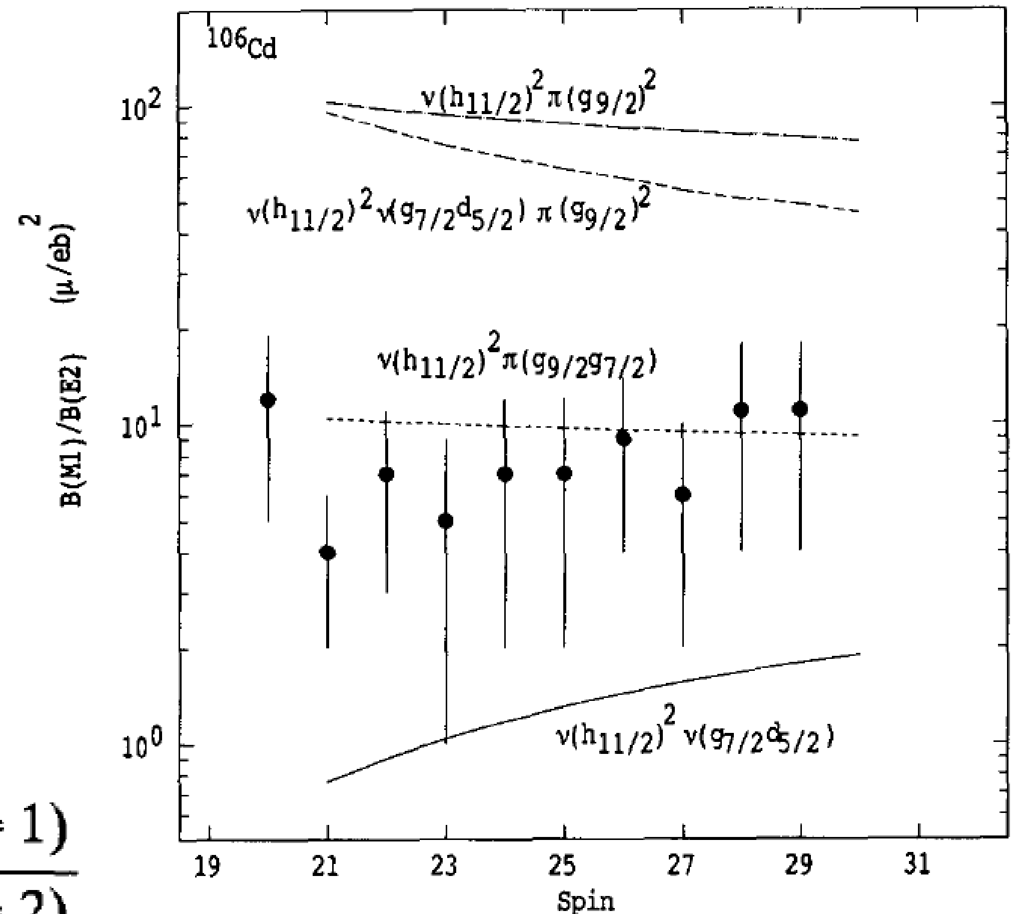

Experimental branching ratios (i.e., relative gamma-ray intensities) can used to be give:

$$\frac{B(\mathrm{M1})}{B(\mathrm{E2})} = 0.697\frac{E_2^5}{E_1^3}\frac{1}{1+\delta^2}\frac{I_\gamma(\Delta I = 1)}{I_\gamma(\Delta I = 2)}$$

Octupole Collectivity

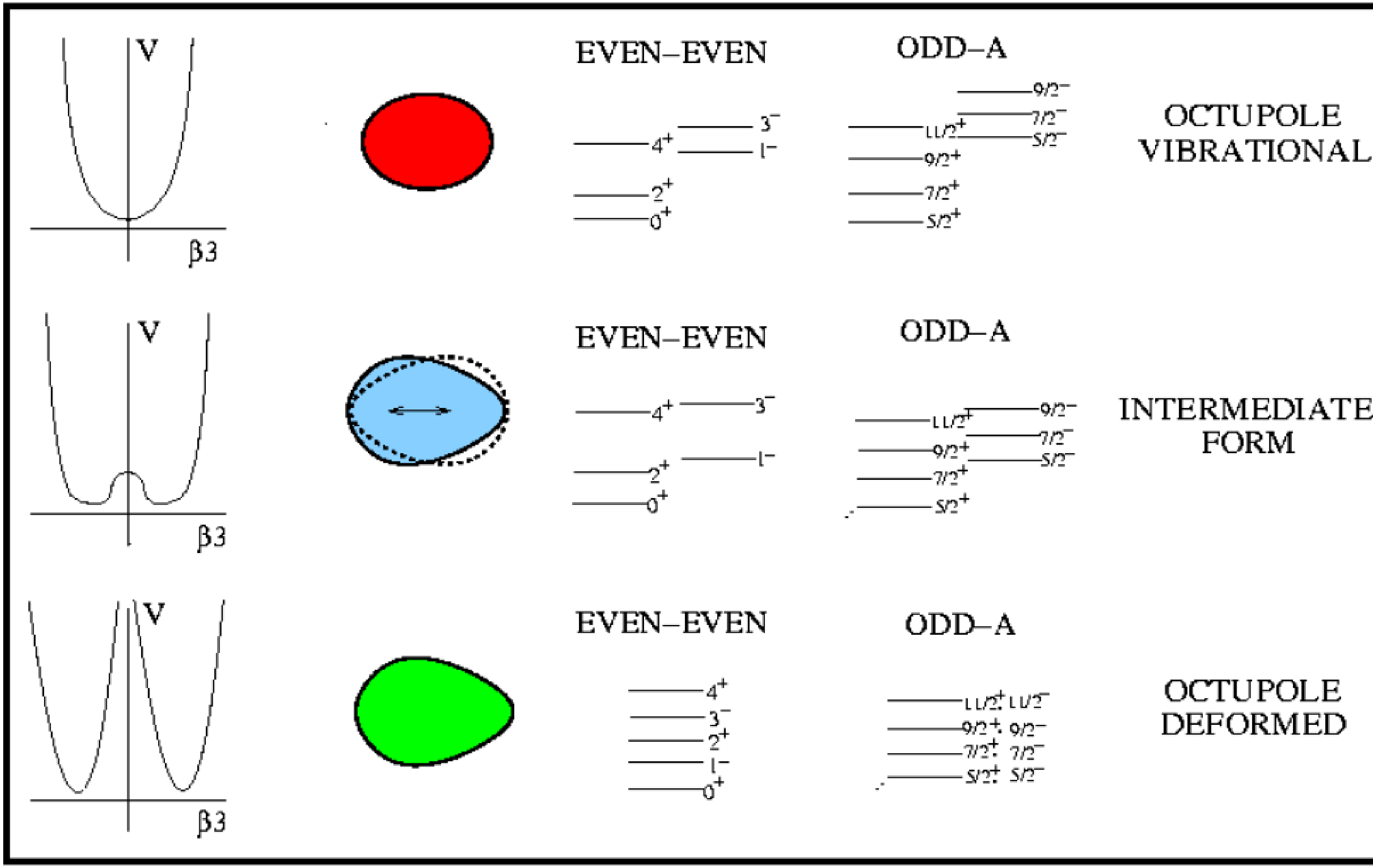

I. Ahmad & P. A. Butler, Annu. Rev. Nucl. Part. Sci. **43**, 71 (1993).

P. A. Butler and W. Nazarewicz, Rev. Mod. Phy. **68**, 349 (1996).

$$B(E1 : I_i \rightarrow I_f) = \frac{3D_0^2}{4\pi} < I_i 010 | I_f 0 >^2 = \frac{3D_0^2}{4\pi} \frac{(I-K)(I+K)}{I(2I+1)}$$

Large Dipole Moments

$$D_0 \sim [B(E1)/\langle I_i 010 | I_f 0\rangle]^{1/2}$$

where

$$D_0 > 0.2 \text{ eb-fm}$$

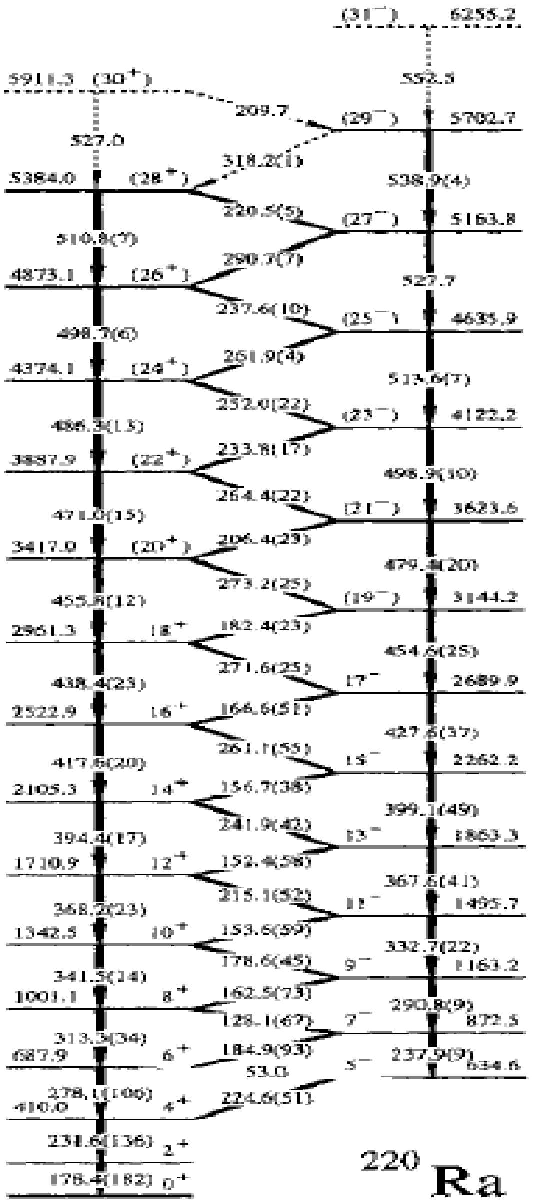

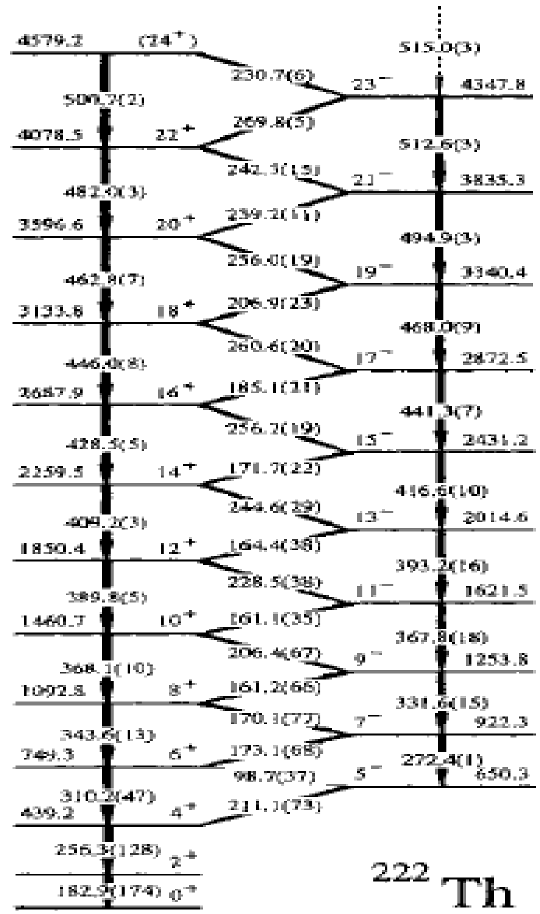

J. Smith *et al.*, Phys. Rev. Lett. 75 (1995) 1050.

Where to find enhanced octupole collectivity

Long-range interactions between single particle states with $\Delta j = \Delta l = 3$;

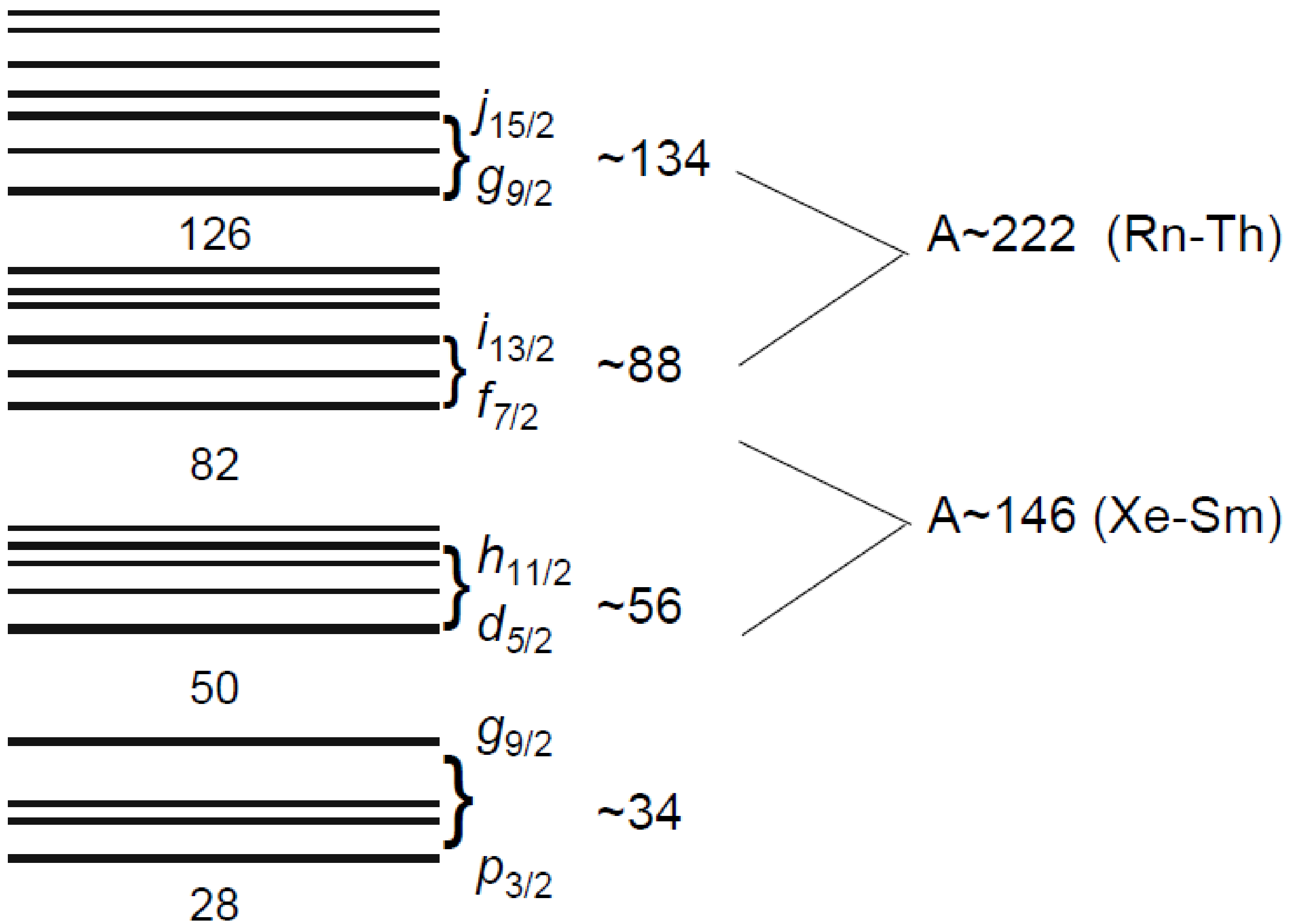

Difficult regions to study experimentally

Problem ?

- Standard fusion-evaporation reactions make (usually) neutron-deficient nuclei.

How do you make and study neutron-rich nuclei ?

- (low-cross-section) fusion evap. reactions, e.g., $^{18}O + ^{48}Ca \rightarrow 2p + ^{64}Fe$
  - Limited compound systems using stable / beam target combinations.
  - Highly selective reactions (if good channel selection applied).

- Spontaneous fission sources (e.g., ^{244}Cm)
  - Good for some regions of the nuclear chart, but little/no selectivity in the 'reaction' mechanism.
  - Can make quite high spins in each fragment ($10 \rightarrow 20\hbar$)

- Fusion fission reactions
  - e.g., $^{18}O + ^{208}Pb \rightarrow ^{226}Th^* \rightarrow f_1 + f_2 + xn$ (e.g., $^{112}_{44}Ru + ^{112}_{46}Pd + 2n$)
  - Doesn't make very neutron-rich, little selectivity.
  - Medium spins (~10 $\hbar$ in each fragment) populated

- Heavy-ion deep-inelastic / multi-nucleon transfer reactions (e.g.,
  - e.g. $^{136}Xe + ^{198}Pt \rightarrow ^{136}Ba + ^{194}Os + 2n$.
  - Populations Q-value dependent; medium spins accessed in products, make nuclei 'close' to the original (stable) beam and target species.
  - Selectivity can be a problem, large Doppler effects.

- Projectile fragmentation (or Projectile Fission)
  - (v. different energy regime)
  - Need a fragment separator.

INSTITUTE OF PHYSICS PUBLISHING JOURNAL OF PHYSICS G: NUCLEAR AND PARTICLE PHYSICS

J. Phys. G: Nucl. Part. Phys. **32** (2006) R151–R192 doi:10.1088/0954-3899/32/6/R01

TOPICAL REVIEW

Spectroscopic studies with the use of deep-inelastic heavy-ion reactions

R Broda

Niewodniczański Institute of Nuclear Physics PAN, Kraków, Poland

Deep-Inelastic Reactions

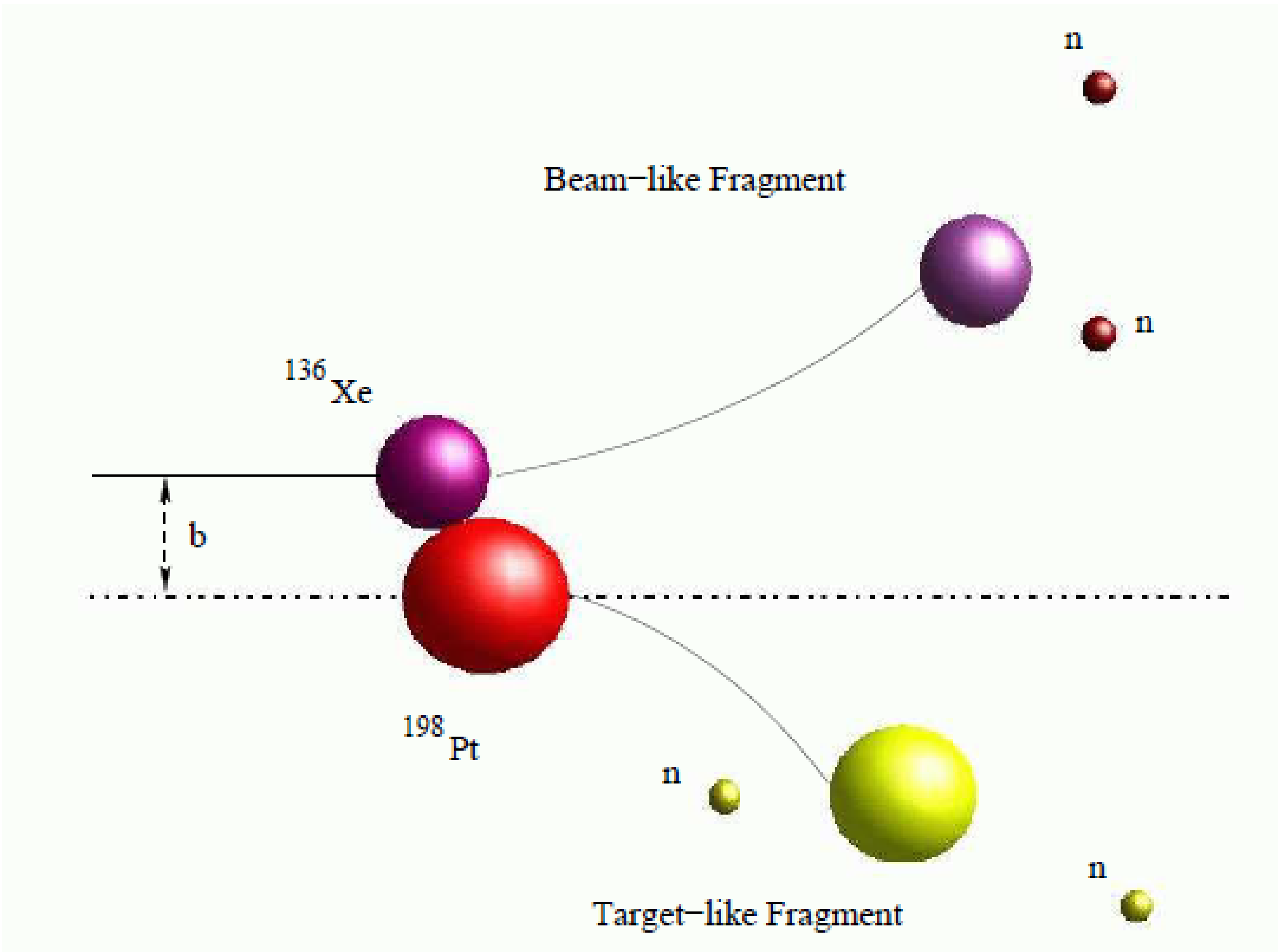

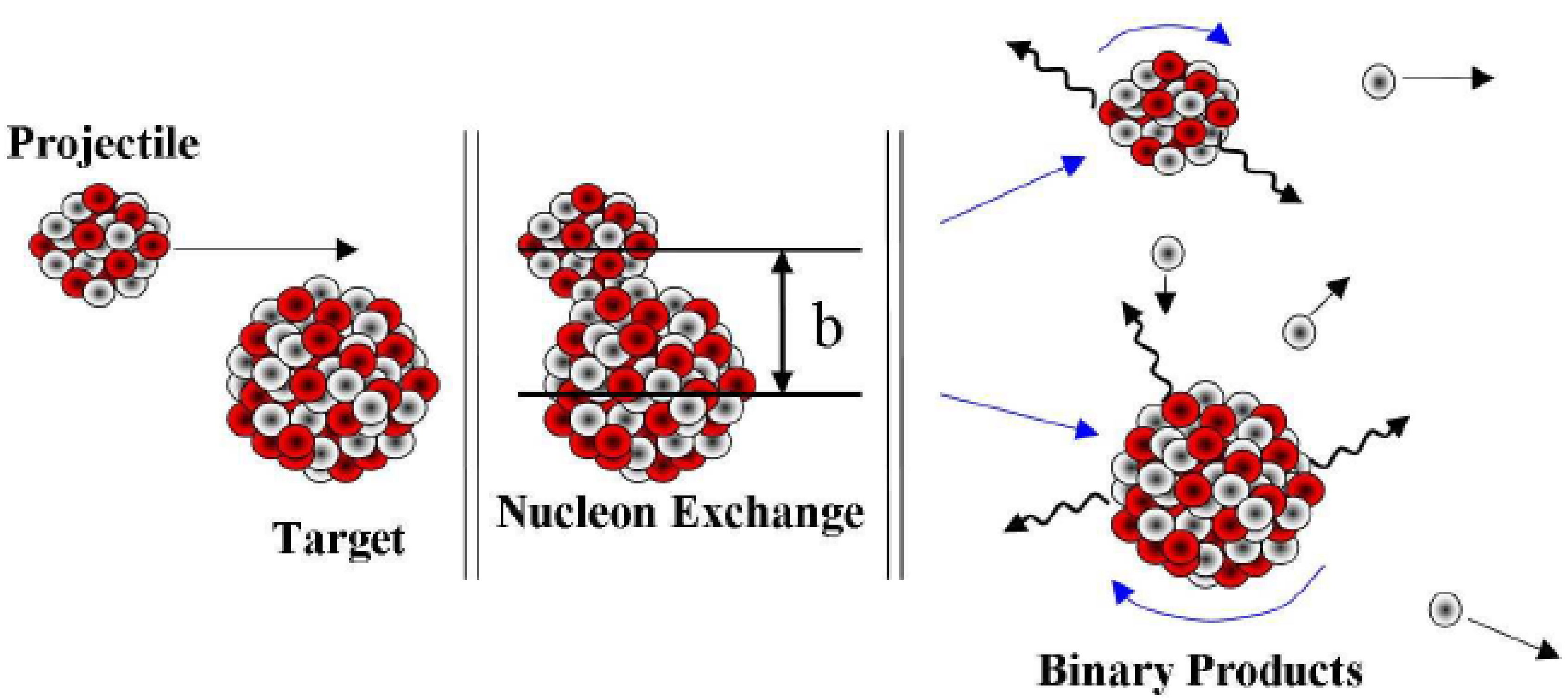

$$L = \mu R^2 \omega + \Im_p \omega_p + \Im_t \omega_t,$$

$$\mu = \frac{A_p A_t}{A_p + A_t}.$$

J. Phys. G: Nucl. Part. Phys. **32** (2006) R151–R192

TOPICAL REVIEW

Spectroscopic studies with the use of deep-inelastic heavy-ion reactions

R Broda

Niewodniczański Institute of Nuclear Physics PAN, Kraków, Poland

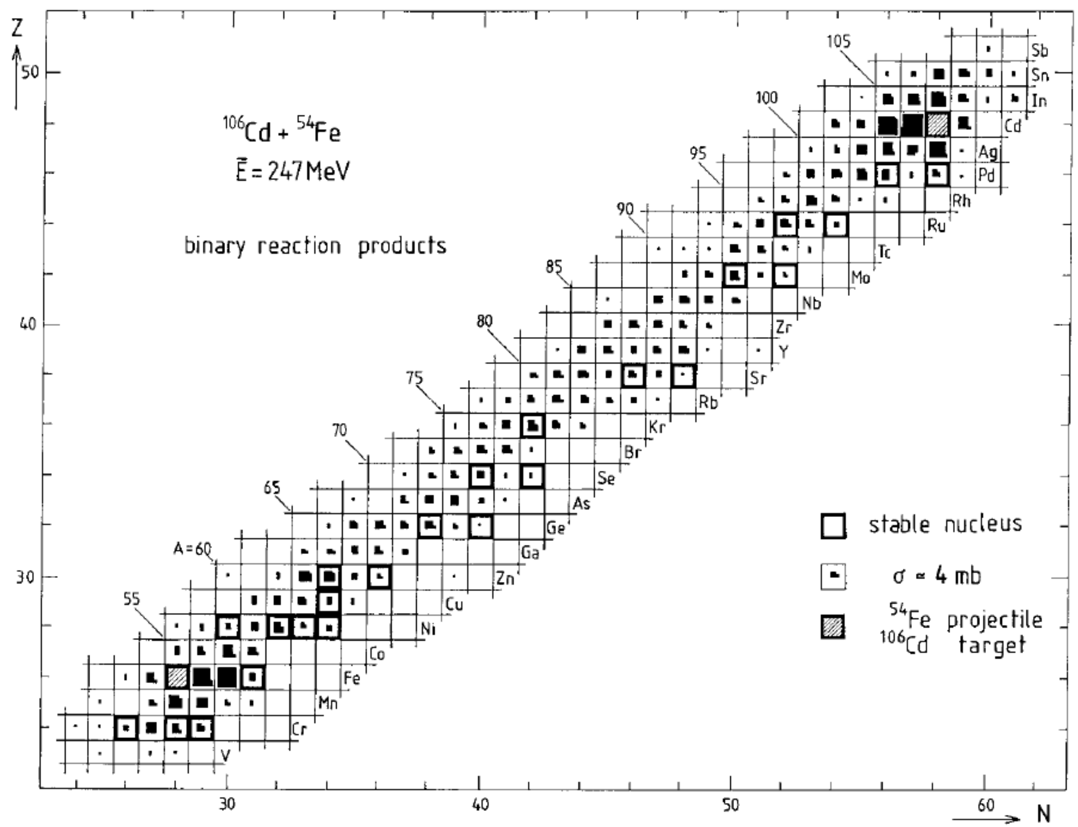

Figure 2. Production cross sections for binary reaction products in ^{54}Fe + ^{106}Cd collisions. In the same experiment cross sections for fusion–evaporation products were determined. Reprinted with permission from [11] © 1994 American Physical Society.

Topical Review R155

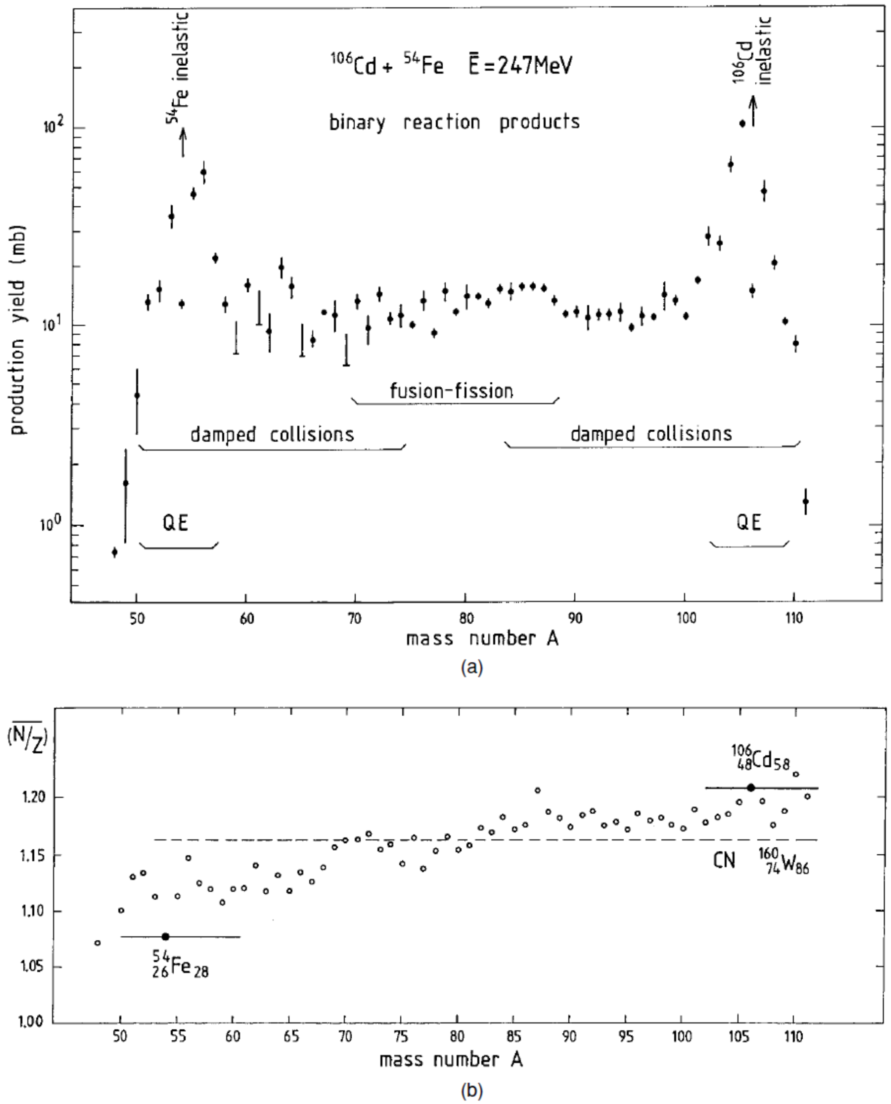

Figure 3. Isobar-integrated production cross sections (a) and the average N/Z ratios (b) as a function of binary reaction product mass in ^{106}Cd + ^{54}Fe collisions. Reprinted with permission from [11] © 1994 American Physical Society.

Both the target-like and beam-like fragments and the intermediated fusion-fission residues are usually **stopped** in a thick/backed target.

For discrete gamma rays decaying from states with effective lifetimes of a few picoseconds, there is **no Doppler shift** effect as the sources are stopped in the target and have v/c=0.

Prompt decays from higher-spin / faster lifetime states (< 1ps) will be ‘smeared’ out by the Doppler broadening effect.

Backed/thick target experiments can not correct for Doppler shifts as the direction and velocity of the emitting fragment is not known.

e.g., ^{82}Se + ^{192}Os at INFN-Legnaro.

Discrete gamma rays detected using GASP array.

Triples gamma-ray coincidences measured within ~ 50 ns timing window.

Discrete states to ~ 12ħ observed in BLF.

More like ~ 20 ħ in some of the TLFs.

PHYSICAL REVIEW C **76**, 054317 (2007)

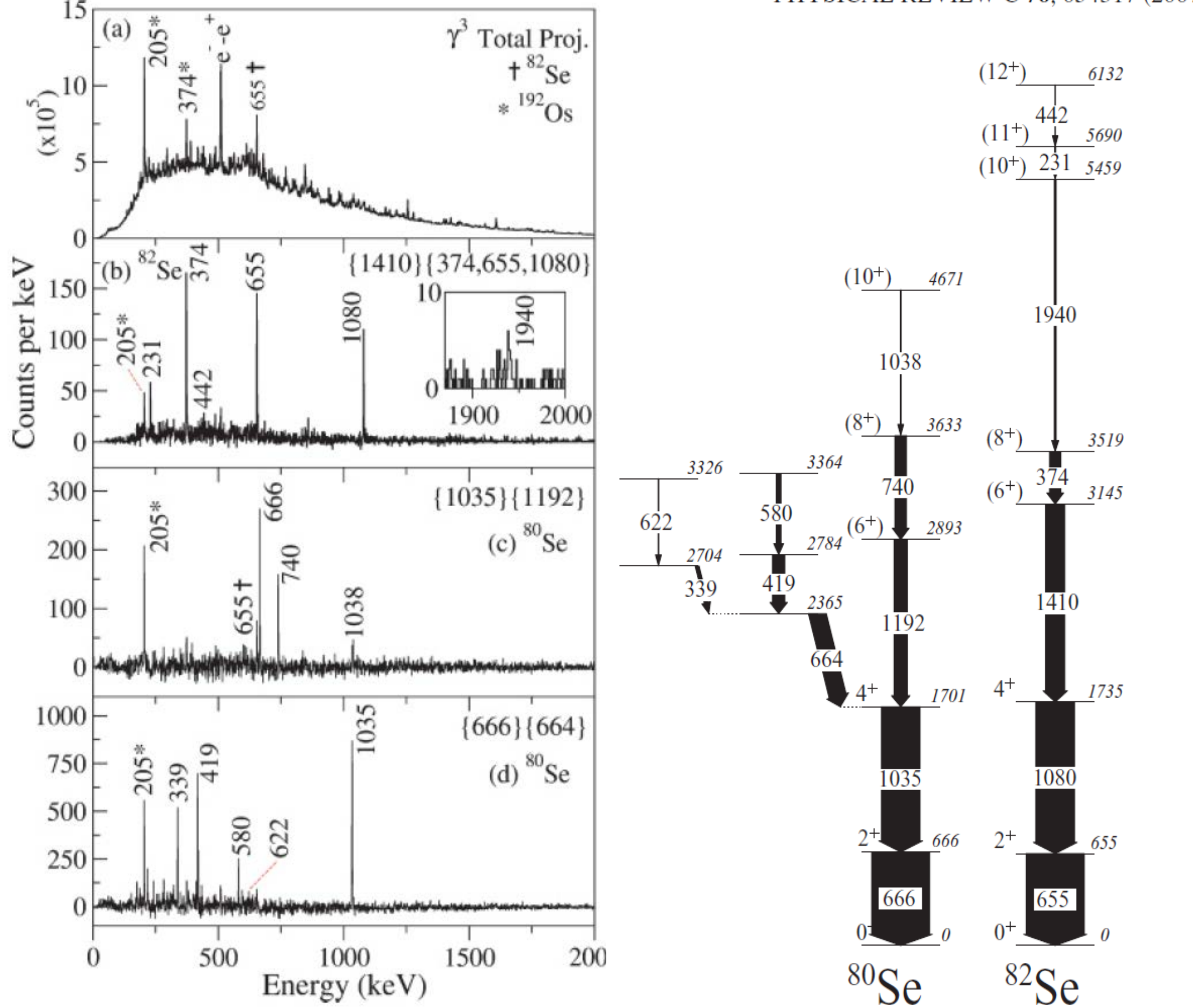

PHYSICAL REVIEW C **76**, 054317 (2007)

Yrast studies of ^{80,82}Se using deep-inelastic reactions

G. A. Jones,[1] P. H. Regan,[1] Zs. Podolyák,[1] N. Yoshinaga,[2] K. Higashiyama,[3] G. de Angelis,[4] Y. H. Zhang,[5] A. Gadea,[4] C. A. Ur,[6] M. Axiotis,[4] D. Bazzacco,[6] D. Bucurescu,[7] E. Farnea,[6] W. Gelletly,[1] M. Ionescu-Bujor,[7] A. Iordachescu,[7] Th. Kröll,[4] S. D. Langdown,[1] S. Lenzi,[6] S. Lunardi,[6] N. Marginean,[4] T. Martinez,[4] N. H. Medina,[8] R. Menegazzo,[6] D. R. Napoli,[4] B. Quintana,[9] B. Rubio,[10] C. Rusu,[11] R. Schwenger,[12] D. Tonev,[4] J. J. Valiente Dobón,[1,4] and W. von Oertzen[13]

Vol. 36 (2005) ACTA PHYSICA POLONICA B No 4

OBLATE COLLECTIVITY IN THE YRAST STRUCTURE OF ^{194}Pt*

G.A. Jones[a], Zs. Podolyák[a], N. Schunck[a], P.M. Walker[a]
G. De Angelis[b], Y.H. Zhang[b], M. Axiotis[b], D. Bazzacco[c]
P.G. Bizzeti[d], F. Brandolini[c], R. Broda[e], D. Bucurescu[f]
E. Farnea[b], W. Gelletly[a], A. Gadea[b], M. Ionescu-Bujor[f]
A. Iordachescu[f], Th. Kröll[b], S.D. Langdown[a], S. Lunardi[c]
N. Marginean[b], T. Martinez[b], N.H. Medina[g], B. Quintana[h]
P.H. Regan[a], B. Rubio[i], C.A. Ur[c], J.J. Valiente-Dobón[a]
and S.J. Williams[a]

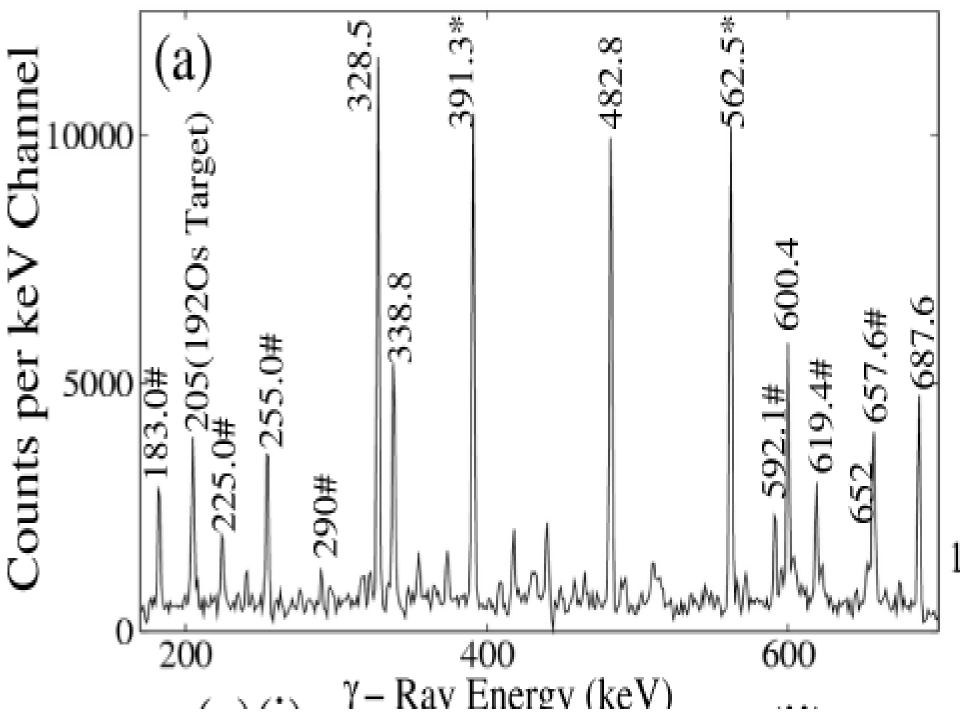

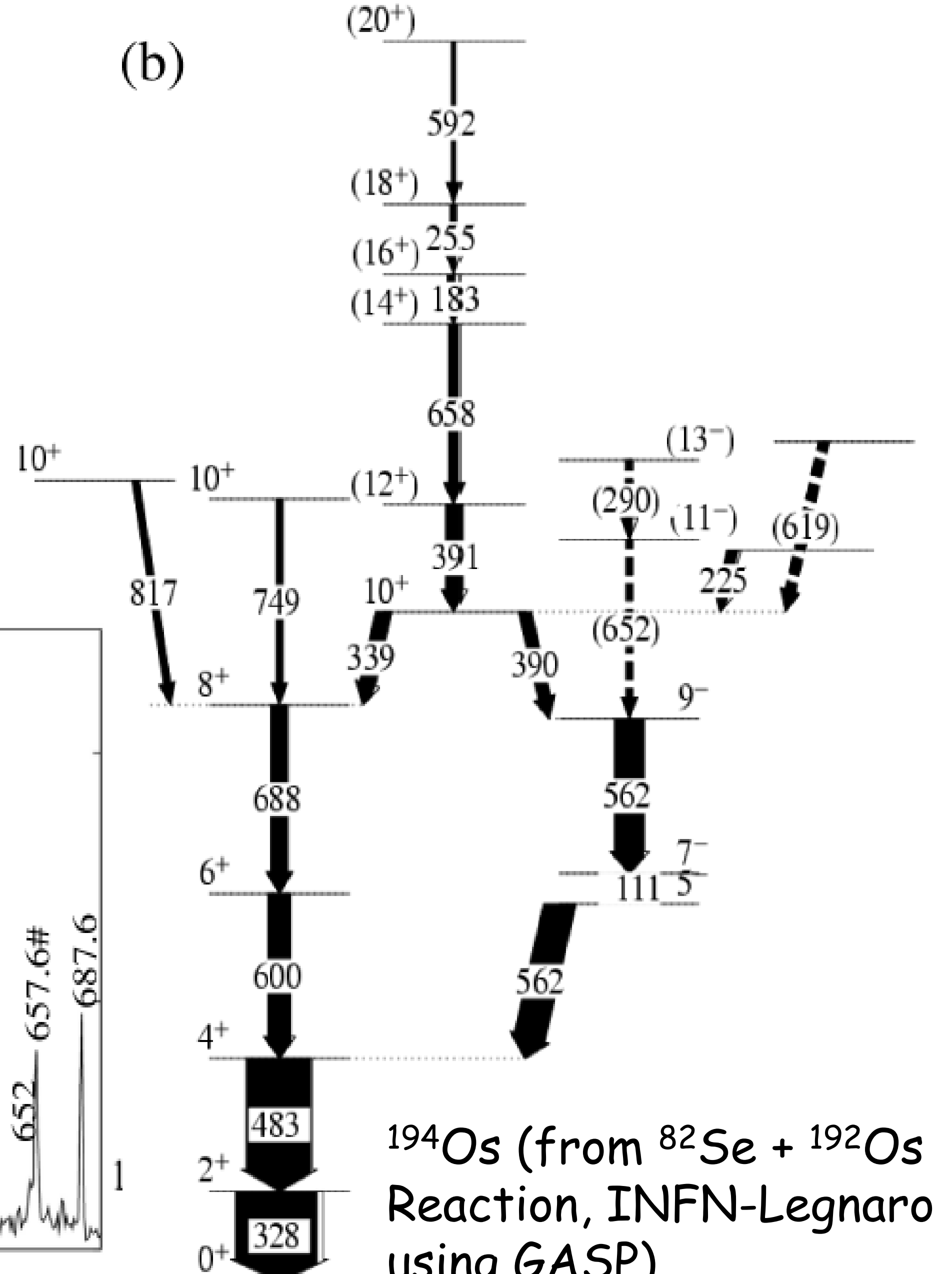

^{194}Os (from ^{82}Se + ^{192}Os Reaction, INFN-Legnaro using GASP)

States to spins of >20 ħ can be populated in DIC.

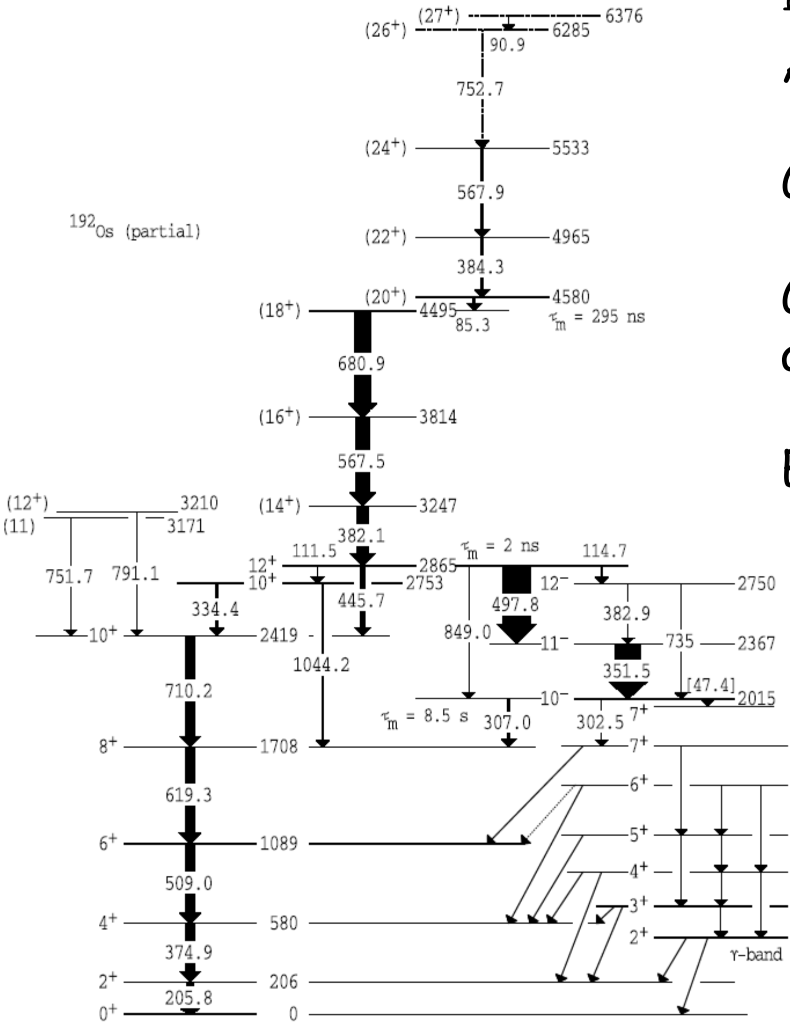

136Xe beam on thick, backed 192Os target at Argonne National Lab.

Gamma rays measured using GAMMASPHERE

Gamma rays decaying following isomeric states are all stopped in the target, no Doppler shifts.

Evidence for population of states with I>25 ħ.

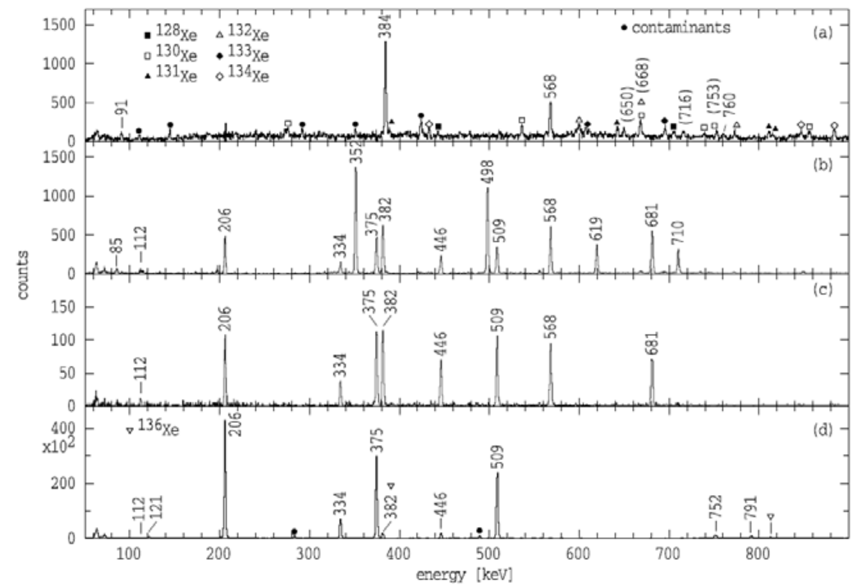

Physics Letters B 720 (2013) 330–335

Isomers and excitation modes in the gamma-soft nucleus ^{192}Os

G.D. Dracoulis [a,*], G.J. Lane [a], A.P. Byrne [a], H. Watanabe [a,b,1], R.O. Hughes [a,2], F.G. Kondev [c], M. Carpenter [d], R.V.F. Janssens [d], T. Lauritsen [d], C.J. Lister [d], D. Seweryniak [d], S. Zhu [d], P. Chowdhury [e], Y. Shi [f], F.R. Xu [f]

Conservation of linear angular momentum gives,

$$P_0 = P_p \cos\theta_p + P_t \cos\theta_t$$
$$0 = P_p \sin\theta_p - P_t \sin\theta_t$$

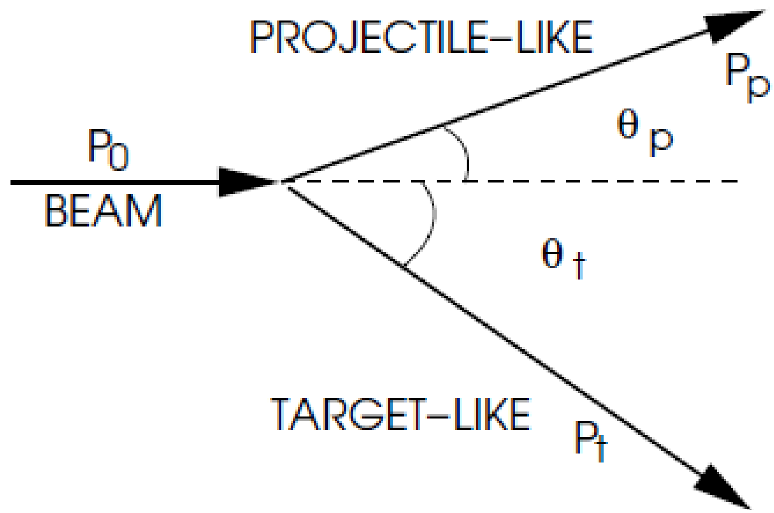

After some algebra manipulation, the relation of the recoil momenta to the initial beam momentum is given by,

$$P_{p,t} = P_0 \frac{\sin(\theta_t, \theta_p)}{\sin(\theta_p + \theta_t)} \tag{2.2}$$

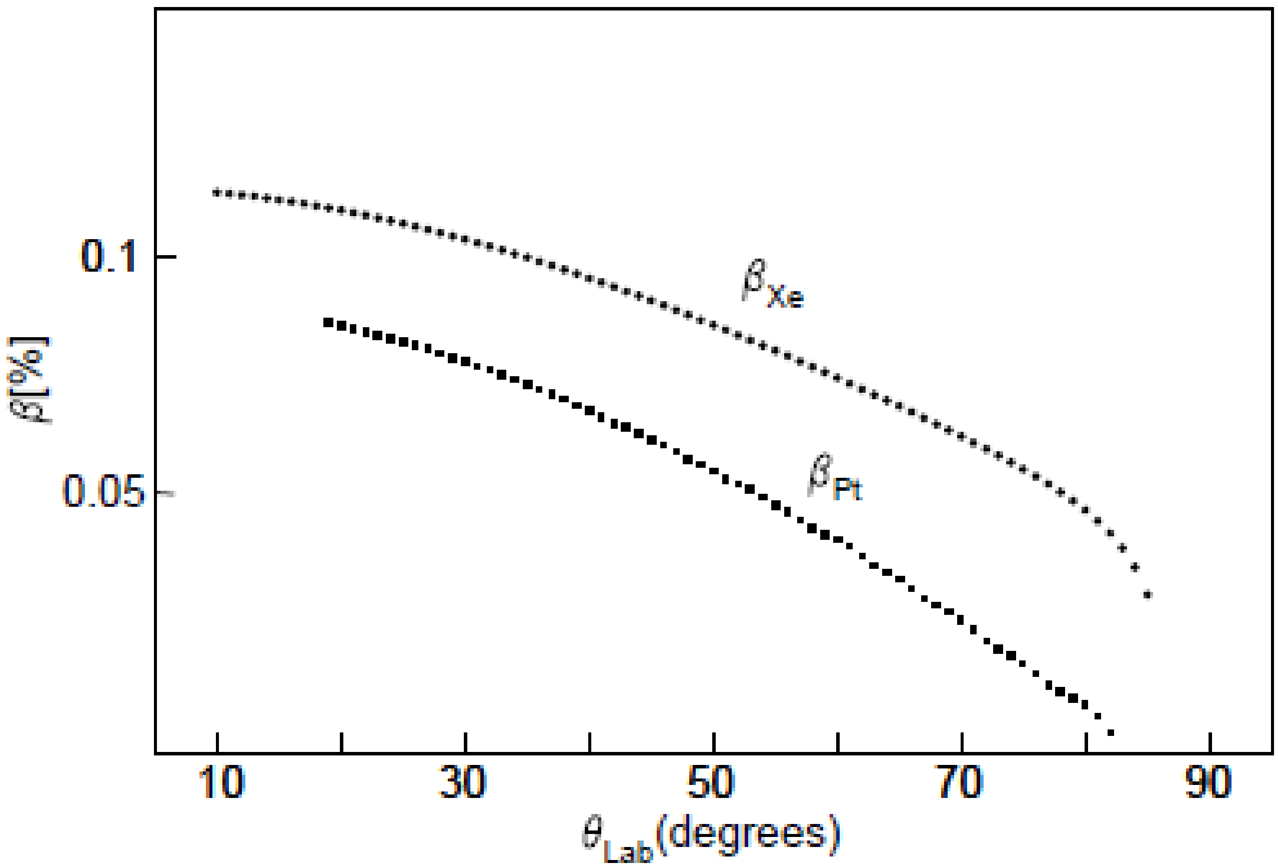

Figure 2.3: Calculated velocities of the projectile and the target recoils for the particular case of a ^{136}Xe beam at 850 MeV in the laboratory frame impinging on a ^{198}Pt target. An elastic collision and simple two-body kinematics have been assumed.

PHYSICAL REVIEW C **69**, 024316 (2004)

^{136}Ba studied via deep-inelastic collisions: Identification of the $(\nu h_{11/2})^{-2}_{10+}$ isomer

J. J. Valiente-Dobón,[1,*] P. H. Regan,[1,2] C. Wheldon,[1,3] C. Y. Wu,[4] N. Yoshinaga,[5] K. Higashiyama,[5] J. F. Smith,[6] D. Cline,[4] R. S. Chakrawarthy,[6] R. Chapman,[7] M. Cromaz,[8] P. Fallon,[8] S. J. Freeman,[6] A. Görgen,[8] W. Gelletly,[1] A. Hayes,[4] H. Hua,[4] S. D. Langdown,[1,2] I. Y. Lee,[8] X. Liang,[7] A. O. Macchiavelli,[8] C. J. Pearson,[1] Zs. Podolyák,[1] G. Sletten,[9] R. Teng,[4] D. Ward,[8] D. D. Warner,[10] and A. D. Yamamoto[1,2]

^{136}Xe beam on a thin ^{198}Pt target.

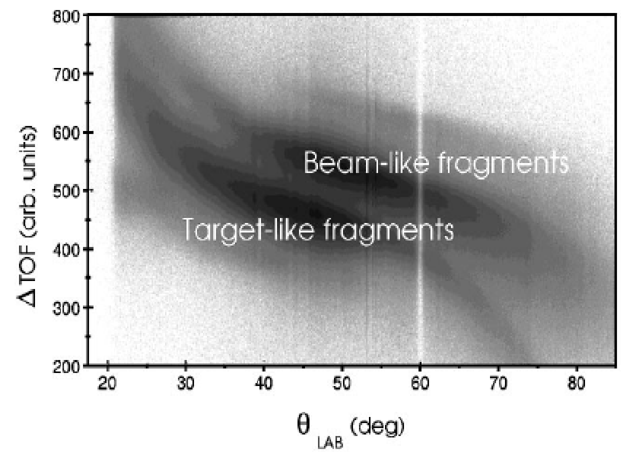

Residual reaction nuclei measured in 'binary' pairs using CHICO, a position sensitive gas detector.

Gamma rays from beam and target-like fragments measured in GAMMASPHERE.

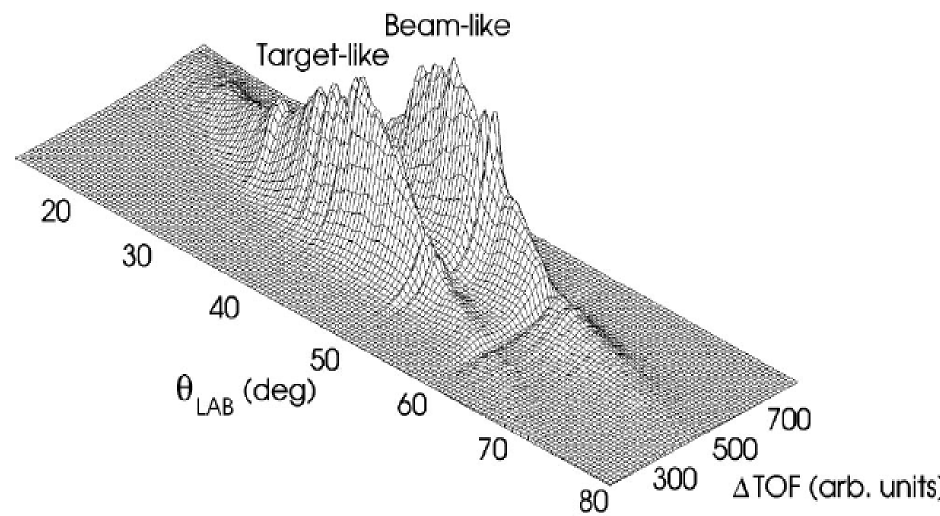

Difference in time of flight between BLF and TLF hitting CHICO can be used to deduce which fragments is which (heavier one usually moved more slowly due to COLM).

Angle differences between CHICO and GAMMASPHERE can be used for Doppler Corrections.

PHYSICAL REVIEW C 69, 024316 (2004)

^{136}Ba studied via deep-inelastic collisions: Identification of the $(\nu h_{11/2})^{-2}_{10^+}$ isomer

J. J. Valiente-Dobón,[1,*] P. H. Regan,[1,2] C. Wheldon,[1,3] C. Y. Wu,[4] N. Yoshinaga,[5] K. Higashiyama,[5] J. F. Smith,[6] D. Cline,[4] R. S. Chakrawarthy,[6] R. Chapman,[7] M. Cromaz,[8] P. Fallon,[8] S. J. Freeman,[6] A. Görgen,[8] W. Gelletly,[1] A. Hayes,[4] H. Hua,[4] S. D. Langdown,[1,2] I. Y. Lee,[8] X. Liang,[7] A. O. Macchiavelli,[8] C. J. Pearson,[1] Zs. Podolyák,[1] G. Sletten,[9] R. Teng,[4] D. Ward,[8] D. D. Warner,[10] and A. D. Yamamoto[1,2]

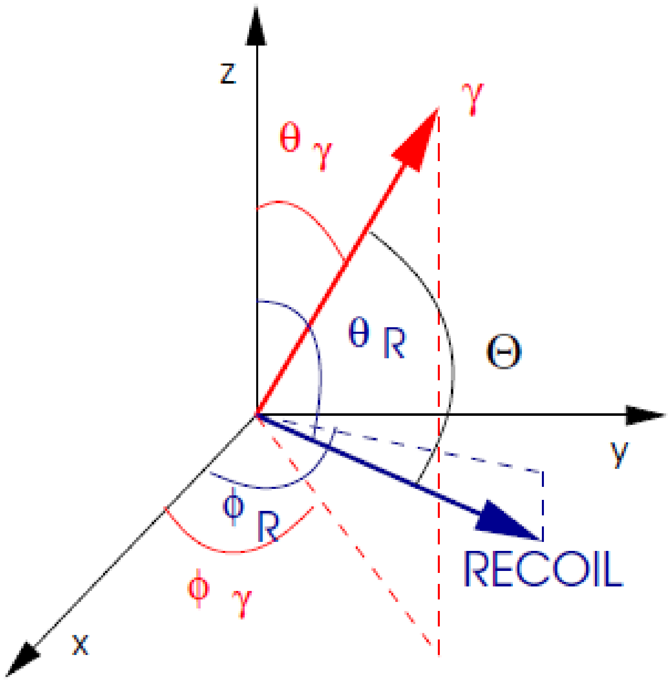

$$\cos\Theta = \sin\theta_R \sin\theta_\gamma(\cos\phi_R\cos\phi_\gamma + \sin\phi_R \sin\phi_\gamma) + \cos\theta_R\cos\theta_\gamma, \quad (3)$$

where θ_R and ϕ_R are the scattering angles of the recoils (BLFs and TLFs), and θ_γ and ϕ_γ are the detection angles of the γ rays from GAMMASPHERE.

e.g., ^{136}Xe beam on thin ^{198}Pt target at 850 MeV (~20% above the coulomb barrier)

The maximum velocities of the binary partners were $\beta \approx 11\%$, as determined from the two-body kinematics of the reaction. Therefore, the prompt γ rays emitted in flight were heavily Doppler shifted. However, it was possible to correct the prompt γ-ray energies for the Doppler effect on an event-by-event basis using the interaction position of the recoils as measured by Chico. The interaction position determined the velocities β_{BLF} and β_{TLF} of the recoiling beam and target nuclei, respectively. By conservation of linear momentum [20] and assuming the limiting case of no particle evaporation,

$$P_{BLF,TLF} = \frac{P_0 \sin(\theta_{TLF,BLF})}{\sin(\theta_{BLF}+\theta_{TLF})}, \quad (1)$$

where $P_{BLF}=m_{(^{136}\mathrm{Xe})}\beta_{BLF}c$ and $P_{TLF}=m_{(^{198}\mathrm{Pt})}\beta_{TLF}c$ are the momenta of the recoiling beam and target nuclei, respectively; θ_{BLF} and θ_{TLF} are the laboratory scattering angles of the recoiling beam and target nuclei, respectively, and P_0 is the momentum of the incident beam. Note that since it is not possible to determine the mass of the recoils with Chico, the momenta of the recoils are calculated assuming the beam ^{136}Xe and target ^{198}Pt masses.

The Doppler-shifted γ rays were corrected according to [22]

$$E_S = E_0 \frac{\sqrt{1-\beta^2}}{1-\beta\cos\Theta}, \quad (2)$$

where E_0 is the energy in the rest frame of the nucleus and Θ is the emission angle relative to the trajectory of the nucleus in the laboratory frame. The angle Θ was determined using the expression

Timing of fragments and measured reaction gamma rays correlated to beam pulse.

PHYSICAL REVIEW C **69**, 024316 (20(

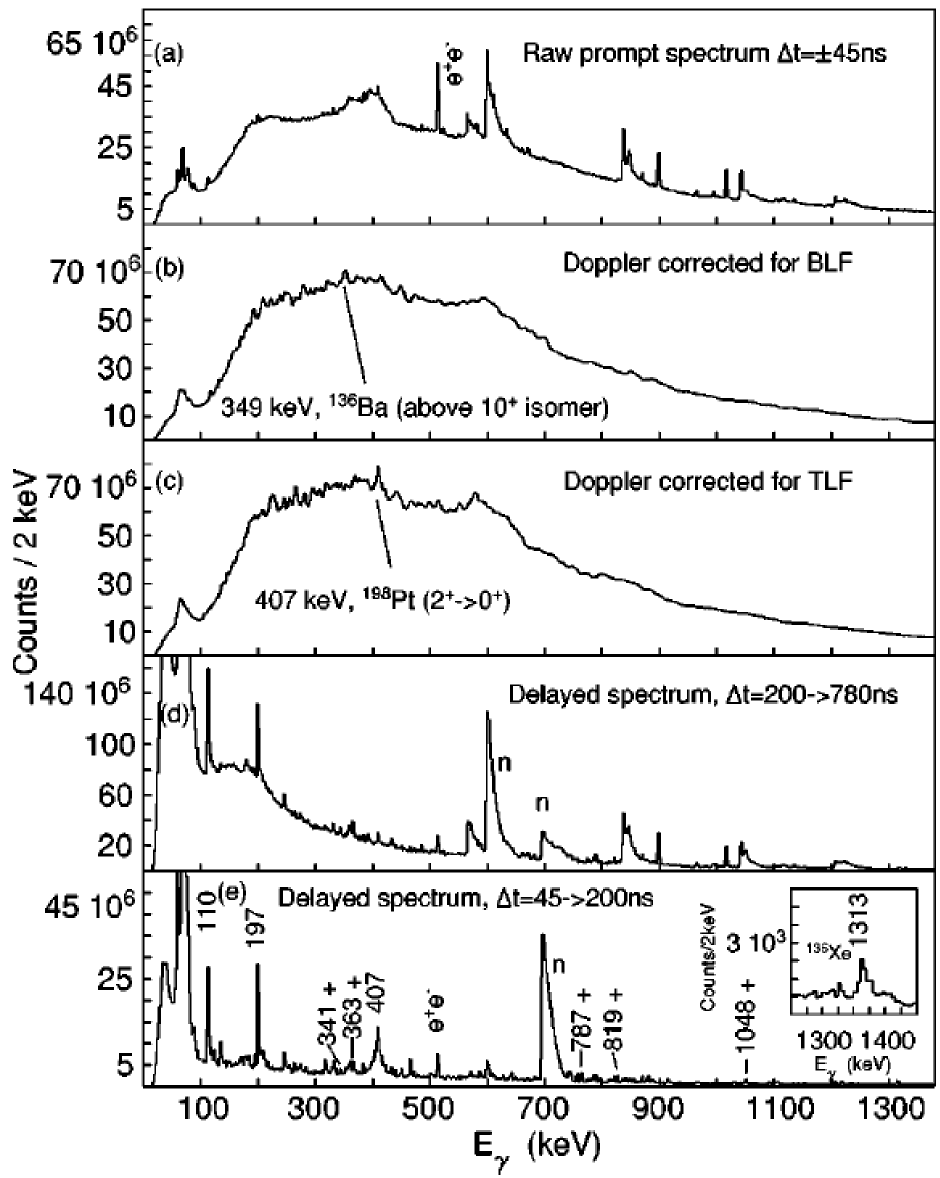

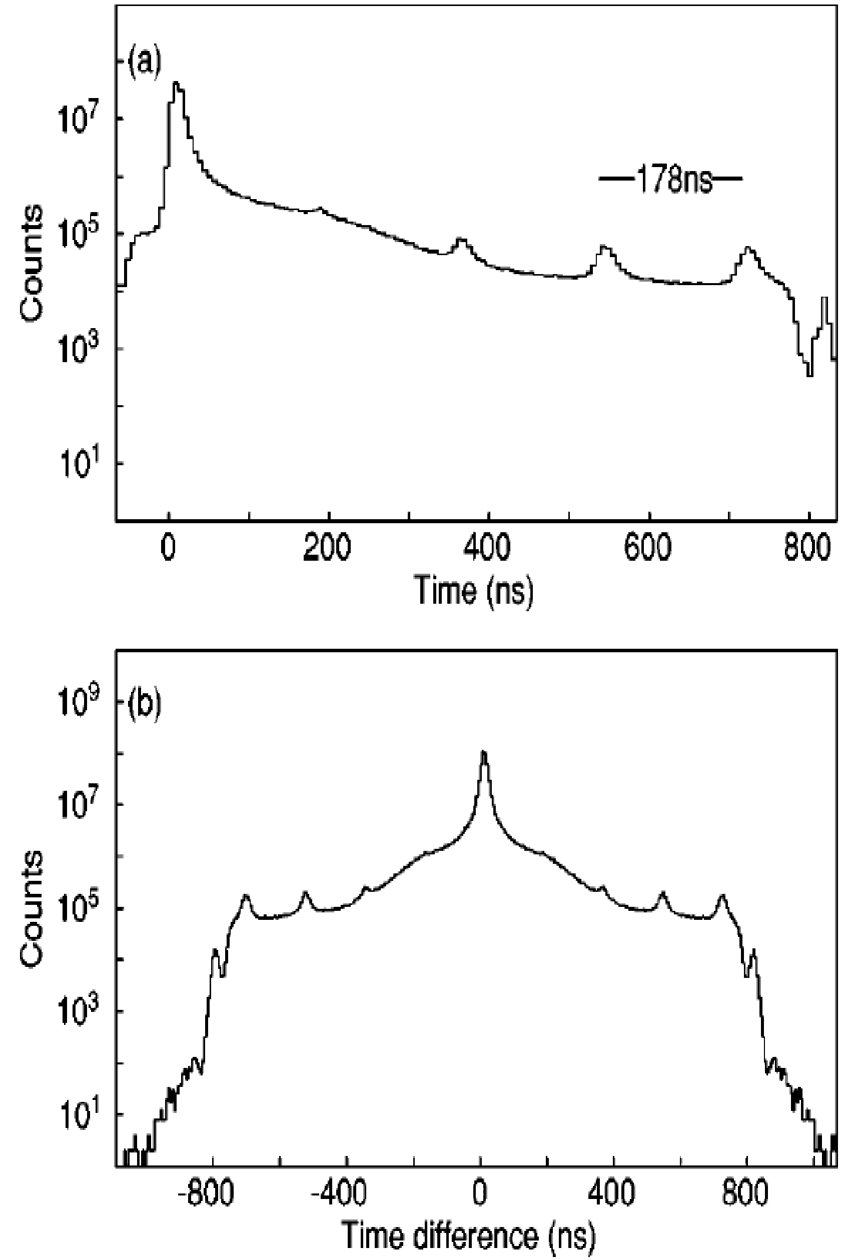

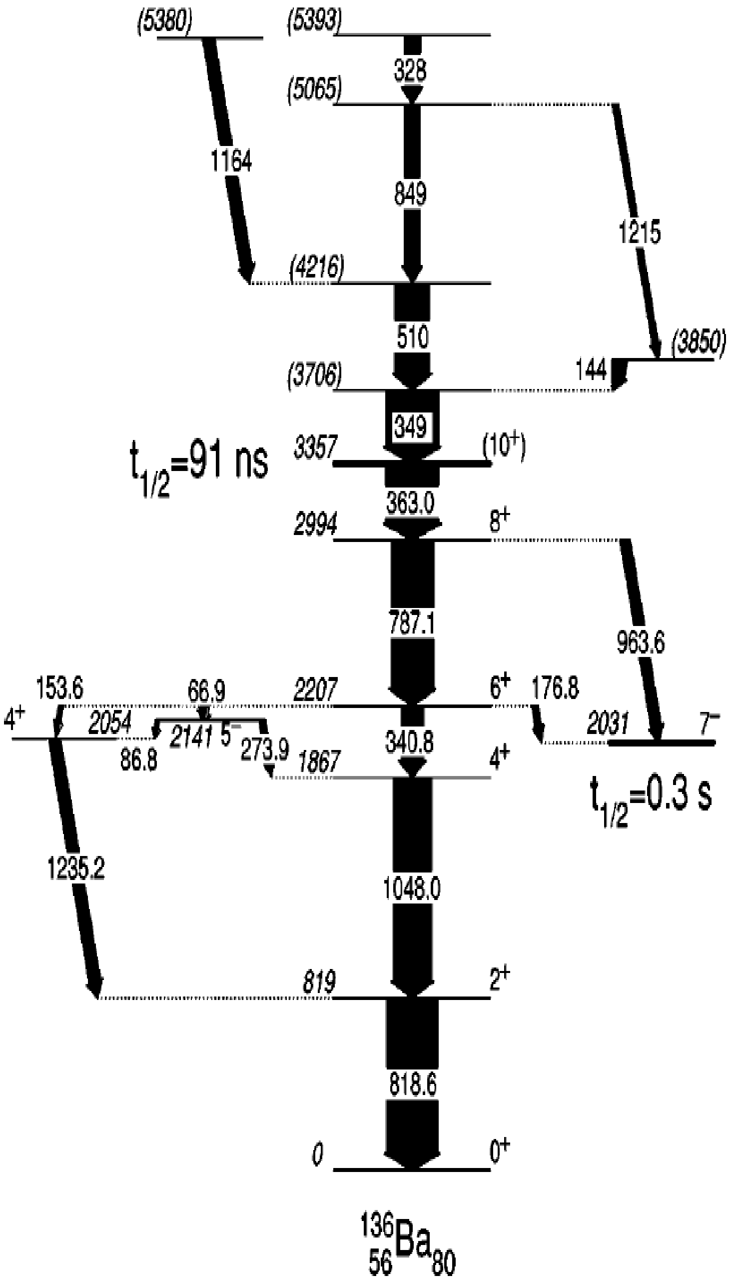
(5380)
(5393)
328
(5065)
1164
849
1215
(4216)
510
(3850)
(3706)
144
349
3357
(10+)
t1/2=91 ns
363.0
2994
8+
787.1
963.6
153.6
66.9
2207
6+
176.8
4+
2054
2141 5−
2031
7−
86.8
273.9
1867
340.8
4+
t1/2=0.3 s
1235.2
1048.0
819
2+
818.6
0
0+
136 56 Ba 80

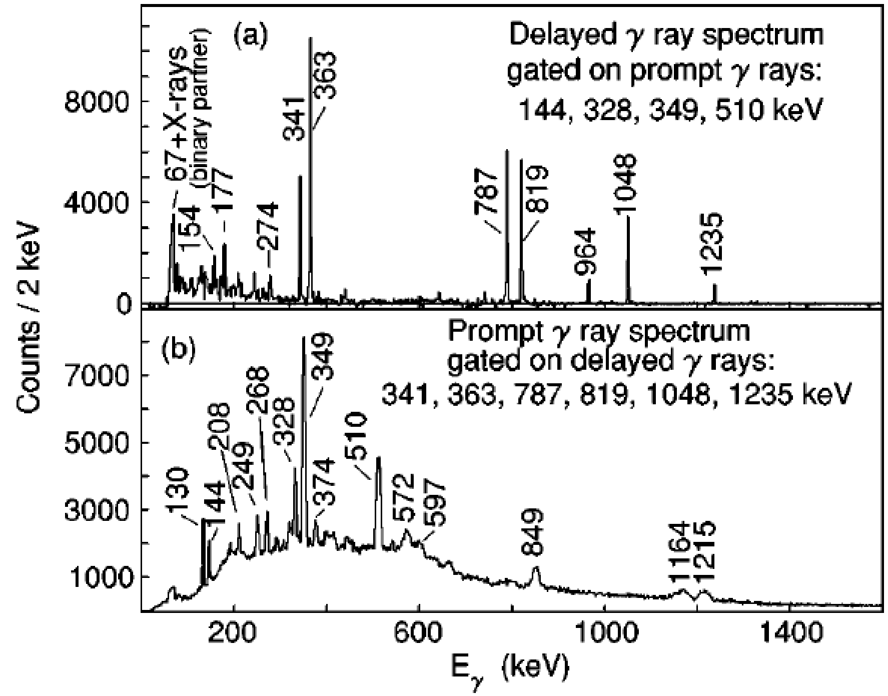
(a)
Delayed γ ray spectrum
gated on prompt γ rays:
144, 328, 349, 510 keV
67+X-rays
(binary partner)
154
177
274
341
363
787
819
964
1048
1235
(b)
Prompt γ ray spectrum
gated on delayed γ rays:
341, 363, 787, 819, 1048, 1235 keV
130
144
208
249
268
328
349
374
510
572
597
849
1164
1215
Counts / 2 keV
Eγ (keV)

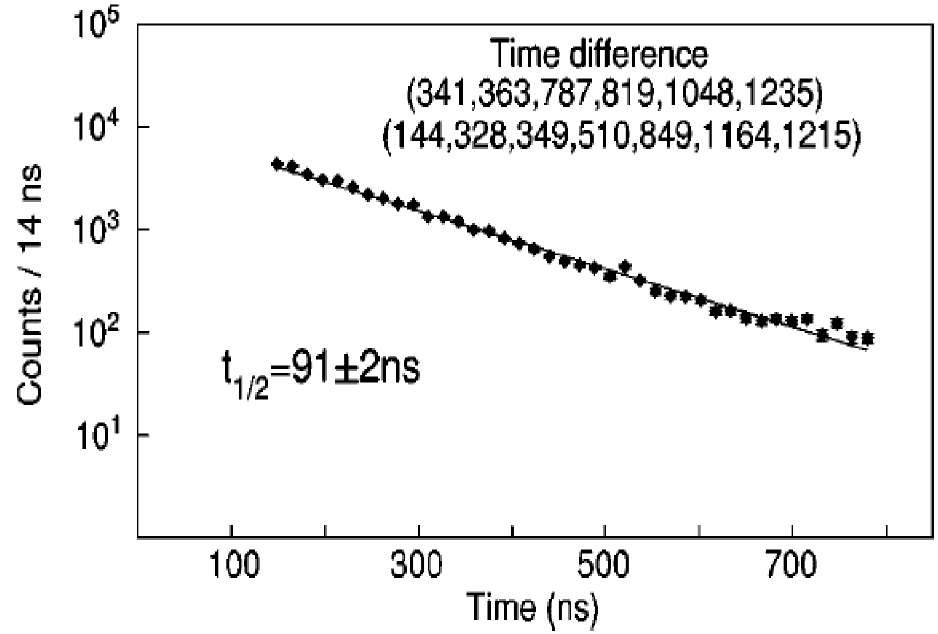
Time difference
(341,363,787,819,1048,1235)
(144,328,349,510,849,1164,1215)
t1/2=91±2ns
Counts / 14 ns
Time (ns)

Use spectrometer to 'tag' on one of the reaction fragments for Doppler Correction.
e.g., ^{82}Se (Z=34) beam on thin ^{170}Er (Z=68) target at INFN-Legnaro.

PHYSICAL REVIEW C **81**, 034310 (2010)

Spectroscopy of neutron-rich ^{168,170}Dy: Yrast band evolution close to the $N_p N_n$ valence maximum

P.-A. Söderström,[1] J. Nyberg,[1] P. H. Regan,[2] A. Algora,[3] G. de Angelis,[4] S. F. Ashley,[2] S. Aydin,[5] D. Bazzacco,[5] R. J. Casperson,[6] W. N. Catford,[2] J. Cederkäll,[7,8] R. Chapman,[9] L. Corradi,[4] C. Fahlander,[8] E. Farnea,[5] E. Fioretto,[4] S. J. Freeman,[10] A. Gadea,[3,4] W. Gelletly,[2] A. Gottardo,[4] E. Grodner,[4] C. Y. He,[4] G. A. Jones,[2] K. Keyes,[9] M. Labiche,[9] X. Liang,[9] Z. Liu,[2] S. Lunardi,[5] N. Mărginean,[4,11] P. Mason,[5] R. Menegazzo,[5] D. Mengoni,[5] G. Montagnoli,[5] D. Napoli,[4] J. Ollier,[12] S. Pietri,[2] Zs. Podolyák,[2] G. Pollarolo,[13] F. Recchia,[4] E. Şahin,[4] F. Scarlassara,[5] R. Silvestri,[4] J. F. Smith,[9] K.-M. Spohr,[9] S. J. Steer,[2] A. M. Stefanini,[4] S. Szilner,[14] N. J. Thompson,[2] G. M. Tveten,[7,15] C. A. Ur,[5] J. J. Valiente-Dobón,[4] V. Werner,[6] S. J. Williams,[2] F. R. Xu,[16] and J. Y. Zhu[16]

Measure BLFs directly in PRISMA spectrometer and gammas in CLARA gamma-ray array. Reverse correct for heavier TLF using 2-body kinematics.

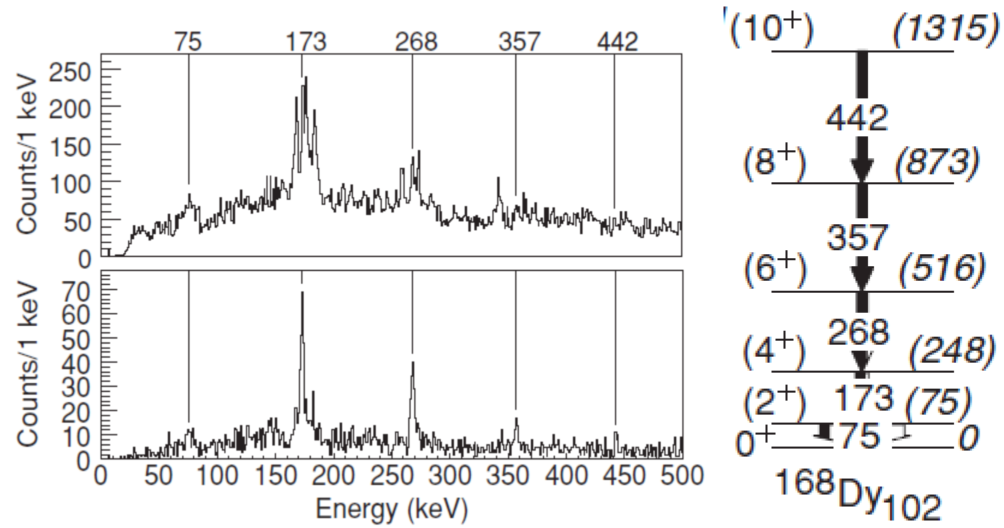

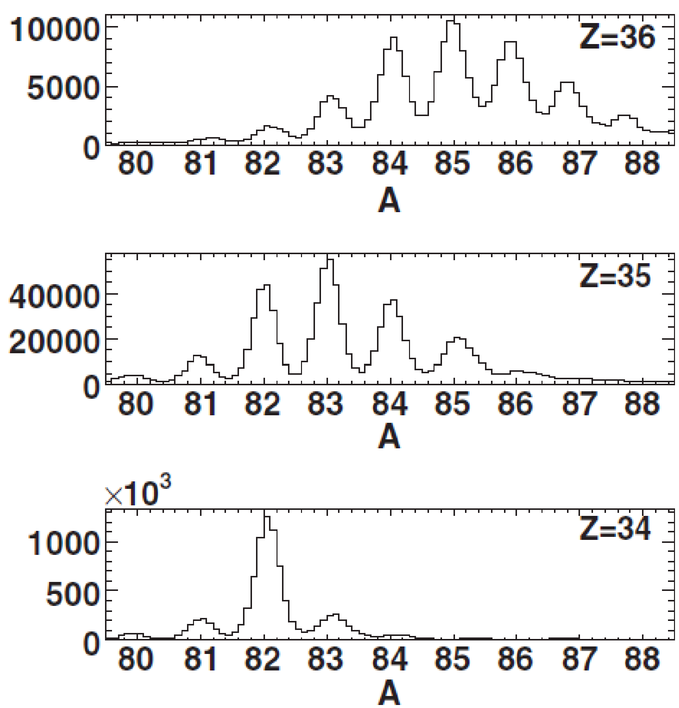

FIG. 3. Spectrum of γ-ray energies from targetlike fragments gated on the beamlike fragments ^{84}Kr (top) and on beamlike fragments ^{84}Kr plus a short time of flight (bottom). The transitions identified as the rotational band in ^{168}Dy are marked with solid lines.

Gate on ^{84}Kr (Z=36) fragment in PRISMA. Complementary fragment (assuming no neutron evaporation) for ^{82}Se+^{170}Er reaction for ^{84}Kr is ^{168}Dy (Z=66) (+2p transfer channel). Shortest time of flight in PRISMA associated with least neutron evaporation.